

**Breakdown of Thymic Tolerance –  
an Etiologic Link Between Acute and  
Chronic Graft-versus-Host Disease**

**Inauguraldissertation**

zur

Erlangung der Würde eines Doktors der Philosophie  
vorgelegt der  
Philosophisch-Naturwissenschaftlichen Fakultät  
der Universität Basel

von

**Simone Dertschnig**

aus Herznach, AG

Basel, 2014

Genehmigt von der Philosophisch-Naturwissenschaftlichen Fakultät  
auf Antrag von

Prof. Dr. Georg A. Holländer

Prof. Dr. Jean Pieters

Prof. Dr. Christoph Hess

Basel, den 18. Februar 2014

Prof. Dr. Jörg Schibler  
Dekan

## SUMMARY

Allogeneic haematopoietic stem cell transplantation (HSCT) is the standard therapy for many disorders of the haematological system. Its use is limited by the major complication acute graft-versus-host disease (GVHD). Development of acute GVHD predisposes to chronic GVHD whose autoimmune manifestations are integral components of disease. It remains uncertain, however, whether and how autoimmunity is linked to antecedent alloimmunity. A hallmark of murine acute GVHD is the *de novo* generation of autoreactive T cells that suggests breakdown of thymic tolerance induction. Central tolerance is dependent on the intrathymic expression of a full scope of tissue-restricted self-antigens (TRA), which is a distinct property of mature medullary thymic epithelial cells (mTEC<sup>high</sup>). The ectopic expression of TRA in mTEC<sup>high</sup> is partly controlled by the autoimmune regulator (Aire). Since the thymus epithelium is a target of donor T-cell alloimmunity, I hypothesised that thymic acute GVHD interfered with the mTEC<sup>high</sup> capacity to sustain TRA diversity. I found that reductions in mTEC<sup>high</sup> compartment sizes are universal manifestations of thymic acute GVHD in murine models of haploidentical, fully MHC-disparate and MHC-identical allogeneic HSCT. Moreover, acute GVHD weakens the platform for central tolerance induction because individual TRA are purged from the total repertoire secondary to a decline in the Aire<sup>+</sup>mTEC<sup>high</sup> subset. The most substantially reduced TRA are enriched for genes specific for known target tissues of chronic GVHD. I provide direct evidence in a transgenic mouse system using ovalbumin (OVA) as a model neo-TRA that the *de novo* production of TRA-specific CD4<sup>+</sup> T cells during acute GVHD is a consequence of impaired ectopic TRA expression. OVA-specific CD4<sup>+</sup> T cells are present in the periphery in mice with acute GVHD. Peritransplant administration of an epithelial cytoprotective agent, fibroblast growth factor-7, maintains a stable pool of Aire<sup>+</sup>mTEC<sup>high</sup>, which is due to enhanced proliferation of cells within the total mTEC compartment. In parallel, Fgf7 improves the TRA transcriptome despite acute GVHD. Taken together, these data indicate the presence of an etiologic link between acute GVHD and autoimmunity during subsequent chronic GVHD. The present results also suggest that approaches for epithelial cytoprotection may prove to prevent the emergence of thymus-dependent autoreactive T cells.

# TABLE OF CONTENTS

|  |           |
|--|-----------|
| <b>1. INTRODUCTION.....</b>  | <b>7</b>  |
| <b>1.1 Haematopoietic Stem Cell Transplantation.....</b>                     | <b>7</b>  |
| 1.1.1 Current Status.....  | 7         |
| 1.1.2 Principles of allogeneic HSCT .....                                    | 8         |
| 1.1.3 Successful Outcome of HSCT.....  | 9         |
| <b>1.2 T-cell Reconstitution post-HSCT .....</b>                             | <b>10</b> |
| 1.2.1 Overview.....  | 10        |
| 1.2.2 Thymus-dependent T cell regeneration.....                              | 11        |
| The Thymic Lymphoid Compartment .....  | 13        |
| The Thymic Stromal Compartment.....  | 14        |
| Negative Selection in the Thymus Medulla .....                               | 15        |
| OVA – a tool to study thymic negative selection .....                        | 17        |
| 1.2.3 Thymus-independent T cell regeneration .....                           | 17        |
| <b>1.3 Graft-versus-host Disease .....</b>                                   | <b>19</b> |
| 1.3.1 Clinical Features of Graft-versus-host Disease .....                   | 19        |
| 1.3.2 Pathophysiology of acute GVHD .....                                    | 20        |
| 1.3.3 Pathophysiology of chronic GVHD .....                                  | 22        |
| 1.3.4 Prophylaxis and Treatment of GVHD .....                                | 24        |
| Prevention of GVHD .....   | 24        |
| Treatment of GVHD.....   | 24        |
| 1.3.5 Post-transplant immune deficiency .....                                | 25        |
| 1.3.6 Immune reconstitution in the presence of acute GVHD.....               | 25        |
| 1.3.7 Thymic GVHD .....  | 26        |
| Pathomechanism of Thymic Injury – Preclinical Mouse Models .....             | 26        |
| Thymic dysfunction during acute GVHD – a link to chronic GVHD? ..            | 28        |
| 1.3.8 Strategies to Improve post-transplant Immune Deficiency.....           | 29        |
| Fibroblast growth factor-7 .....   | 29        |
| <b>2. HYPOTHESES AND AIM OF THE THESIS .....</b>                             | <b>31</b> |
| <b>3. MATERIALS AND METHODS .....</b>  | <b>32</b> |
| <b>3.1 Mice.....</b>   | <b>32</b> |
| <b>3.2 BMT and GVHD induction.....</b>                                       | <b>32</b> |
| <b>3.3 Fgf7 treatment .....</b>  | <b>33</b> |
| <b>3.4 Flow cytometry reagents .....</b>                                     | <b>33</b> |
| <b>3.5 Analysis of the mTEC<sup>high</sup> compartment by flow cytometry</b> |           |
| .....  | 34        |
| <b>3.6 Immunofluorescence confocal microscopy.....</b>                       | <b>35</b> |



|       |  |    |
|-------|--|----|
| 3.7   | Quantitative PCR .....   | 36 |
| 3.8   | DNA microarray analysis .....  | 37 |
| 3.9   | Bioinformatics .....   | 38 |
| 3.10  | Statistical analysis .....   | 39 |
| 4.    | <b>RESULTS</b> .....   | 40 |
| 4.1   | <b>Impaired ectopic expression of tissue-restricted antigens in the thymus during murine acute GVHD</b> .....  | 40 |
| 4.1.1 | Identification and characterisation of medullary thymic epithelial cell subsets by flow cytometry .....  | 40 |
| 4.1.2 | Induction of thymic acute GVHD .....   | 41 |
| 4.1.3 | Acute GVHD impairs mTEC <sup>high</sup> compartment size .....   | 44 |
| 4.1.4 | Acute GVHD impairs thymic Aire expression.....   | 47 |
| 4.1.5 | Acute GVHD impairs TRA expression.....   | 49 |
| 4.2   | <b>Impaired thymic expression of tissue-restricted antigens licenses the <i>de novo</i> generation of autoreactive CD4<sup>+</sup> T cells during murine acute GVHD</b> .....  | 57 |
| 4.2.1 | A transgenic model to study generation of thymus-dependent autoreactive T cells during acute GVHD.....   | 57 |
| 4.2.2 | Thymic GVHD induction in RIP-mOVA recipients.....  | 58 |
| 4.2.3 | Acute GVHD reduces the thymic ectopic expression of the neo-self-antigen ovalbumin .....   | 63 |
| 4.2.4 | OVA-specific T cell clones escape negative selection during acute GVHD .....   | 64 |
| 4.2.5 | <i>De novo</i> generated OT-II T cells display a non-tolerant effector phenotype .....   | 67 |
| 4.3   | <b>Epithelial cytoprotection with fibroblast growth factor-7 (Fgf7) sustains ectopic expression of tissue-restricted antigens in the thymus during murine acute GVHD</b> ..... | 70 |
| 4.3.1 | Fgf7 sustains the thymic mTEC <sup>high</sup> compartment including Aire expression .....  | 70 |
| 4.3.2 | Fgf7 administration sustains a more diverse TRA transcriptome in mTEC <sup>high</sup> during acute GVHD.....   | 76 |
| 4.3.3 | Fgf7 administration alters thymic expression of TRA independently of their tissue specificity and acute GVHD .....   | 83 |
| 5.    | <b>DISCUSSION</b> .....  | 85 |
|       | Loss of mTEC – a universal manifestation of acute GVHD .....   | 86 |
|       | Acute GVHD weakens the platform for central tolerance.....   | 87 |

|   |            |
|---|------------|
| Use of the RIP-mOVA system to study thymic negative selection in the presence of acute GVHD.....            | 89         |
| Potential mechanism of autoreactive T-cell neogenesis following allogeneic HSCT.....                        | 92         |
| Fgf7 restores the thymic mTEC <sup>high</sup> compartment and sustains the diversity of TRA expression..... | 96         |
| <b>6. CONCLUSIONS.....</b>  | <b>100</b> |
| <b>7. REFERENCES .....</b>  | <b>101</b> |
| <b>8. ACKNOWLEDGEMENTS.....</b>   | <b>126</b> |
| <b>9. APPENDIX .....</b>  | <b>127</b> |

# 1. INTRODUCTION

## 1.1 Haematopoietic Stem Cell Transplantation

### 1.1.1 Current Status

Haematopoietic stem cell transplantation (HSCT) has developed into the standard therapy for several disorders of the haematopoietic system.<sup>1-4</sup> In 2011, more than 35,000 transplantations were performed annually in Europe, of which 42% were allogeneic and 58% autologous procedures.<sup>4,5</sup> The main indications for allogeneic HSCT were malignancies of the haematopoietic system, in particular acute myeloid and lymphoblastic leukaemias (AML and ALL, respectively), myelodysplastic syndromes (MDS) and non Hodgkin lymphoma (Figure 1). Autologous HSCT was mainly performed to treat lymphoid neoplasias and non-Hodgkin and Hodgkin lymphomas.<sup>4,6</sup> The success of allogeneic HSCT therapy depends on a multitude of parameters, including the type and stage of the underlying disease, patient age, genetic disparity between donor and host, type and intensity of the pretransplantation conditioning regimen, and the presence of transplant-related toxicities (TRTs).<sup>6,7</sup> For instance, allogeneic HSCT is highly efficacious for patients with AML or ALL, since long term leukaemia-free survival can be achieved in 20-60% of these patients. Increased disease-free survival with allogeneic HSCT therapy can even be obtained in older patients (>65yrs): Here, the 5-year survival is <2% when treated with chemotherapy alone,<sup>8</sup> whereas treatment with allogeneic HSCT increases the 5-year survival rate to 33%.<sup>9</sup> For patients with MDS allogeneic HSCT is the only therapy with curative potential.

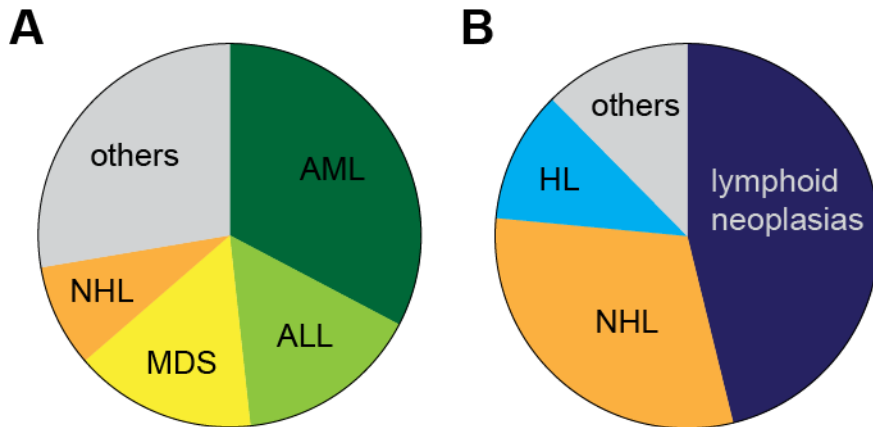


**Figure 1. Indications for HSCT in Europe in 2011.** (A) Proportions of disease indications for an allogeneic HSCT in Europe in 2011. (B) Proportions of disease indications for an autologous HSCT in Europe in 2011. AML = acute myeloid leukaemia; ALL = acute lymphoblastic leukaemia; MDS = myelodysplastic syndromes; NHL = non-Hodgkin lymphoma; HL = Hodgkin lymphoma.

Adapted from *Passweg et al., Bone Marrow Transplantation (2013)*<sup>5</sup>

### 1.1.2 Principles of allogeneic HSCT

Patients that are chosen for HSCT therapy first undergo preparative cytoreductive conditioning with chemotherapy and/or total body irradiation (TBI). This treatment has several purposes as it serves, firstly, to reduce tumour burden in case of cancer treatment; secondly, to suppress the recipient's immune system and thus prevent rejection of the donor graft; and lastly, to ablate the recipient's haematopoietic system in order to create space in the stem cell niche and to enable proper engraftment of donor HSC. The preparative conditioning therapy can be applied in different intensities, resulting in either reduction or full ablation of the host's haematopoietic system.<sup>10</sup> The use of reduced intensity regimens (RIC) instead of myeloablative treatments was a major advance in allogeneic HSCT. The principle of RIC is to treat with an intensity that is high enough to prevent graft rejection, but that induces less tissue injury.<sup>11</sup> Conditioning is followed by allogeneic HSCT whose goal is two-fold: firstly, to replace the patient's diseased haematopoietic system with new HSCs stemming from a genetically disparate healthy donor, and secondly, to

exploit the immunotherapeutic effect of the donor graft (i.e. graft-versus-tumour effect, GVT; see below, section 1.2.3).

HSCs can be harvested from different sources. HSC mobilised by granulocyte colony-stimulating factor (G-CSF) into the peripheral blood (PB) are the preferred source for transplantation today (peripheral blood stem cells; PBSC; 99% of autologous and 71% of allogeneic HSCT).<sup>4,6</sup> Alternative sources for HSCs used clinically are bone marrow (BM) and umbilical cord blood (UCB).

### 1.1.3 Successful Outcome of HSCT

The rates for 1-year and disease-free survival following allogeneic HSCT have significantly improved over the last few years.<sup>12,13</sup> For allogeneic HSCT to be successful, three main objectives need to be fulfilled. Firstly, the underlying disease needs to be cured. The use of cytoreductive conditioning in combination with the capacity of donor T cells to mediate an anti-tumour effect is essential for tumour control. Secondly, the patient should not experience transplant-related toxicities (TRTs) that arise as a consequence of conditioning and donor T cell immunity that is directed against healthy host tissues. Unfortunately, TRTs are still major obstacles of allogeneic HSCT that hamper therapeutic success.<sup>14,15</sup> TRTs include acute and chronic graft-versus-host disease (GVHD, see below chapter 1.3) and organ failure caused by the preparative conditioning regimen.<sup>16,17</sup> When present, such adverse events put the patient at risk for transplant-related morbidity and mortality. Thirdly, immunity needs to be efficiently reconstituted in patients receiving HSCT. This is important, since the cytoreductive conditioning not only elicits an anti-tumour effect, but also compromises the patient's innate and adaptive immune responses. This effect predisposes the HSCT recipient to opportunistic infections, increases the risk for malignancy relapse and the development of secondary malignancies, and hence, contributes to poor clinical outcome.<sup>18-22</sup> Timing and quality of immune reconstitution following allogeneic HSCT have therefore a significant impact on the patient's well-being. Acute GVHD increases the likelihood to be diagnosed with an opportunistic infection.<sup>23</sup> Hence, this particular TRT is a confounding factor for the re-establishment of immune competence. The following two chapters will first present

knowledge concerning (i) the immune regeneration after transplantation and (ii) the immunopathophysiology of GVHD, and then address (iii) the known mechanistic relationships between these two events.

## 1.2 T-cell Reconstitution post-HSCT

### 1.2.1 Overview

Following cytoreductive treatment and allogeneic HSCT, there are two complementary pathways that restore immune competence. Firstly, residual host-derived haematopoietic cells and mature cells present in the donor graft undergo clonal expansion in peripheral host tissues secondary to homeostatic and alloantigenic stimuli; and secondly, myeloid and lymphoid cells are generated *de novo* from the donor HSCs. Whereas the innate immune system, including monocytes, granulocytes and natural killer (NK) cells, is restored within a few weeks, the regeneration of the adaptive immune system takes months (B cells) to years (T cells) to be completed.<sup>24-29</sup> Adequate T cell regeneration is pivotal for the patient's survival. The absence of competent T cell immunity is associated with an increased risk for viral, bacterial and fungal infections.<sup>18,30-34</sup> The speed of T-cell reconstitution depends on several in part interconnected factors, as diverse as recipient age and gender, underlying disease, type of conditioning, genetic disparity between donor and host, HSC source, acute and chronic GVHD, opportunistic infections and relapse of malignancy.<sup>35</sup> Two pathways act in parallel to contribute to the regeneration of the T cell pool. First, donor graft- and residual host-derived mature T cells undergo peripheral clonal expansion in a thymus-independent manner. The second pathway comprises the *de novo* generation of T cells from the transplanted HSCs in a functionally intact thymus (Figure 2).

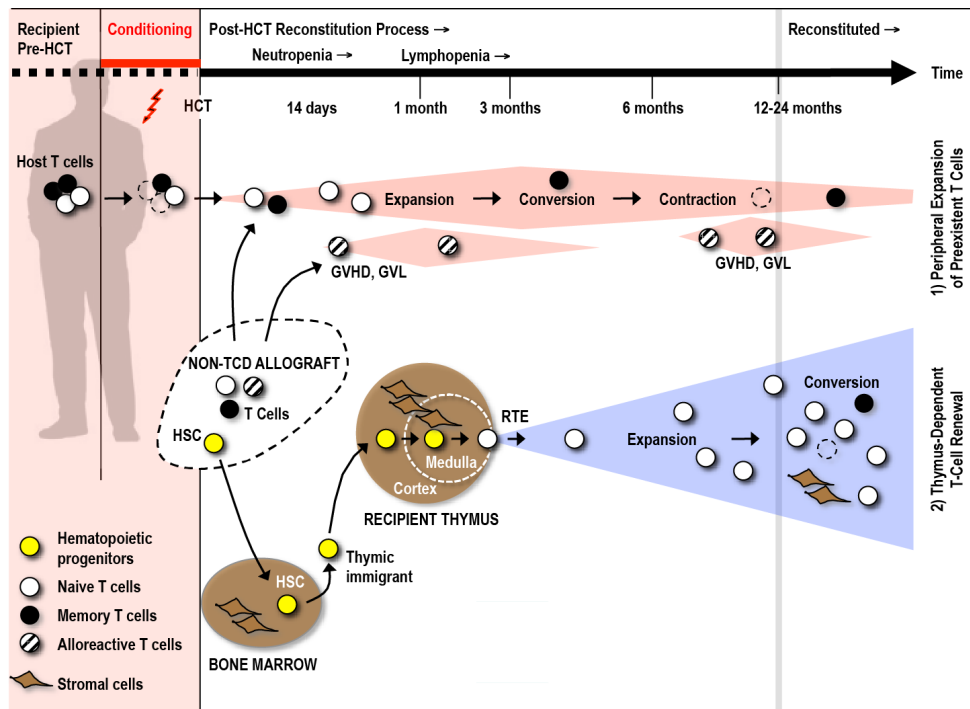


**Figure 2. T-cell reconstitution after allogeneic HSCT.** T-cell regeneration post-HSCT is accomplished by two pathways. 1) Thymus-independent pathway. Residual host and mature donor T cells expand initially in response to homeostatic signals or cognate antigen. Alloreactive donor T cells can mediate both GVHD and GVT, but contribute also to the peripheral T cell compartment. Peripheral expansion of pre-existent T cells results in a conversion to memory phenotype, skewing of the TCR repertoire and contracted pool size. 2) Thymus-dependent pathway. The *de novo* generation of naïve T cells from haematopoietic progenitors requires a functional thymus. The thymic microenvironment is a three-dimensional network that attracts T cell progenitors and supports their survival, expansion, differentiation and selection. Naïve, pathogen specific, non-self reactive T cells emerge from the thymus to the periphery. Adapted from *Krenger et al., Blood (2011)*<sup>36</sup>

## 1.2.2 Thymus-dependent T cell regeneration

The primary site for T cell development during fetal and early postnatal life is the thymus.<sup>37-41</sup> The cellular architecture of the thymus is highly conserved between vertebrate species and is organised in subcapsular region, cortex, cortico-medullary junction and medulla. Since the thymus does not contain numbers of HSC sufficient for permanent T-cell

regeneration, the thymus therefore needs to be continuously replenished with T cell progenitors from the BM via the blood circulation.<sup>42</sup> Once these progenitors enter the thymus at the cortico-medullary junction, they pass through different maturation steps during which they develop into mature T cells (Figure 3).<sup>43</sup>

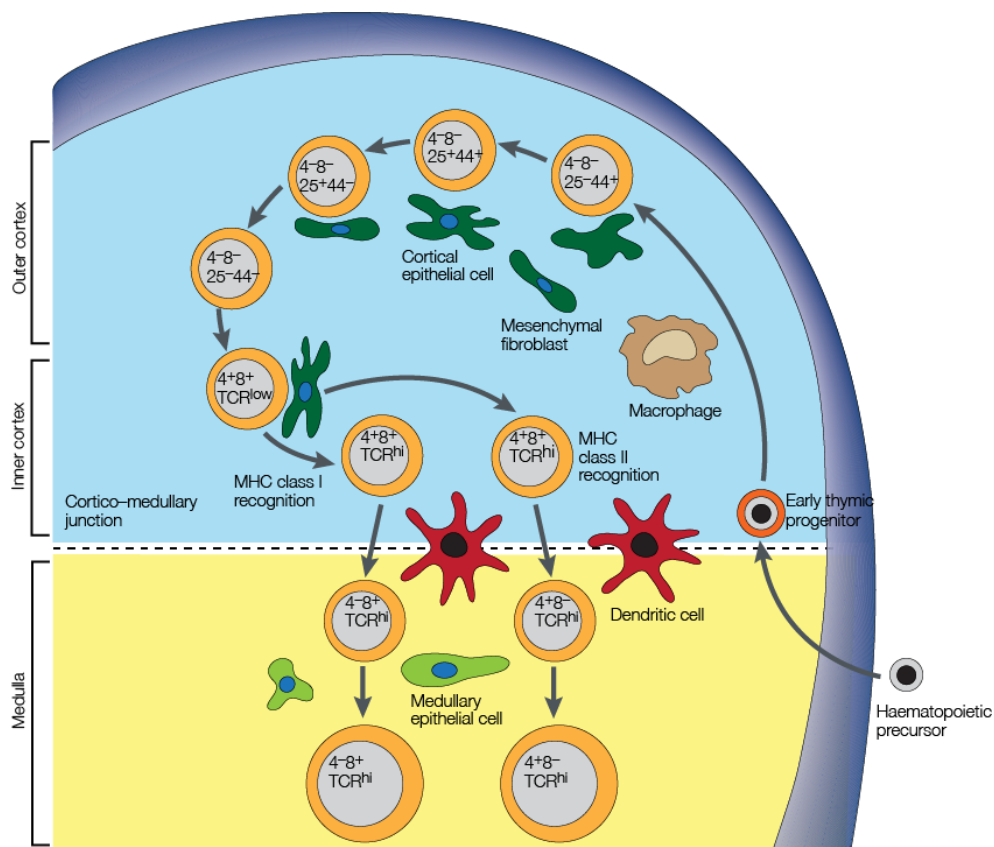


**Figure 3. Thymic crosstalk – TEC-thymocyte interactions.** The thymus is organised in discrete cortical and medullary areas. T cell progenitors enter the thymus at the cortico-medullary junction and their development can be followed by different expression of cell surface markers. Interactions between thymocytes and the thymus stroma are important to drive T-cell maturation.

Adapted from *Anderson et al., Nature Reviews Immunology (2001)*<sup>44</sup>



### *The Thymic Lymphoid Compartment*

T cell progenitors that have entered the thymus bear a CD3<sup>+</sup>CD4<sup>-</sup>CD8<sup>-</sup> triple negative (TN) phenotype and are commonly referred to as early thymic precursors (ETPs). Throughout their differentiation, ETPs interact with the thymic microenvironment (discussed in more detail below).<sup>45</sup> The initial developmental stages of the TN ETPs are identified by the surface expression of CD25 and CD44 (double negative (DN) 1: CD25<sup>-</sup>CD44<sup>+</sup>; DN2: CD25<sup>+</sup>CD44<sup>+</sup>; DN3: CD25<sup>+</sup>CD44<sup>-</sup>; DN4: CD25<sup>-</sup>CD44<sup>-</sup>; Figure 3).<sup>46,47</sup> DN thymocytes that are located in the thymic cortex and restricted to the  $\alpha/\beta$  TCR lineage rearrange their *Tcrb* locus and then assemble the TCR $\beta$  and pre-TCR $\alpha$  (pT $\alpha$ ) chains. This results in the expression of the pre-TCR complex on the cell surface, which is associated with CD3.<sup>48</sup> The expression of the CD3:pre-TCR complex induces extensive proliferation, expression of the surface proteins CD4 and CD8 and hinders further  $\beta$ -chain rearrangement. These CD4<sup>+</sup>CD8<sup>+</sup> double positive (DP) thymocytes then rearrange the  $\alpha$ -chain locus, which results in expression of a complete, randomly chosen TCR $\alpha\beta$ :CD3 complex with an antigen specificity. At the DP stage, thymocytes undergo a first selection process, termed positive selection, to assure TCR reactivity to self-peptide/self-major histocompatibility complex (MHC) complexes. The latter are presented by thymic stroma cells and thymocytes with sufficiently high affinity are selected and consequently receive further differentiation signals,<sup>49</sup> whereas no interactions induce apoptosis (“death by neglect”) of DP. Positively selected thymocytes with a TCR restricted to MHC class II express CD4 on the surface, whereas CD8 is expressed on thymocytes with a TCR restricted to MHC class I (CD4<sup>+</sup> single positive (SP) and CD8<sup>+</sup> SP, respectively).<sup>50</sup> Only 3-5% of thymocytes receive a survival signal and migrate from the cortex to the medulla,<sup>51,52</sup> where they are subject to thymic negative selection. In this process, SP thymocytes are checked for reactivity to self-peptides, among them many antigens with tissue-specific expression of proteins (i.e. tissue-restricted antigens, TRA). These self-antigens are presented by medullary thymic epithelial cells (mTEC) and dendritic cells (DC) (discussed in more detail below). SP thymocytes with a TCR that binds with an inadequately high affinity to the self-peptide/MHC complexes are removed from the repertoire by apoptosis.<sup>53</sup> Positive and negative selection processes together shape the T cell repertoire such that the

adaptive immune system is competent to react to a seemingly unlimited diversity of foreign antigens (“nonself”) whilst not being responsive to self-antigens (“self”).<sup>54</sup> This pivotal mechanism to assure self-tolerance is termed central (i.e. thymic) T cell tolerance induction. Before being exported to the periphery, thymocytes go through post-selection maturation in the medulla.<sup>43</sup>

### ***The Thymic Stromal Compartment***

The thymic stroma is a three-dimensional network composed of different cell types. Major components of this scaffold are thymic epithelial cells (TEC), but mesenchymal cells and cells of haematopoietic origin such as DCs and macrophages are also present. Together they build a unique structural and functional microenvironment that attracts T cell progenitors and supports their survival, expansion, differentiation and selection.<sup>38,55</sup> The TEC compartment itself is composed of phenotypically, functionally and structurally different cortical and medullary subsets, which are completely replaced every 10 to 14 days.<sup>56,57</sup> Several surface and intracellular markers characterise the TEC subsets of the murine thymus. The major markers are cytokeratins (CK) which include CK5, CK14, CK8 and CK18. Cortical TEC express CK8 and CK18 and can be further defined by flow cytometry by their expression of epithelial cell adhesion molecule (EpCam; CD326) and Ly51.<sup>38,58-60</sup> In addition to the expression of both MHC class I and class II molecules, cTEC have the unique ability to support positive selection by antigen-processing and antigen-presentation capacities that are different from other cell types like mTEC and DCs present in the thymus.<sup>61</sup> The mTEC subset is characterised by its expression of CK5 and CK14.<sup>58-60</sup> Recent progress further allowed a more precise identification of mTEC by flow cytometry. These cells express EpCam (CD326) and are reactive with *Ulex europaeus* agglutinin-1 (UEA-1), but do not express Ly51 and CD45.<sup>56,57,62-67</sup> Similar to cTEC, mTEC express both MHC class I and class II.<sup>43</sup> Since mTEC are major contributors to thymic negative selection they are of central importance to generate a self-tolerant T cell repertoire.

### *Negative Selection in the Thymus Medulla*

The medullary TEC compartment contains cells at different maturational stages that can be classified according to the expression of costimulatory molecules, such as CD40, CD80, CD86, the intensity of MHC class II expression and the intracellular expression of the transcription factor Autoimmune Regulator (Aire).<sup>64,68</sup> While immature mTEC express low levels of CD40, CD80, CD86 and MHC class II (referred to as mTEC<sup>low</sup>), mature mTEC express high levels of CD40, CD80, CD86 and MHC class II (mTEC<sup>high</sup>) and express Aire at either low or high levels. A large array of TRA is produced by mTEC and presented to developing thymocytes either by mTEC themselves or by DCs via cross-presentation.<sup>69</sup> These TRA encode for antigens normally present in the periphery.<sup>64,70</sup> During mTEC maturation, TRA expression levels increase, as mTEC<sup>high</sup> show the highest extent of TRA diversity.<sup>70</sup> The process of TRA expression is called promiscuous gene expression (pGE). TRA expression by mTEC “mirrors the peripheral self” and is crucial for induction of central tolerance.<sup>71,72</sup> Expression levels in mTEC are 50- to 170-fold lower when compared to the corresponding peripheral tissues.<sup>73-75</sup> Given the fact that each TRA is only expressed by 1-3% of mTEC, which are dispersed in the medulla,<sup>75</sup> the process of TRA presentation needs to be efficient. It is still poorly understood how mTEC<sup>high</sup> transcribe and translate these promiscuous genes. One control mechanism that drives TRA expression is mediated via the transcription factor Aire (Figure 4). Within the thymus, Aire is expressed in mature mTEC<sup>high</sup>,<sup>72,76,77</sup> and lack of appropriate Aire expression predisposes to autoimmune disease. In humans, mutations in the Aire gene cause Autoimmune polyendocrinopathy-candidiasis ectodermal dystrophy (APECED; also known as autoimmune polyendocrine syndrome type 1, APS-1),<sup>78,79</sup> a rare monogenic autoimmune disease that affects multiple organs.<sup>80,81</sup> Aire<sup>+</sup>mTEC<sup>high</sup> are typically post-mitotic and acquire features that are characteristic for professional APCs (e.g. high expression of MHC class II, CD40, CD80, CD86).<sup>56,77,82</sup> Mice deficient for Aire (Aire-knock out) show autoimmune manifestations that mimic the human APECED including the presence of autoantibodies against various tissues and mononuclear cell infiltrations of several organs.<sup>83,84</sup> Gene expression analysis of mTEC isolated from Aire-knock out (Aire<sup>-/-</sup>) and Aire-wild type (Aire<sup>+/+</sup>) mice revealed that a fraction of ~30% of TRA is controlled by

Aire.<sup>54,72</sup> Among them are for example insulin, salivary protein 1, and fatty acid-binding protein.<sup>72</sup> Importantly, inadequate Aire gene dosage or the absence of Aire expression and the loss of TRA diversity is associated with impaired negative selection.<sup>73</sup> Consequently, T cells bearing a high-affinity TCR for a specific Aire-dependent TRA can emerge in the periphery.<sup>85,86</sup> The precise molecular mechanisms how Aire promotes TRA expression are still unsolved. Transcriptional regulation via epigenetic modifications is likely to be a candidate mechanism.<sup>64,70</sup>

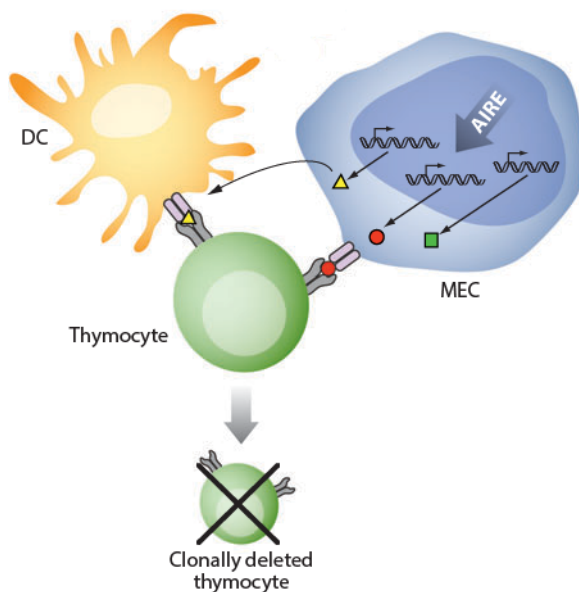


**Figure 4. Aire promotes negative selection of self-reactive thymocytes.** Aire induces the expression of a broad array of TRA, which are processed and presented by mTEC themselves or DCs via cross-presentation. Inadequate binding of the TCR with a TRA/MHC complex results in clonal deletion of thymocytes.

Adapted from *Mathis et al., Annual Review of Immunology (2009)*<sup>87</sup>

Efficient tolerance induction is only achieved when thymocytes are exposed to the whole spectrum of self-antigens present in the thymic medulla. Hence, this process needs to be tightly regulated.<sup>88</sup> Small interruptions such as a reduced number of mature mTEC and ensuing distraction of the three-dimensional network can obstruct this process.<sup>89,90</sup> Thymic negative selection is not 100% efficient. Additional mechanisms are in place that contribute to assure self-tolerance and prevent autoimmunity. For example, natural regulatory T cells ( $T_{reg}$ ) that are characterised by their  $CD4^+CD25^+$  phenotype and the intracellular expression of the transcription factor Foxp3 are generated in the thymus.<sup>91-93</sup> Recent data has demonstrated that the mTEC compartment provides a developmental niche for  $T_{reg}$  cells and is therefore critically required for the proper generation of the latter.<sup>94-96</sup>

### ***OVA – a tool to study thymic negative selection***

To study negative selection specially adapted mouse models are required that include the thymic expression of neo-self-antigen (model TRA). RIP-mOVA mice express membrane-bound ovalbumin (mOVA; OVA<sub>139-385</sub>) under the control of the rat insulin promoter (RIP).<sup>97</sup> In these mice, mOVA is expressed in the pancreas but the transgene is also ectopically expressed in the thymus specifically in mTEC.<sup>98</sup> Rag2-deficient OT-II mice have a transgenic V $\alpha$ 2V $\beta$ 5 TCR specific for OVA<sub>323-339</sub> in the context of MHC class II (I-A<sup>b</sup>).<sup>99,100</sup> In bone marrow chimeras the developing OVA-specific thymocytes are deleted in a thymus of a RIP-mOVA mouse. This indicated that negative selection is mediated by thymic OVA expression.<sup>98</sup> In contrast, OT-II thymocytes are not negatively selected in a wildtype thymus and emerge to the periphery. This experimental system allows the investigation of central tolerance to a known antigen and consequently the identification of autoreactive T cells that have escaped negative selection.

### **1.2.3 Thymus-independent T cell regeneration**

Early T cell competence following allogeneic HSCT is provided both by residual host T cells that have survived conditioning and by mature donor T cells present in the non T cell depleted (non-TCD) graft (Figure 2).<sup>27,101-106</sup> Donor-derived T cells are the major contributors to T cell competence in cases of high-intensity conditioning.<sup>107,108</sup> After use of RIC residual host T cells also play a prominent role in complementing early T cell immunity.<sup>10,109,110</sup> Under physiological conditions T cells either expand in response to stimulation by cognate antigen or undergo homeostatic proliferation in case of lymphopenia.<sup>111,112</sup> The diversity of the T cell pool generated through homeostatic peripheral expansion, largely depends on the diversity of the mature T cells that served as the source for expansion. Interactions with pathogens skew the repertoire because of oligoclonal expansion of pathogen-specific T cells, which may acquire a memory phenotype.<sup>113</sup> Thymus-independent T cell immunity is largely transient and characterised by clonal exhaustion of cells caused by extensive replication and increased sensitivity to apoptosis.<sup>27,106,114-116</sup> The transferred donor T

cells not only defend against post-HSCT infections, but also provide tumouricidal activity, which is termed graft-versus-tumour (GVT) effect,<sup>117</sup> and may cure malignancies in the context of allogeneic HSCT.<sup>118</sup> In the case of leukaemia, this phenomenon is referred to as the graft-versus-leukaemia (GVL) effect.<sup>119</sup> Donor T cells and histocompatibility differences between donor and host are pivotal for the GVT effect.<sup>120</sup> In MHC-mismatched transplantation settings, alloreactive donor T cells react against both MHC molecules and antigens presented by the MHC molecule. However, in MHC-matched settings genetic differences between donor and recipient are restricted to minor histocompatibility antigens (miHAs).<sup>120</sup> The epitopes that promote the GVT effect are also mostly expressed on normal, non-malignant host cells and promote a GVH reaction (see chapter 1.3).<sup>119</sup> However, unique tumour associated antigens and miHA specifically expressed in haematopoietic cells, such as HA-1 and HA-2, can serve as preferential targets of GVT responses without developing GVHD.<sup>121-125</sup> GVT and GVHD are thus tightly linked processes.

## 1.3 Graft-versus-host Disease

### 1.3.1 Clinical Features of Graft-versus-host Disease

The development of novel transplantation strategies has contributed to the expansion of indications for allogeneic HSCT. However, GVHD remains a major complication and limits the use of transplantation therapy.<sup>126</sup> GVHD manifests in an acute and/or chronic form. Acute GVHD is classified in a classic and a late-onset form according to the time when symptoms are visible.<sup>127</sup> Acute GVHD predominantly affects the skin (81% of patients), gastrointestinal tract (GI; 54%), and liver (50%) (Figures 5 and 6).<sup>126,128</sup>



**Figure 5. Acute GVHD of the skin (grade I).**  
Taken from *Ferrara et al., Lancet (2009)*<sup>126</sup>

The severity of acute GVHD depends on the extent of organ involvement and is graded as follows: grade I (mild); II (moderate); III (severe); and IV (very severe).<sup>129</sup> Five-year survival for grade III acute GVHD is 25%. Grade IV disease diminishes long-term survival to 5%.<sup>130</sup> The development of acute GVHD depends on several factors, including genetic differences between donor and host, donor's sex, and the stem cell source replete with donor T cells.<sup>131-134</sup> While the incidence of acute GVHD in patients receiving fully-matched sibling donor grafts varies from 35 to 45%,<sup>134</sup> recipients of one-antigen HLA-mismatched unrelated donor grafts have an incidence of acute GVHD occurrence of up to 60-80%.<sup>135</sup>

Chronic GVHD is the major cause for non-relapse death occurring late after allogeneic HSCT.<sup>136</sup> Additionally, its presence prolongs the need for immune suppressive therapy.<sup>14,137,138</sup> Two forms of chronic GVHD were defined; a classic type without features of acute GVHD and an overlap

syndrome with features of both, acute and chronic GVHD (Figure 6).<sup>127,139</sup> The overlap syndrome can arise in two different ways. Firstly, chronic GVHD occurs progressively, thus the acute form merges into chronic pathology. Secondly, chronic GVHD can appear quiescently, when fully resolved acute GVHD is followed by the chronic form. However, classic chronic GVHD is initiated *de novo*. The occurrence of chronic GVHD varies widely between 6-80%,<sup>136,140,141</sup> with a mortality of 30%.<sup>126</sup> Older recipient age and the presence of prior acute GVHD predispose to chronic GVHD.<sup>132,141,142</sup> Chronic GVHD is a multiorgan pathology that affects the skin, eyes, mouth, gut, liver, lungs, joints and genitourinary system, which results in organ failure and decreased survival.<sup>139,143-147</sup> According to the number and severity of organs involved, chronic GVHD is scored as mild, moderate or severe.<sup>139,148</sup>

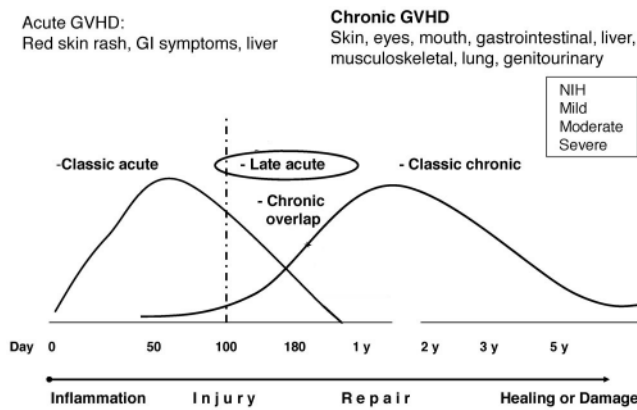


**Figure 6. GVHD classification.** Clinical manifestations determine whether the syndrome is considered as acute or chronic GVHD.

Adapted from Pavletic *et al.*, *Hematology (2012)*<sup>149</sup>

### 1.3.2 Pathophysiology of acute GVHD

The use of mouse models was crucial for the understanding of the pathophysiology of acute GVHD.<sup>150</sup> The development of acute GVHD can be summarised to occur in three sequential steps: 1) activation of host APCs; 2) activation, expansion and differentiation, and trafficking of donor T cells; and 3) target tissue destruction by cellular and inflammatory effectors (Figure 7).<sup>126</sup>



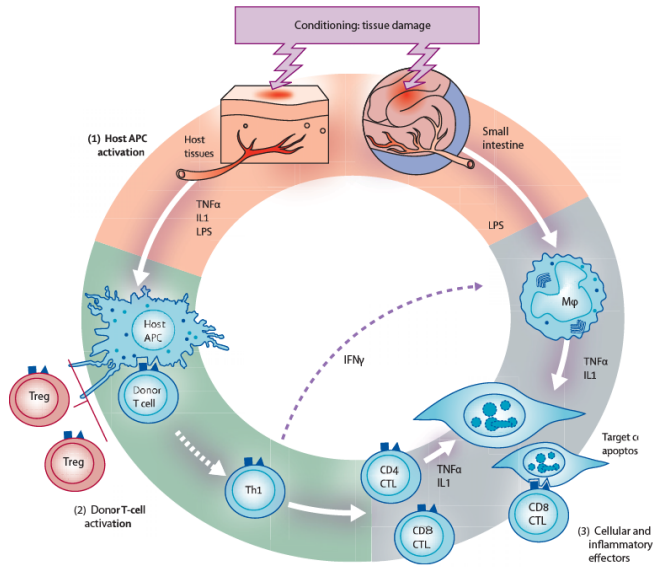


**Figure 7. Pathophysiology of acute GVHD.** The development of acute GVHD consists of three different phases: 1) Host APC activation; 2) Donor T cell activation; 3) Cellular and inflammatory effectors. Taken from Ferrara et al., *Lancet* (2009)<sup>126</sup>

Prior to transplantation, the underlying disease and cytoreductive conditioning cause damage to patient’s tissues. The latter respond to this damage with the secretion of “danger signals”, including proinflammatory cytokines, such as tumour necrosis factor- $\alpha$  (TNF- $\alpha$ ) and interleukins 1 and 6 (IL-1 and -6, respectively), and chemokines. Furthermore, expression of adhesion molecules, costimulatory molecules, and MHC antigens on host APCs is increased. Together, these danger signals result in the activation of host APCs.<sup>151-154</sup>

The central step of the GVH reaction is the second phase, in which donor T cells proliferate and differentiate upon recognition of signals from host APC.<sup>155,156</sup> Donor/host disparities in MHC class I initiate a CD8-driven GVHD response, while differences in MHC class II result in stimulation of CD4<sup>+</sup> T cells.<sup>157</sup> However, recipients of HLA-identical grafts can still develop acute GVHD mediated by both CD4<sup>+</sup> and CD8<sup>+</sup> T cells because of genetic disparities outside of the MHC loci referred to as minor histocompatibility antigens (miHA).<sup>158,159</sup> The combination of signals mediated by antigen-specific receptors and costimulatory molecules results in the activation of donor T cells and consequently their expression of cytokines. T-helper 1 (T<sub>H</sub>1) cytokines, which include interferon- $\gamma$  (IFN- $\gamma$ ), IL-2 and TNF- $\alpha$ , but also T<sub>H</sub>2 cytokines (IL-4, -5, -10, and -13), are extensively released during acute GVHD. A unique combination of chemokines expressed by host tissues that target receptors expressed on

donor T cells regulates the migration of alloreactive T cells from lymphoid tissues to specific target tissues. Once migrated to target tissues, alloreactive effector T cells can mediate tissue damage through both direct cytotoxicity and the recruitment of additional leukocytes, such as NK cells.<sup>152</sup>

The third phase of acute GVHD is a complex cascade of cellular mediators, such as cytotoxic T cells and NK cells, and soluble inflammatory agents, such as TNF- $\alpha$ , IFN- $\gamma$ , IL-1 and nitric oxide.<sup>126</sup> These molecules work synergetically to amplify local tissue injury and further promote inflammation and target tissue destruction. IFN- $\gamma$  has an ambivalent role in acute GVHD and can either enhance or reduce the disease.<sup>160,161</sup> But my lab has demonstrated a central role for IFN- $\gamma$  in thymic injury (see 1.3.7).<sup>162</sup>

### 1.3.3 Pathophysiology of chronic GVHD

In comparison to acute GVHD, the pathophysiology of chronic GVHD is less well understood. This restriction is due to a limited availability of suitable mouse models.<sup>147,150</sup> Four mechanisms may likely contribute to the development of chronic GVHD. Firstly, cytokines such as transforming growth factor- $\beta$  (TGF- $\beta$ ) may play a crucial role in chronic GVHD, since neutralisation of TGF- $\beta$  in experimental models ameliorated the manifestations of chronic GVHD.<sup>163</sup> Secondly, the role of B cells in the pathophysiology of chronic GVHD is supported by both experimental and clinical data. For example, experimental models showed that the development of a chronic GVHD syndrome with cutaneous sclerosis and glomerulonephritis phenotype is dependent on the presence of both, donor CD4 T and B cells.<sup>164</sup> Patients treated with a anti-CD20 antibody showed improvement of clinical symptoms of chronic GVHD, indicating a role for B cells.<sup>165</sup> Thirdly, a defect in the T<sub>reg</sub> population was associated with the development of chronic GVHD. Acute GVHD affects the development of T<sub>reg</sub> cells, which might be capable of preventing chronic GVHD.<sup>166</sup> Experimental data from different GVHD models showed that donor and host T<sub>reg</sub> cells were able to prevent or even reverse already existing GVHD.<sup>164,167,168</sup> Clinical data from chronic GVHD in humans are not consistent, but an association between low T<sub>reg</sub> levels and increased GVHD risk is likely.<sup>169-175</sup> Lastly, defective thymic negative selection has been

implicated in the development of chronic GVHD. Thymic damage caused by prior acute GVHD (discussed in more detail below) has been reported to impair negative selection of developing thymocytes in mice.<sup>176</sup> Evidence that the disruption in the thymic microenvironment plays a role for the typical autoimmune syndrome observed in chronic GVHD has been gained from experimental transplantation models. The *de novo* generation of autoreactive T cells from donor HSC is a hallmark of murine acute GVHD.<sup>177,178</sup> These autoreactive T cell clones can mediate the evolution from the acute to the chronic GVHD form.<sup>179-181</sup> Moreover, thymic damage in the course of acute GVHD has been connected to a severely altered TCR repertoire selection.<sup>180</sup> Taken together, the impairment of the T<sub>reg</sub> development and thymic negative selection provide two possibilities how acute GVHD can predispose to chronic GVHD. Since some studies<sup>182,183</sup> showed that chronic GVHD recipients do not necessarily have a defect in thymic negative selection, and that transplantation of healthy thymic tissue did not ameliorate chronic GVHD, thymus-independent pathways can also give rise to autoreactive T cells breaking the tolerance and mediating chronic GVHD. Supporting this notion, Zhao *et al.*<sup>183</sup> showed that autoimmune-like chronic GVHD can be induced in euthymic, T cell-deficient athymic, and thymectomised MHC-matched recipients by donor CD4<sup>+</sup> T cells. As a possible mechanism, mature donor CD4<sup>+</sup> T cells that are transferred in the donor stem cell graft show both, host and donor reactivity, and are activated and expanded by alloimmune response. This results in a skewed TCR repertoire that is able to mediate autoimmune manifestations in the absence of effective T-cell regulation.<sup>146</sup> After being activated, these donor T cells contribute to the development of autoimmune-like manifestations characteristic of chronic GVHD.<sup>183,184</sup> A crucial role for donor APCs in the evolution from alloreactivity to autoreactivity was suggested in this context.<sup>185</sup> In a first phase of GVHD, donor T cells recognise alloantigen presented on host APCs. However, these APCs are replaced by donor APCs, which present host alloantigen via the indirect pathway of allorecognition to donor T cells. During this transition, breaking of self-tolerance occurs and donor T cells acquire the ability to recognise both host and donor.

### 1.3.4 Prophylaxis and Treatment of GVHD

#### *Prevention of GVHD*

The primary strategy to prevent GVHD is to suppress the patient's immune competence.<sup>186</sup> Since T cells play a central role in initiating GVHD many clinical studies used T-cell depletion (TCD) in order to effectively prevent GVHD. TCD can be done either by negative selection of T cells *ex vivo*; by positive selection of CD34<sup>+</sup> stem cells *ex vivo*; and/or by antibodies targeting T cells *in vivo*.<sup>126</sup> Unfortunately, TCD is associated with high rates of graft failure, malignancy relapse, and opportunistic infections.<sup>8,187-189</sup> At present, no therapy or combination of therapies exist to effectively prevent clinical acute GVHD. The current standard prophylaxis of acute GVHD is a combination of immunophilin ligands, such as cyclosporine and tacrolimus, and/or antimetabolites, such as methotrexate.<sup>128</sup> Since both beneficial anti-tumour effects and deleterious anti-host effects responses are based on T-cell immunity, a generalised immunosuppression will inhibit both effects equally. The separation of GVT and GVH responses is hence a major challenge to transplant immunologists. The use of RIC results in diminished conditioning-caused tissue damage and consequently the secretion of inflammatory cytokines is decreased. This could explain the reduced frequency of severe acute GVHD after RIC compared to full myeloablative conditioning.<sup>190-193</sup> Current approaches to prevent chronic GVHD are strategies to deplete donor T cells before HSCT. The efficacy of this approach is low and the overall survival is not increased, however, clinical studies suggest the use of *in vivo* T-cell depletion to prevent chronic GVHD.<sup>194,195</sup>

#### *Treatment of GVHD*

Despite preventive efforts, GVHD develops in a large number of patients and treatment is required. The gold standard for acute GVHD treatment are steroids, which have potent anti-lymphocyte and anti-inflammatory activity.<sup>126,128,186</sup> However, to treat steroid-refractory acute GVHD other therapy options need to be available, including antilymphocyte antibody, infusion of mesenchymal stromal cells,

extracorporeal photopheresis or the blockade of the inflammatory cytokine TNF- $\alpha$ .<sup>126,128</sup> To control acute GVHD, often multiple agents are used in combination. Still, treatment responses remain incomplete and complications occur frequently, which puts the patient at risk of morbidity and mortality. Chronic GVHD is treated with a variety of immunosuppressive drugs. The treatment response varies dramatically not only among patients, but also among the patient's different organs, which makes chronic GVHD difficult to treat. Prolonged treatment with steroids is highly toxic and predisposes the patient to higher risk for infections.<sup>126,196</sup>

### **1.3.5 Post-transplant immune deficiency**

Post-transplant immune reconstitution is affected by several factors including advanced age of the patient, type of preparative conditioning regimen, use of TCD stem cell grafts, genetic differences between donor and host, presence of GVHD, and immunosuppressive drugs in order to prevent or treat GVHD. GVHD impacts on the restoration of the patient's immune competence in two separate ways; firstly, GVHD directly affects the thymus,<sup>197,198</sup> and secondly, treatment of GVHD with immunosuppressive drugs impairs immune reconstitution.<sup>199-204</sup>

### **1.3.6 Immune reconstitution in the presence of acute GVHD**

The presence of acute GVHD has been inversely associated with the capacity to reconstitute immune competence. In both patients with and without acute GVHD immune competence drops post-transplantation. At one year post-transplantation total T cell counts are only slightly higher in patients without acute GVHD compared to patients suffering from acute GVHD. However, the reconstitution of naïve CD4<sup>+</sup> T cells (CD45RA<sup>+</sup>CD62L<sup>+</sup>) is significantly delayed in patients suffering from acute GVHD (Figure 8).<sup>197,205-207</sup>

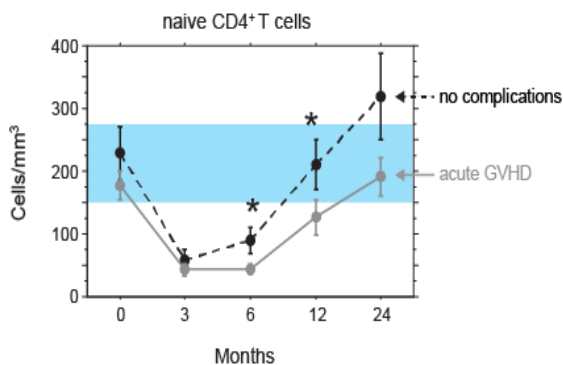


**Figure 8. Acute GVHD delays reconstitution of naïve CD4<sup>+</sup> T cells.** Without complications, normal numbers of naïve CD4<sup>+</sup> T cells are reached between 12 and 24 months post-transplantation. In the presence of acute GVHD, this reconstitution process is slowed down. (blue shading indicates the normal range for naïve peripheral CD4<sup>+</sup> T cells)

Adapted from *Clave et al., Blood (2009)*<sup>197</sup>

In addition to the total cellularity, the quality of the TCR repertoire is also affected. The generation of a polyclonal repertoire is restricted in the presence of acute GVHD and takes longer than the usual 1-2 years in patients without complications.<sup>197</sup> Since the thymus is essential for the generation of a naïve polyclonal T cell pool, these data argue for a defect in thymus-dependent T cell development.

### 1.3.7 Thymic GVHD

Morphological changes in the lymphoid and epithelial components of the thymus have been observed in transplanted patients more than 30 years ago, which led to the identification of the thymus as a target of GVHD.<sup>208-211</sup> The histological features of thymic dysplasia caused by acute GVHD include the depletion of cortical and medullary thymocytes, changes in number and composition of the different TEC subpopulations, disappearance of the corticomedullary demarcation, phagocytosis of cellular debris, and the elimination of Hassall's bodies.<sup>212</sup> In parallel to the destruction of the thymic architecture, deficits in thymopoiesis are observed. This results in a distorted TCR repertoire and lower thymic output in comparison to healthy controls.<sup>197,205,206,213-215</sup>

#### *Pathomechanism of Thymic Injury – Preclinical Mouse Models*

Preclinical mouse models of allogeneic HSCT can provide insight into the pathophysiology of thymic GVHD. Thymic dysplasia induced in

experimental mouse models resembles the typical features observed in human thymic GVHD (see above).<sup>162,178,216,217</sup> The impact of radiation and chemotherapy on thymic structure and function are well described.<sup>218</sup> However, the mechanisms by which an alloreaction causes thymic injury are still incompletely understood. To investigate the effect of acute GVHD on thymic structure and function independently of conditioning, experimental transplantation models that do not necessitate radiation are required. In a haploidentical transplantation model, parental T cells (for example: C57BL/6; H-2<sup>b</sup>) are infused into a F<sub>1</sub> strain (for example: BDF1; H-2<sup>bd</sup>). Since host immune cells recognise the donor T cells as “self” (in the example given they share the b haplotype), there is no risk of graft rejection and pre-conditioning can be omitted. Donor T cells react in turn against the other parental alloantigens presented on host cells (in the example provided H-2<sup>d</sup>), which leads to the destruction of thymic tissue in addition to tissue injury of typical GVHD target organs.<sup>162</sup> In this system, the reduced thymic cellularity in the context of acute GVHD is primarily a consequence of the depletion of the most abundant DP thymocyte population. There are two independent mechanisms that contribute to this defect. Under physiological conditions, cell numbers of the most immature thymocytes increase 20- to 50-fold during progression of TN to DP thymocytes.<sup>219,220</sup> However, in the presence of acute GVHD the proliferation of TN thymocytes is impaired, resulting in an elevated frequency of stage I TN thymocytes compared to stage III TN thymocytes.<sup>221</sup> Hence, acute GVHD causes a failure of survival and further maturation of thymocytes to the DP stage. The second mechanism that accounts for the profound loss of the DP population is the increased apoptosis of DP thymocytes themselves.<sup>222</sup> As an underlying mechanism, alloreactive donor T cells target the host thymic microenvironment, thereby indirectly causing impairments in thymopoiesis and thymic output.<sup>162,212</sup> Donor T cells infiltrate the recipient’s thymus in the absence of pre-conditioning and their number corresponds to the degree of the defect in thymopoiesis.<sup>221</sup> Recent detailed analysis of the thymic stromal network in the course of acute GVHD revealed that TEC undergo apoptosis in response to IFN- $\gamma$  secreted by donor T cells (Figure 9).<sup>162,223-225</sup> IFN- $\gamma$  activates STAT1 and consequently initiates apoptosis in TEC.<sup>162</sup> These data suggest that TEC are competent to directly prime naïve allogeneic donor T cells.<sup>162</sup> The approach of depletion of host APCs would

therefore not be sufficient to protect the recipient from TEC injury caused by alloreactive T cells.

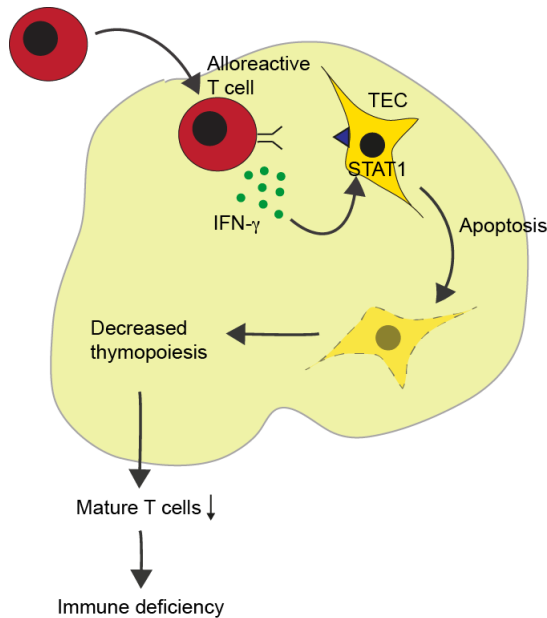


**Figure 9. Alloreactive T cells cause TEC injury in acute GVHD.** Alloreactive T cells present in the donor graft infiltrate the host's thymus (1) where they recognise alloantigens presented by TEC. This results in their activation and secretion of IFN- $\gamma$  (2), which in turn upregulates STAT1 in TEC. Upregulation of STAT1 in TEC leads to an apoptotic programme and consequently TEC death (3). The loss of TEC results in a defective support of T cell development and therefore decreased thymopoiesis (4). Consequently, less mature T cells emerge to the periphery and post-HSCT immune deficiency arises (5).

Adapted from Weinberg KL, *Blood* (2007)<sup>226</sup>

### ***Thymic dysfunction during acute GVHD – a link to chronic GVHD?***

A hypothesis can be formulated that impairment of TEC function in early acute GVHD, and consequently the impaired TCR selection, provide an etiological link between alloreactivity of acute GVHD and the autoimmunity features observed in chronic GVHD. Hence, measures that protect, repair, and enhance TEC function may become the focus of future treatment strategies to prevent thymic acute GVHD and consequently post-transplantation immune deficiency and autoimmunity.



### 1.3.8 Strategies to Improve post-transplant Immune Deficiency

Since thymic injury in the course of acute GVHD contributes to deficits in post-transplantation T-cell regeneration, strategies that seek to boost thymic function hold promise for ameliorating immune deficiency following allogeneic HSCT. Interventions may include therapies that act directly on TEC in order to increase their numbers, and consequently, to enlarge the availability of developmental niches within the thymic stromal network.<sup>227</sup> Various concepts to stimulate thymus function have been proposed that include for example growth hormone or androgen blockage, interference with signalling pathways as for example p53 inhibition and stimulation of Flt3 signalling, and exogenous administration of cytokines and growth factors such as IL-7, IL-22, and fibroblast growth factor-7 (Fgf7).<sup>227</sup> Since my studies dealt with Fgf7, I focus here on this epithelial growth factor.

#### *Fibroblast growth factor-7*

Fibroblast growth factor-7 (Fgf7; also known as keratinocyte growth factor, KGF; Palifermin, Kevivance®) is an epithelial growth factor that belongs to the family of fibroblast growth factors.<sup>228</sup> Palifermin, which is a recombinant human Fgf7, is currently an approved drug for the prevention of oral mucositis in patients undergoing HSCT.<sup>229-231</sup> Fgf7 induces differentiation and proliferation in a variety of epithelial cell tissues via binding and activation of its receptor Fgfr2IIIb, which is a splice variant of the Fgf receptor 2.<sup>232</sup> This receptor is expressed on several epithelial tissues in the intestine, skin, lung, liver, and thymus.<sup>233</sup> Within the thymus, Fgfr2IIIb is expressed on TEC,<sup>216</sup> but not on haematopoietic cells.<sup>234</sup> In the thymus, Fgf7 is endogenously produced by mesenchymal cells and by mature thymocytes of the  $\alpha\beta$ -lineage.<sup>235,236</sup> Experimental studies with mice deficient for Fgfr2IIIb revealed an important role for Fgf7 during thymus organogenesis.<sup>236-238</sup> The fact that thymic Fgf7 production is sustained throughout life and Fgfr2IIIb is expressed on both immature and mature TEC argues for a continued requirement of Fgf7 by the postnatal thymic stromal compartment.<sup>239,240</sup> Fgf7 has the capacity to correct thymus

senescence<sup>241</sup> and to repair thymus injury caused by irradiation.<sup>240</sup> Exogenous postnatal administration of Fgf7 results in enhanced proliferation of the TEC compartment and consequently in increased thymopoiesis (Figure 10).<sup>239</sup>

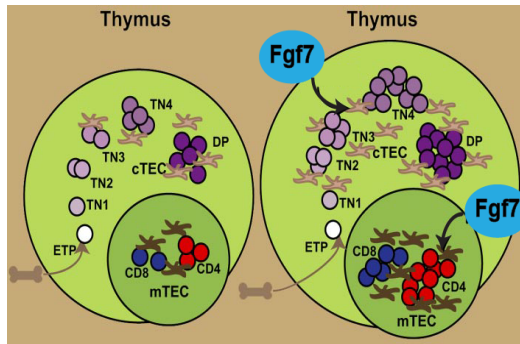


**Figure 10. Fgf7 increases thymic size and cellularity.** Fgf7 administration directly acts on TEC and increases the number of both cortical and medullary TEC. As a consequence, enlarged TEC compartment boosts thymopoiesis, which results in an increase in CD4<sup>+</sup>CD8<sup>+</sup> DP and mature CD4<sup>+</sup> and CD8<sup>+</sup> SP T cells. Adapted from *Chu et al., Blood (2007)*<sup>242</sup>

Moreover, the increased thymopoiesis correlates with enhanced thymic export. Applied in experimental mouse models of acute GVHD, Fgf7 preserved normal function and architecture of the TEC subpopulations.<sup>216</sup> Importantly, regular T cell development is supported despite the presence of alloreactive donor T cells. Moreover, thymus protection by Fgf7 prevents the emergence of self-reactive T cells from the thymus to the periphery,<sup>180</sup> and promotes faster immune recovery following transplantation.<sup>243</sup> These data indicate that early Fgf7 administration corrects thymic injury caused by acute GVHD, and therefore supports and boosts normal thymic T cell development and output. Nevertheless, Fgf7's impact on the immune reconstitution in humans following allogeneic HSCT has not been established yet and further studies are needed.

## **2. HYPOTHESES AND AIM OF THE THESIS**

The overall hypothesis underlying this thesis postulates that GVHD-mediated injury to the thymus, in particular to the thymic epithelial cell compartment, is a major limitation responsible for defective T-cell immune reconstitution after allogeneic HSCT. This defect results in adverse effects as diverse as post-transplantation immune deficiency and autoimmunity.

The aim of the present study was to address whether altered TEC function as a consequence of acute GVHD is causative for the autoimmune syndrome typically seen in chronic GVHD. To address this question, I have tested several specific hypotheses: 1) acute GVHD causes a loss of mTEC number and integrity, 2) impairment of the mTEC compartment alters intrathymic ectopic self-antigen expression which is required for normal central tolerance induction, 3) lack of appropriate thymic negative selection causes autoreactive T cells to emerge during acute GVHD, and 4) TEC cytoprotection consequently allows normal mTEC function.

## 3. MATERIALS AND METHODS

### 3.1 Mice

Female C57BL/6 (B6; H-2<sup>b</sup>), (C57BL/6xDBA/2)F<sub>1</sub> (BDF<sub>1</sub>; H-2<sup>bd</sup>), Balb/c (H-2<sup>d</sup>), CBy.PL(B6)-Thy1<sup>a</sup>/ScrJ (Balb/c-Thy1.1; H-2<sup>d</sup>), 129/Sv (H-2<sup>b</sup>), B6.SJL-Ptprc<sup>a</sup>Pep3<sup>b</sup>/BoyJ (B6.CD45.1; H-2<sup>b</sup>) and C57BL/6-Tg(Ins2-TFRC/OVA)296Wehi/WehiJ (RIP-mOVA; H-2<sup>b</sup>) mice were kept in accordance with federal regulations. B6.OT-II-Rag2<sup>-/-</sup>CD45.1 mice (OT-II.CD45.1; H-2<sup>b</sup>) were bred at Benaroya Research Institute at Virginia Mason, Seattle, USA.

### 3.2 BMT and GVHD induction

Thymic acute GVHD was induced in unirradiated or total body irradiated (TBI) recipients. In an unconditioned haploidentical allo-HSCT model, acute GVHD was induced in 8-week old non-irradiated BDF<sub>1</sub> (H-2<sup>bd</sup>) mice by i.v. injection of 15x10<sup>6</sup> B6.CD45.1 (CD45.1<sup>+</sup>; H-2<sup>b</sup>) splenic T-cells as described.<sup>162,225</sup> As controls, 15x10<sup>6</sup> syngeneic BDF<sub>1</sub> splenic T-cells were infused into syngeneic recipients which were age-matched with recipients of allogeneic donor cells. The same haploidentical transplantation model was studied following myeloablative conditioning. Acute GVHD (*b*→*bd*) was induced in 8-week old lethally irradiated BDF<sub>1</sub> mice (1000 cGy) by i.v. co-injection of 2.5x10<sup>6</sup> B6.CD45.2 splenic T-cells and 5x10<sup>6</sup> B6.CD45.1 T-cell depleted (TCD) bone marrow cells. As controls without disease, recipients of 5x10<sup>6</sup> B6.CD45.1 TCD bone marrow cells alone were used. In a fully MHC-disparate transplantation model, acute GVHD (*d*→*b*) was induced in 9-week old lethally irradiated B6 mice (975 cGy) by i.v. co-injection of 3x10<sup>6</sup> Balb/c-Thy1a (H-2<sup>d</sup>) splenic T-cells and 5x10<sup>6</sup> Balb/c TCD bone marrow cells. As controls without disease, recipients of 5x10<sup>6</sup> Balb/c TCD bone marrow cells were used. In a MHC-matched, minor histocompatibility antigen-mismatched transplantation model, acute GVHD (*b*→*b*) was induced in 8-week old lethally irradiated B6 mice (1000 cGy) by i.v. co-injection of 4x10<sup>6</sup> splenic T-cells and 7x10<sup>6</sup> TCD bone marrow cells from 129/Sv (H-2<sup>b</sup>) donors. As controls without disease, recipients of 7x10<sup>6</sup> TCD

bone marrow cells were used. To induce thymic acute GVHD into RIP-mOVA mice, Balb/c T cells ( $3 \times 10^6$ ) isolated from the spleen were transplanted into total body irradiated (TBI)-fully MHC-mismatched RIP-mOVA recipients ( $H-2^d \rightarrow H-2^b$ ). Control mice (no GVHD) received T-cell depleted Balb/c-Thy1.1 bone marrow ( $10 \times 10^6$ ) only. Four weeks after generation of [Balb/c  $\rightarrow$  RIP-mOVA] chimeras (GVHD<sup>-</sup> or GVHD<sup>+</sup>), recipients were reirradiated and transplanted with T-cell depleted OT-II bone marrow ( $5 \times 10^6$  TCDBM; CD45.1) mixed with B6 TCDBM ( $15 \times 10^6$ ; CD45.2). OVA-specific T cells stemming from the OT-II BM were analysed 4-6 weeks after the 2<sup>nd</sup> HSCT in the thymus and periphery (spleen and lymph nodes). These OVA-specific T cells were defined as CD4<sup>+</sup>, CD45.1<sup>+</sup>, V $\alpha$ 2<sup>+</sup>, V $\beta$ 5<sup>+</sup>.

### 3.3 Fgf7 treatment

Recombinant human Fgf7 (palifermin, Kepivance<sup>®</sup>, Biovitrum, Sweden) was injected i.p. from day -3 to day +3 after allogeneic HSCT at a dose of 5 mg/kg/day.<sup>216,225,239</sup>

### 3.4 Flow cytometry reagents

For six- and seven colour flow cytometric analyses, the moAbs directed against the following murine proteins were used: CD4 (clone RM4-5 and GK1.5), CD8 (53-6.7), CD45.1 (A20), CD45 (30-F11), CD90.1 (19E12), I-A<sup>b</sup> (AF6-120.1), I-A/I-E pan MHCII (clone M5/114.15.2), Ly51 (6C3/BP-1, clone 6C3), H-2K<sup>b</sup> (AF6-88.5), H-2K<sup>d</sup> (SF1-1.1), Va2 (B20.1), TCR $\beta$  (H57-597), H-2K<sup>b</sup> (25-D1.16), CD44 (IM7), CD73 (TY/11.8), FR4 (eBio12A5), Foxp3 (FJK-16s) and 5'-bromo-2'-deoxyuridine (BrdU, clone 3D4; Mouse Anti-BrdU Set). These reagents were obtained from BD Biosciences Pharmingen (San Diego, CA) or eBioscience (San Diego, CA). The moAbs against EpCam (CD326; clone G8.8),<sup>62</sup> and Aire (clone 5H12) were obtained from The Developmental Studies Hybridoma Bank (University of Iowa, IA) and Dr. H. Scott (Melbourne, Australia),<sup>77</sup> respectively. UEA1 lectin was purchased from Vector Laboratories (Burlingame, CA, USA) and 7-amino-actinomycin D (7-AAD) was obtained

from BD Biosciences. Primary moAbs were conjugated to either biotin, fluorescein isothiocyanate (FITC), phycoerythrin (PE), cyanin 5 (Cy5), allophycocyanin (APC), Alexa Fluor®700 or the tandem dyes PECy5, PECy7, PerCPCy5.5, APCCy7 (BD Biosciences, eBioscience, BioLegend, San Diego, CA). Biotin-conjugated primary moAbs were detected using secondary anti-rat polyclonal antibodies conjugated to streptavidin/APCCy7 or streptavidin/PerCPCy5.5 (BioLegend, San Diego, CA).

### **3.5 Analysis of the mTEC<sup>high</sup> compartment by flow cytometry**

Thymi were isolated at the indicated time points after transplantation and enzymatically digested with collagenase/dispase/DNAse I (Roche Diagnostics, Switzerland). For RNA isolation and detection of Aire expression in mTEC, the enzymatic digests were incubated with biotin-conjugated EpCam (G8.8) followed by anti-biotin magnetic microbeads (Miltenyi Biotec, Bergisch Gladbach, Germany) and enrichment of EpCam<sup>+</sup> stromal cells by positive selection on an AutoMACS Pro (Miltenyi). For analysis of BrdU incorporation, mice were either injected intraperitoneally (i.p.) twice with 1mg BrdU 16 and 8 hours prior to analysis, or were fed from day -3 to 3 after HSCT with drinking water supplemented with 0.8mg/ml BrdU. The first method aims to analyse cell cycle during a short time window, whereas the latter provides information about the kinetics of cell proliferation.<sup>244</sup> For both BrdU analysis methods the enzymatic digests were incubated with anti-CD45 magnetic microbeads (Miltenyi) followed by depletion via negative selection of CD45<sup>+</sup> cells. Depending on the experimental goal, enriched cell preparations were stained with different combinations of primary moAbs against surface and intracellular proteins and the lectin UEA1. Prior to intracellular staining, cells were fixed and permeabilised using the BD Cytotfix/Cytoperm Fixation/Permeabilization Kit (BD Bioscience) according to the manufacture's guidelines. For intracellular Foxp3 staining, cells were fixed and permeabilised using the Foxp3/Transcription Factor Staining Buffer Set (eBioscience) according to the manufacture's instructions. Non-fixed labelled cells were stained with DAPI; (4',6-

Diamidine-2'-phenylindole dihydrochloride; Roche Diagnostics, Switzerland) and were analysed or sort purified using a FACSAria® flow cytometer (Becton Dickinson, Mountain View, CA) and FACSDiva (Becton Dickinson) and FlowJo software (Tree Star Inc, Ashland, OR). MHC class II<sup>low</sup> and class II<sup>high</sup> mTEC were defined as DAPI<sup>-</sup>CD45<sup>-</sup>EpCam<sup>+</sup>Ly51<sup>-</sup>UEA1<sup>+</sup>MHCII<sup>low/int</sup> and MHCII<sup>high</sup> cells, respectively (Table 1). For the purpose of RNA isolation, non-fixed viable (DAPI<sup>-</sup>) cells were sorted on ice to a purity of >99% and immediately processed. To analyse cell proliferation, cells were also treated with DNase I (Sigma, St. Louis, USA) followed by BrdU staining and re-staining of tandem dyes.

### 3.6 Immunofluorescence confocal microscopy

For analysis of Aire expression in TEC, thymi were isolated at 2, 4 and 7 weeks after transplantation (which corresponded to recipient ages of 10, 12 and 15 weeks) and frozen in OCT. Sections (8 µm) were cut on a cryostat, dried and fixed with acetone (-20°C). Primary antibodies were biotin-conjugated cytokeratin (CK)-18 (Ks18.04, Progene GmbH, Heidelberg, Germany), CK14 (rabbit) (Covance, Princeton, NJ, USA), and Aire/Cy5 (5H12, provided by H. Scott, Adelaide, Australia). Secondary reagents were streptavidin/Cy3 (BioLegend) and goat anti-rabbit IgG A488 (Invitrogen). Sections were stained with DAPI and mounted with hydromount. All images were captured on a Zeiss LSM 510 Meta Laser Scanning Confocal Microscope system (Carl-Zeiss AG, Feldbach, Switzerland). Isotype controls were used in all experiments. Images were acquired with a 20x Plan-Neofluar air objective with NA 0.5 at room temperature. The microscope used photomultiplier tubes (PMT) for detection. Overlays of blue (Cy5), red (Cy3), and green (Alexa488) stainings were coloured by computer-assisted management of confocal microscopy data generated with Zeiss LSM 510 software version 3.2. Image analysis was done using the software ImageJ (<http://imagej.nih.gov/ij>).

### 3.7 Quantitative PCR

RNA was isolated from sorted mTEC<sup>high</sup> using the RNeasy Micro Kit (Qiagen, Switzerland) according to the manufacturer's protocol. RNA was transcribed into cDNA with the SuperScript III Reverse Transcriptase (Invitrogen) according to the manufacturer's instructions. Real-time PCR was performed on a Rotor-Gene 3000A (Qiagen) using SensiMix SYBR Kit (Bioline, London, United Kingdom) for quantitative expression analyses.

Primer sequences were:

EpCam:

forward, 5'-TGAGGACCTACTGGATCATC;

reverse, 5'-TATCGAGATGTGAACGCCTC;

Foxn1:

forward, 5'-TCTACAATTTTCATGACGGAGCACT;

reverse, 5'-TCCACCTTCTCAAAGCACTTGTT;

GAPDH:

forward, 5'-GGTGAAGGTCGGTGTGAACG;

reverse, 5'-ACCATGTAGTTGAGGTCAATGAAGG;

salivary protein 1 (Spt1):

forward, 5'-GGCTCTGAAACTCAGGCAGA;

reverse, 5'-TGCAAACCTCATCCACGTTGT;

major urinary protein 1 (Mup1):

forward, 5'-CTATCCAATGCCAATCGCTG;

reverse, 5'-GATAGGAAGGGATGATGGTGG;

casein  $\gamma$  (Csn1s2a):

forward, 5'-ATTACACCTTCCCAAATGCT;

reverse, 5'-CAGTTAATACGGCTCCACAG;

Ovalbumin (OVA):

forward, 5'-TGCCTTTCAGAGTGACTGAG;

reverse, 5'-GAAGCCATTGATGCCACTC;

autoimmune regulator (Aire):

forward, 5'-TGTGCCACGACGGAGGTGAG;

reverse, 5'-GGTTCTGTTGGACTCTGCCCTG



### 3.8 DNA microarray analysis

To determine gene expression profiles in mTEC<sup>high</sup> cells, biotin-labelled and fragmented cRNA from sorted cells was hybridized to DNA microarrays (Affymetrix Mouse Expression Set MOE430A). MIAME compliant microarray data was generated by analysis of triplicates for each of the experimental conditions which included syngeneic (*bd*→*bd*) and allogeneic (*b*→*bd*) transplantation with or without Fgf7 treatment. RNA from sorted mTEC<sup>high</sup> (approximately 1000-3000 cells per sample) was isolated on 2, 4 and 7 weeks after transplantation using the RNeasy Micro Kit (Qiagen, Switzerland) according to the manufacturer's protocol. High quality RNA was confirmed with the Experion RNA HighSens Analysis Kit (Bio-Rad, Reinach, Switzerland). cRNA target synthesis was done starting from a minimum of 1.16 ng total RNA using the Ovation Pico WTA System (NuGEN Technologies, The Netherlands) following standard recommendations. Following second reverse transcription, fragmentation and labelling of amplified cDNA were performed using the WT Terminal Labelling Kit (Affymetrix, Santa Clara, CA). Synthesis reactions were carried out using a PCR machine (TProfessional, Biometra, Goettingen, Germany). DNA was loaded on Mouse Gene 1.0 ST Array (Affymetrix), hybridised for 17 hours, washed and stained using Affymetrix protocol FS450\_0007. The GeneChips were processed with an Affymetrix GeneChip Scanner 3000 7G. DAT images and CEL files of the microarrays were generated using Affymetrix GeneChip Command Control 3.0.0.1214. Data quality controls were led using Expression console 1.1 (Affymetrix). Affymetrix CEL files were normalised<sup>245</sup> and data were log<sub>2</sub>-transformed using Partek<sup>®</sup> Genomics Suite v.6 software (Partek Inc, St. Louis, MO). To select differently expressed genes a one-way ANOVA model was applied. Genes were filtered on the basis of an adjusted p-value lower than 0.01. Microarray data of triplicate samples of pure mTEC<sup>high</sup> preparations are available under accession number E-MEXP-3745 at <http://www.ebi.ac.uk/arrayexpress>.

### 3.9 Bioinformatics

Bioinformatics was done using R software (R Foundation for Statistical Computing, Vienna, Austria, <http://www-r-project.org>). Gene expression data from the public databases Mouse GNF1M and MOE430 Gene Atlases (<http://biogps.org>) were taken as a starting point for the identification of TRA among the total number of transcripts expressed in mTEC<sup>high</sup> cells. Using data from the GEO platform ([www.ncbi.nlm.nih.gov/geo](http://www.ncbi.nlm.nih.gov/geo), GEO series accession number GSE85) and the literature,<sup>64,70,72</sup> genes were annotated as ubiquitously expressed genes (Ub) and TRA, respectively. We initially used the same algorithm for Aire-dependent and independent TRA as previously described.<sup>64,70</sup> Briefly, transcripts with expression in <5 different tissues in combination with a lower threshold of 5-fold signal intensity of the average of all tissues were designated as tissue restricted. The annotated gene lists were further curated by incorporating recent sequencing data generated from thymic epithelial subpopulations (data not shown). Transcripts whose expression levels increased or decreased greater than three-fold in relation to the control group (corresponding to relative expression values of <0.33 and >3.0, respectively) were considered to be altered in consequence of acute GVHD. To test hypothesis of transcript distribution, O/E analyses were performed. In this ratio, O is the observed number of events, and E is the expected number of events.<sup>246</sup> Using hypergeometric statistical analysis, the accuracy of the O/E ratio was tested. Pearson's correlation coefficient (Pearson's r) was calculated including only 50% of the genes that had a inter quartile range (IQR) higher than the median of the IQR values of all genes. IQR is a measure of statistical dispersion. Tissue representation of TRA was analysed using the public databases Mouse GNF1M and MOE430 Gene Atlases (<http://biogps.org>). For display of heatmaps, signal intensities ( $\log_2$ ) were colour coded and plotted for selected genes.

### **3.10 Statistical analysis**

All values are depicted as mean  $\pm$  SD. The nonparametric unpaired Mann-Whitney U test was used for two-group comparisons, whereas for multiple group comparisons Kruskal-Wallis one-way ANOVA with Dunn's post test was performed using GraphPad Prism version 6 for Mac OS X (GraphPad Software, San Diego California USA, *www.graphpad.com*).

## 4. RESULTS

### 4.1 Impaired ectopic expression of tissue-restricted antigens in the thymus during murine acute GVHD

#### 4.1.1 Identification and characterisation of medullary thymic epithelial cell subsets by flow cytometry

Advances in the understanding of thymic epithelial cell (TEC) biology have allowed for a more precise identification of the terminally differentiated, postcycling medullary TEC (mTEC) that are responsible for central tolerance induction. This EpCam<sup>+</sup>UEA1<sup>+</sup> cell subset is distinguished from other immature or mature epithelial subsets in the thymic cortex and medulla by its expression of Aire, lack of Ly51 surface protein and its high surface density of MHC class II (mTEC<sup>high</sup> cells) (Figure 11, Table 1).<sup>56,57,62-66</sup>

| Marker | Phenotype           |                      |
|--------|---------------------|----------------------|
|        | mTEC <sup>low</sup> | mTEC <sup>high</sup> |
| DAPI   | -                   | -                    |
| CD45   | -                   | -                    |
| EpCam  | +                   | +                    |
| UEA-1  | +                   | +                    |
| Ly51   | -                   | -                    |
| MHCII  | + / +++             | +++                  |
| Aire   | -                   | - / +                |

**Table 1. Surface markers to identify TEC subsets.** Depending on the experimental goal, thymic cell preparations were stained with different combinations of primary moAbs against surface and intracellular proteins and the lectin UEA-1

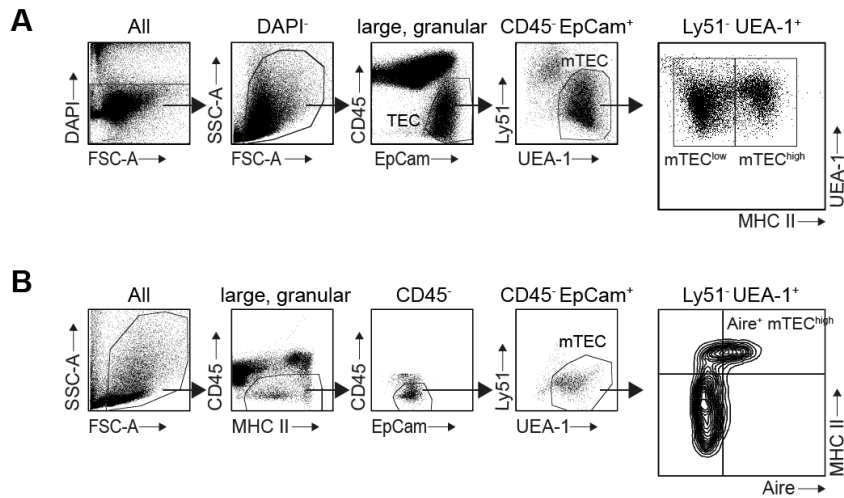


**Figure 11. Identification and characterisation of medullary thymic epithelial cell subsets by flow cytometry.** I used a modified isolation method for thymic stromal cells which preferentially enriched for medullary thymic epithelial cells (mTEC).<sup>67</sup> (A) Gating strategy for mTEC<sup>high</sup> cells. The flow cytometry plot on the far right shows the mature MHC class II<sup>high</sup> and the immature MHC class II<sup>low</sup> mTEC subpopulations as cells with CD45<sup>-</sup>EpCam<sup>+</sup>Ly51<sup>-</sup>UEA-1<sup>+</sup>MHCII<sup>high</sup> and MHCII<sup>low/int</sup> phenotypes, respectively. (B) Gating strategy for identification of postcycling mTEC that are responsible for central tolerance induction and express Aire. The flow cytometry plot on the far right shows intracellular Aire staining of CD45<sup>-</sup>EpCam<sup>+</sup>Ly51<sup>-</sup>UEA-1<sup>+</sup> mTEC. Doublet discrimination was applied in all flow cytometry analyses.

#### 4.1.2 Induction of thymic acute GVHD

To study the effect of acute GVHD on mTEC number and function, I used four different murine models of lethal acute GVHD with or without pre-transplantation conditioning. Firstly, to investigate thymic acute GVHD independently of total body irradiation or other preconditioning regimens, I employed a haploidentical transplantation model (Figure 12A). In this model, acute GVHD was induced in 8-week old non-irradiated BDF<sub>1</sub> (H-2<sup>bd</sup>) mice by i.v. injection of 15x10<sup>6</sup> B6.CD45.1 (CD45.1<sup>+</sup>; H-2<sup>b</sup>) splenic T cells (designated as B6→BDF<sub>1</sub> group, *b*→*bd*) as described.<sup>225</sup> BDF<sub>1</sub> recipients injected with 15x10<sup>6</sup> BDF<sub>1</sub> splenic T cells served as syngeneic controls (BDF<sub>1</sub>→BDF<sub>1</sub> group, *bd*→*bd*).

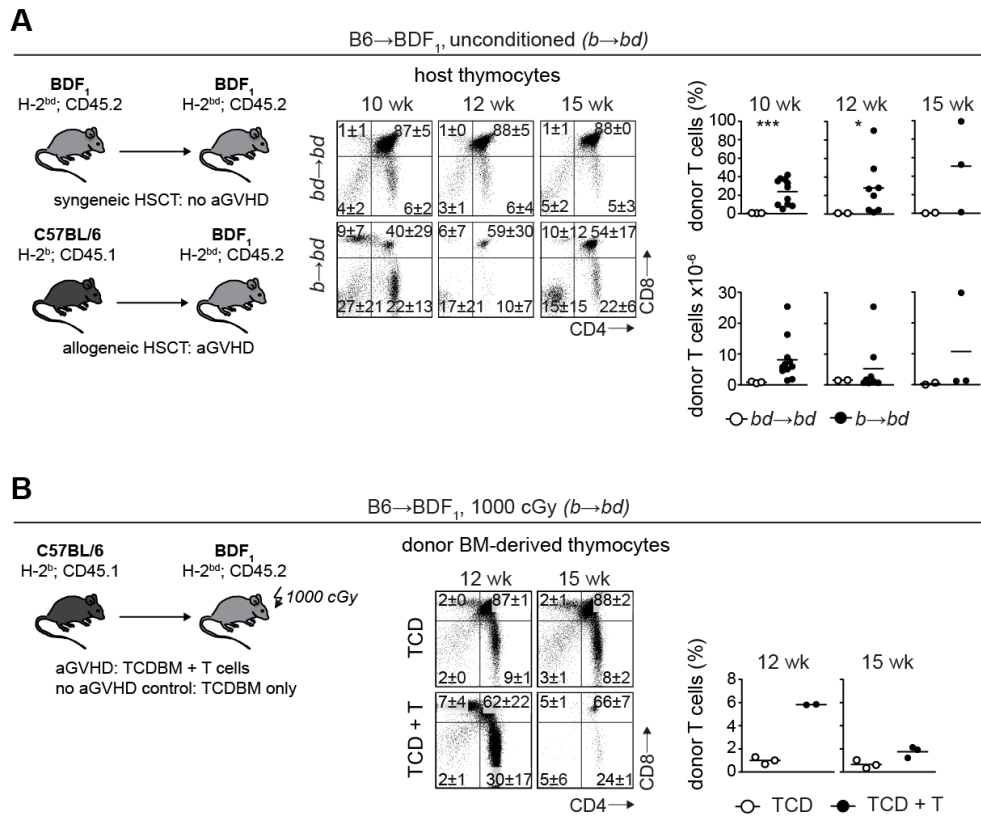


**Figure 12. Induction of thymic acute GVHD in two haploidentical HSCT models.** (A) In an unconditioned haploidentical allogeneic HSCT model, acute GVHD was induced in 8-week old non-irradiated BDF<sub>1</sub> (H-2<sup>bd</sup>) mice using B6.CD45.1 (CD45.1<sup>+</sup>; H-2<sup>b</sup>) as donors (B6→BDF<sub>1</sub> group; *b*→*bd*, ●). As controls, BDF<sub>1</sub> mice were transplanted with syngeneic donor cells (BDF<sub>1</sub>→BDF<sub>1</sub> group; *b*→*bd*, ○). The flow cytometry dot plots depict surface expression of CD4 and CD8 on host thymocytes. Cell analysis was restricted to live thymocytes as defined by forward/side scatter and exclusion of cells staining positive for propidium iodide. The numbers shown in each quadrant represent frequencies (% of the respective populations, mean ± SD). The figure represents combined data from four separate experiments; with an aggregate of 11 mice analysed for each group. Infiltration of donor-derived CD45.1<sup>+</sup> T cells into host thymi is given as frequency (% among total thymic cells) and absolute cell numbers (x 10<sup>6</sup>, mean ± SD). \**p*<0.05, Mann-Whitney U-test, acute GVHD versus syngeneically transplanted mice without disease. (B) Acute GVHD (*b*→*bd*) was induced in 8-week old lethally irradiated BDF<sub>1</sub> mice by co-injection of T cells and T-cell depleted (TCD) bone marrow from B6.CD45.2 and B6.CD45.1 donors, respectively (TCD+T group, ●). Control recipients without disease received TCD bone marrow only (TCD group, ○). The flow cytometry dot plots depict surface expression of CD4 and CD8 on donor bone marrow derived thymocytes and analysis was done as above. Donor T cell infiltration is given as fraction (%) of CD45.2<sup>+</sup>H-K<sup>b</sup>+K<sup>d</sup>- T cells among thymocytes (mean ± SD).

The development of thymic acute GVHD was assessed by flow cytometric analysis of host thymocyte development and donor T-cell infiltration into the host thymus as a function of age. Here, 10, 12 and 15 week old recipients corresponded to 2, 4 and 7 weeks post-transplantation, respectively. In allogeneically transplanted recipients, the frequency of the CD4/CD8 double positive (DP) population was decreased from ~88% in syngeneic controls to ~50% at all time points (Figure 12A, middle panel). In contrast, an increase in the portion of single positive (SP) thymocytes was observed when compared to syngeneic controls (~1% to ~8% and ~6% to ~18% for CD8<sup>+</sup> SP and CD4<sup>+</sup> SP, respectively). This aberrant thymopoiesis was characteristic for the presence of thymic acute GVHD and reflected enhanced apoptosis of CD4<sup>+</sup>CD8<sup>+</sup> DP thymocytes.<sup>221</sup> Since GVHD-dependent changes in thymocyte maturation correlates directly with the number of infiltrating donor T cells,<sup>221</sup> I next investigated frequencies and absolute numbers of donor T cells present in recipients' at 10, 12 and 15 weeks of age. Donor T cells were detected as early as 2 weeks after transplantation (Figure 12A, right panel) and remained present in thymi for the whole observation period. Next, the same haploidentical transplantation model was studied following myeloablative conditioning: Eight-week old BDF<sub>1</sub> mice were lethally irradiated (1000 cGy) prior to i.v. co-injection of 2.5x10<sup>6</sup> B6.CD45.1 splenic T cells (H-2<sup>b</sup>) and 5x10<sup>6</sup> B6.CD45.2 T-cell depleted (TCD) bone marrow cells (TCD+T group) (Figure 12B). Similar to the non-irradiated haploidentical model, I observed defective thymopoiesis (Figure 12B, middle panel) and the presence of donor T cells (Figure 12B, right panel) in thymi of mice with acute GVHD. To confirm these data in other clinically relevant transplantation models, I further investigated a fully MHC-disparate transplantation model. To this end, acute GVHD (*d*→*b*) was induced in 9-week old lethally irradiated B6 mice (975 cGy) by i.v. co-injection of 3x10<sup>6</sup> Balb/c (H-2<sup>d</sup>) splenic T cells and 10x10<sup>6</sup> Balb/c-Thy1a TCD bone marrow cells (TCD+T group) (Figure 13A). Consistent with the observations before, intrathymic T-cell development was aberrant and donor T cells infiltrated the thymus in the presence of acute GVHD. Lastly, a MHC-matched, minor histocompatibility antigen (miHA)-mismatched transplantation model was analysed (Figure 13B). Here, defective thymopoiesis (higher frequencies of CD4 and CD8 SP thymocytes in the presence of acute GVHD) was also a hallmark of acute

GVHD but defects were not as pronounced as in the MHC-mismatched allo-HSCT models described above.

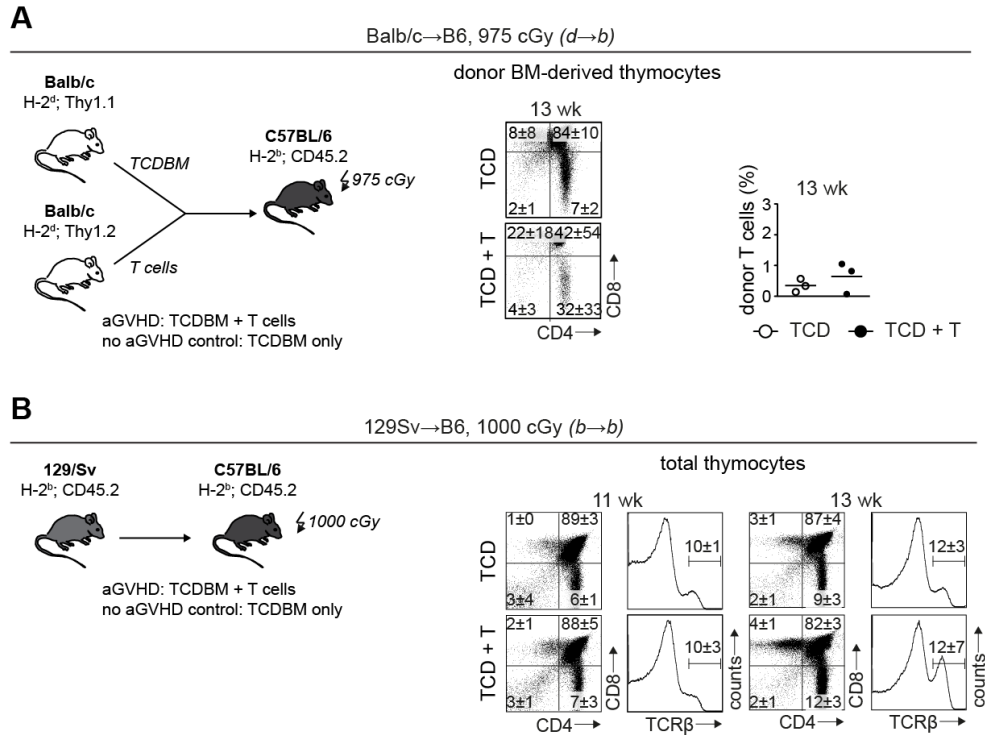


**Figure 13. Induction of thymic acute GVHD in a MHC- and a miHA-mismatched HSCT model.** (A) Acute GVHD (*d*→*b*) was induced in 9-week old lethally irradiated B6 recipients by co-injection of T cells and TCD bone marrow from MHC-mismatched Balb/c and Balb/c-Thy1a donors, respectively (TCD+T group, ●). Control recipients without disease received TCD bone marrow only (TCD group, ○). The same analysis was performed as in panels A and B. Donor T cell infiltration is given as percentages of Thy1a<sup>+</sup>H-2K<sup>d+</sup> T cells among total thymic cells (mean ± SD). (B) Acute GVHD (*b*→*b*) was induced in 8-week old lethally irradiated B6 mice by co-injection of T cells and TCD bone marrow from MHC-matched, minor histocompatibility antigen-mismatched 129/Sv (H-2<sup>b</sup>) donors (TCD+T group, ●). Control recipients without disease received TCD bone marrow only (TCD group, ○). Flow cytometry analysis of total populations was performed as above.

#### 4.1.3 Acute GVHD impairs mTEC<sup>high</sup> compartment size

Based on the aforementioned identification and characterisation scheme for TEC subsets and the fact that the thymic epithelium is a target of donor T-cell alloimmunity,<sup>36,162,223</sup> I next aimed to investigate whether frequencies



and absolute numbers of the different TEC subsets were affected by thymic acute GVHD (Figures 14 and 15). Total numbers of mTEC<sup>high</sup> declined indeed over time in untransplanted adult BDF<sub>1</sub> and B6 mice, confirming age-dependent changes of the thymic stroma in normal mice (Figure 15).<sup>57</sup>

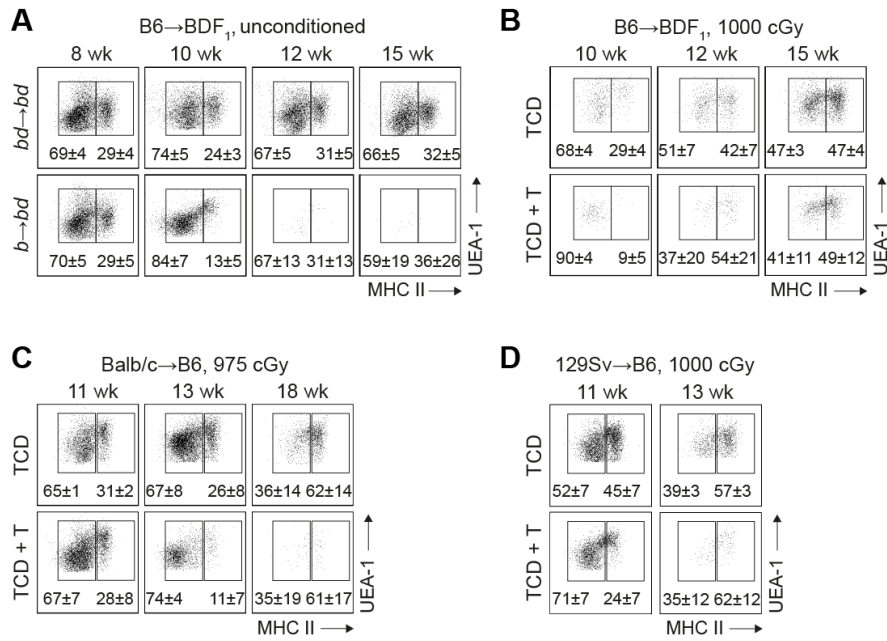


**Figure 14. Flow cytometric analysis of medullary thymic epithelial cell subsets in presence of acute GVHD.** mTEC<sup>high</sup> and mTEC<sup>low</sup> were analysed by flow cytometry as a function of age using the strategy described in Figure 11. (A) mTEC<sup>high</sup> and mTEC<sup>low</sup> analysis in the haploidentical transplantation model described in Figure 12A. The numbers shown in each flow cytometry dot plot represent frequency (% mean ± SD) of the respective population among total mTEC. The figure represents combined data of individual mice from 6 separate experiments. *bd*→*bd*; syngeneic controls, no acute GVHD. *b*→*bd*; allogeneic HSCT, acute GVHD. The same analysis was performed for three other allogeneic HSCT models (described in Figures 12 and 13). (B) Haploidentical HSCT model (*b*→*bd*) with lethal irradiation (1000 cGy). TCD; no acute GVHD, TCD + T; acute GVHD. (C) MHC-mismatched HSCT model (*d*→*b*) with lethal irradiation (975 cGy). TCD; no acute GVHD, TCD + T; acute GVHD. (D) MHC-matched, miHA-mismatched HSCT model (*b*→*b*) with lethal irradiation (1000 cGy). TCD; no acute GVHD, TCD + T; acute GVHD

I then investigated the four mouse models of age-matched allo-HSCT described in section 4.1.2. Flow cytometric analysis revealed that relative frequencies of both mTEC<sup>low</sup> and mTEC<sup>high</sup> subsets were altered in the presence of acute GVHD as early as 2 weeks post-transplantation in

unconditioned recipients of haploidentical HSCT ( $H-2^b \rightarrow H-2^{bd}$ ;  $b \rightarrow bd$ ) (Figure 14). The induction of thymic acute GVHD progressively reduced total  $mTEC^{low}$  and  $mTEC^{high}$  numbers from  $\sim 10^4$  cells/mouse in syngeneically transplanted animals to  $\leq 10^3$  cells/mouse in animals surviving acute GVHD (Figure 15A). This observation was mirrored in allo-HSCT that included total body-irradiation (TBI) before MHC-identical, MHC-disparate, or haploidentical transplantation (Figure 15B-D). In these models, the conditioning initially reduced  $mTEC^{high}$  numbers independently of acute GVHD, but cell loss was either more pronounced ( $b \rightarrow bd$ ) or more protracted ( $d \rightarrow b$ ;  $b \rightarrow b$ ) in the presence of disease. Hence, reduction in  $mTEC^{high}$  compartment size is a universal manifestation of thymic acute GVHD, and radiation injury is not mandatory, as suggested before.<sup>223</sup>

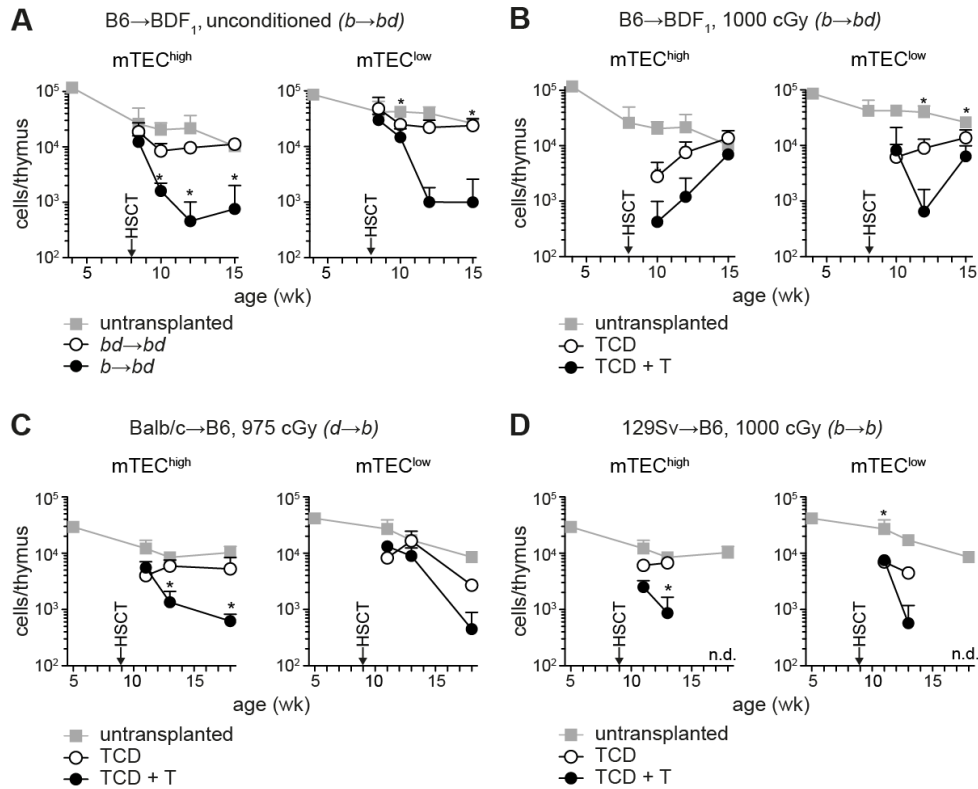


**Figure 15. Absolute cell numbers of  $mTEC^{high}$  and  $mTEC^{low}$  are decreased in the presence of acute GVHD.** Absolute numbers of the  $mTEC$  compartment were analysed as a function of recipient age in 4 different murine models of allogeneic HSCT. (A) Acute GVHD was induced in 8-week old unconditioned BDF<sub>1</sub> recipients ( $b \rightarrow bd$ , black circles). Untransplanted BDF<sub>1</sub> mice (grey squares) or syngeneically transplanted mice ( $bd \rightarrow bd$ , open circles) served as controls. A total of 6 experiments were performed, with 3 to 5 mice per

group and experiment. (B) Acute GVHD (TCD + T group, black circles) was induced in irradiated 8-week old BDF<sub>1</sub> recipients ( $b \rightarrow bd$ ). Untransplanted BDF<sub>1</sub> mice (grey squares) and recipients of TCD bone marrow only (TCD group, open circles) were used as controls without disease. (C) Acute GVHD (TCD + T group, black circles) was induced into 9-week old B6 recipients ( $d \rightarrow b$ ). Untransplanted age-matched B6 mice (grey squares) and B6 mice that received TCD bone marrow only (TCD group, open circles) were used as controls. (D) Acute GVHD (TCD + T group, black circles) was induced into 8-week old B6 recipients ( $b \rightarrow b$ ). Untransplanted age-matched B6 mice (grey squares) and B6 mice that received TCD bone marrow only (TCD group, open circles) were used as controls. A total of 3 experiments were performed. The line graphs show total cell numbers (mean  $\pm$  SD) of mTEC<sup>high</sup> (left) and mTEC<sup>low</sup> (right) cells as a function of recipient age post-transplantation. \* $p < 0.05$ , analysis of variance (ANOVA), acute GVHD versus transplanted mice without acute GVHD. TCD, T-cell depleted; n.d., not done.

#### 4.1.4 Acute GVHD impairs thymic Aire expression

Crucial for negative selection of self-reactive T cells is the exposure of thymocytes to self-antigens including those with highly restricted tissue expression. Within the thymus, the ectopic expression of many tissue-restricted peripheral self-antigens (TRA) is a particular property of cells of the mTEC<sup>high</sup> compartment.<sup>71,72,247,248</sup> Expression of TRA is partly under the control of the transcription factor autoimmune regulator (Aire).<sup>72</sup> Therefore, I next investigated whether acute GVHD affected qualitatively and quantitatively the postcycling medullary TEC subset (Aire<sup>+</sup>mTEC<sup>high</sup>) that expresses Aire and is responsible for central tolerance induction. Confocal microscope analysis of thymic sections stained with cytokeratin 18 (CK18), CK14 and Aire confirmed Aire<sup>+</sup> cells to localise in the thymus medulla (Figure 16A). Syngeneically transplanted mice ( $bd \rightarrow bd$ ) were not different from age-matched untransplanted control mice (data not shown<sup>73</sup>). However, in the presence of acute GVHD in unconditioned recipients ( $b \rightarrow bd$ ) thymic cortical and medullary organisation was lost and Aire<sup>+</sup> cells became virtually undetectable with time. Hence, contraction of the total mTEC<sup>high</sup> pool in  $b \rightarrow bd$  recipients corresponded to a progressive decrease in the subset that expresses Aire.<sup>73,77</sup> This observation was confirmed by FACS analysis of Aire<sup>+</sup> cells among the mTEC<sup>high</sup> population (Figure 16B, C). In 12-week-old recipients, residual Aire<sup>+</sup>mTEC<sup>high</sup> were low in numbers (<300 cells/thymus compared to  $\sim 5 \times 10^3$  cells/thymus in animals without acute GVHD) and were not detectable anymore during progressive disease, owing

to the smaller than normal frequencies of Aire-expressing cells among declining mTEC<sup>high</sup> numbers. Taken together, these data demonstrated that mature medullary thymic epithelial cells were targets of acute GVHD and that the cells most affected belonged to the subset of Aire-expressing mTEC<sup>high</sup>.

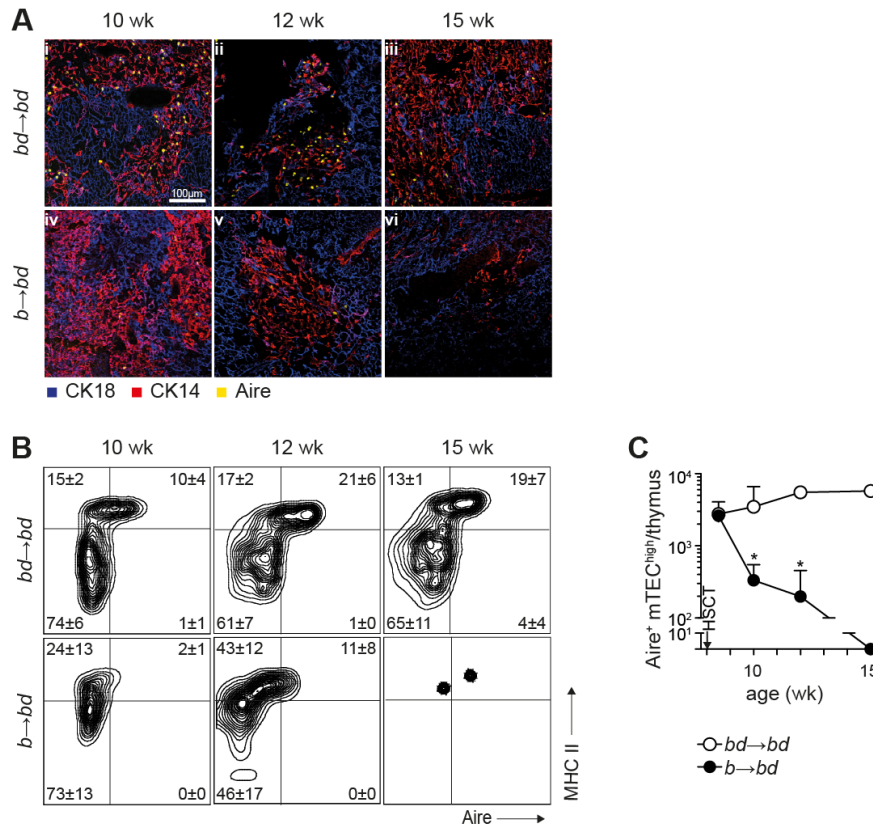


**Figure 16. Acute GVHD causes loss of Aire<sup>+</sup>mTEC<sup>high</sup> cells.** (A-C) Qualitative and quantitative analysis of thymic Aire expression. Immunohistochemistry and confocal microscope analysis (A) was performed on thymic frozen sections taken from unconditioned transplant recipients at ages 10, 12, and 15 weeks (i.e. 2, 4, and 7 weeks after transplantation; [i-iii] *bd*→*bd*, [iv-vi] *b*→*bd*). Cytokeratin-18 (CK18, blue) and CK14-positive cells (red) denote cTEC and mTEC, respectively.<sup>67,162</sup> The flow cytometry plots in (B) depict Aire and MHC class II expression of DAPI<sup>+</sup>CD45<sup>+</sup>EpCam<sup>+</sup>Ly51<sup>+</sup>UEA-1<sup>+</sup> mTEC. Numbers represent frequencies (%) of cells (mean ± SD). Total numbers of Aire<sup>+</sup>mTEC<sup>high</sup> in thymi from individual recipient mice (C) was calculated from flow cytometry data (mean ± SD). (syngeneic HSCT, *bd*→*bd*, open circles; allogeneic HSCT, *b*→*bd*, black circles). A total of 5 experiments were performed with 3 to 5 mice per group. \**p*<0.05, ANOVA, acute GVHD vs. transplanted mice without acute GVHD.

### 4.1.5 Acute GVHD impairs TRA expression

Given the intimate associations between Aire-deficiency, TRA repression, and autoimmunity,<sup>248</sup> I next determined whether acute GVHD interfered with TRA transcription. To this end, I isolated total remaining mTEC<sup>high</sup> cells at HSCT recipient ages of 10, 12 and 15 weeks in the presence or absence of acute GVHD in unconditioned allo-HSCT recipients. Gene expression analysis of these cells was performed using DNA microarray technology. Development of thymic acute GVHD (*b*→*bd*) altered global gene expression profiles in total residual mTEC<sup>high</sup> cell pools isolated at 2 to 4 weeks after transplantation (Figure 17A, Table 2). An increase or decrease in expression level greater than three-fold in relation to the control group (corresponding to relative expression values of <0.33 and >3.0, respectively) was considered as altered gene expression in consequence of acute GVHD. To discriminate between TRA and ubiquitously expressed transcripts (Ub) in mTEC<sup>high</sup>, I used a special algorithm which had previously been described.<sup>64,70,72</sup> (Personal communication by Bruno Kyewski, Heidelberg, Germany) Here, transcripts with expression in <5 different tissues in combination with a lower threshold of 5-fold signal intensity of the average of all tissues were designated as tissue restricted. Recent next generation RNA sequencing data generated from thymic epithelial subpopulations (G. A. Holländer) were incorporated to adjust the annotated gene lists. Using this method, I classified 10017 transcripts as TRA among a total of 17336 transcripts analysed (Figure 17A). It should be noted that due to absence of tissue expression data, not all of the 21759 transcripts present on the microarray chips could be categorised as TRA or Ub. Several hundred transcripts were expressed at reduced levels (>3-fold change; relative expression <0.33) in mice with acute GVHD. For transcripts whose expression was either enhanced or depressed as a consequence of acute GVHD, I expected that TRA and Ub sequestered according to the relative frequencies of TRA and Ub in normal adult mice. To test the accuracy of this hypothesis, O/E analysis was performed, an easy to interpret and widely used statistic for measuring performance (Figure 17B).<sup>246</sup> In this ratio, O is the observed number of events, and E is the expected number of events. An O/E ratio = 1 represents an expected observation, which in my case would be a distribution among TRA and Ub according to the relative frequencies of TRA and Ub in normal adult mice.

Using hypergeometric statistical analysis I could demonstrate, however, that among the transcripts with lowered expression levels (relative expression  $<0.33$ ) the O/E ratios were  $>1.0$  for TRA and  $<1.0$  for Ub (Figure 17B). These data indicated that TRA were significantly enriched among the downregulated transcripts at both time points (i.e. 2 and 4 weeks post-transplantation). To quantify the observed changes between the two experimental groups, a correlation matrix was generated (Figure 17C).

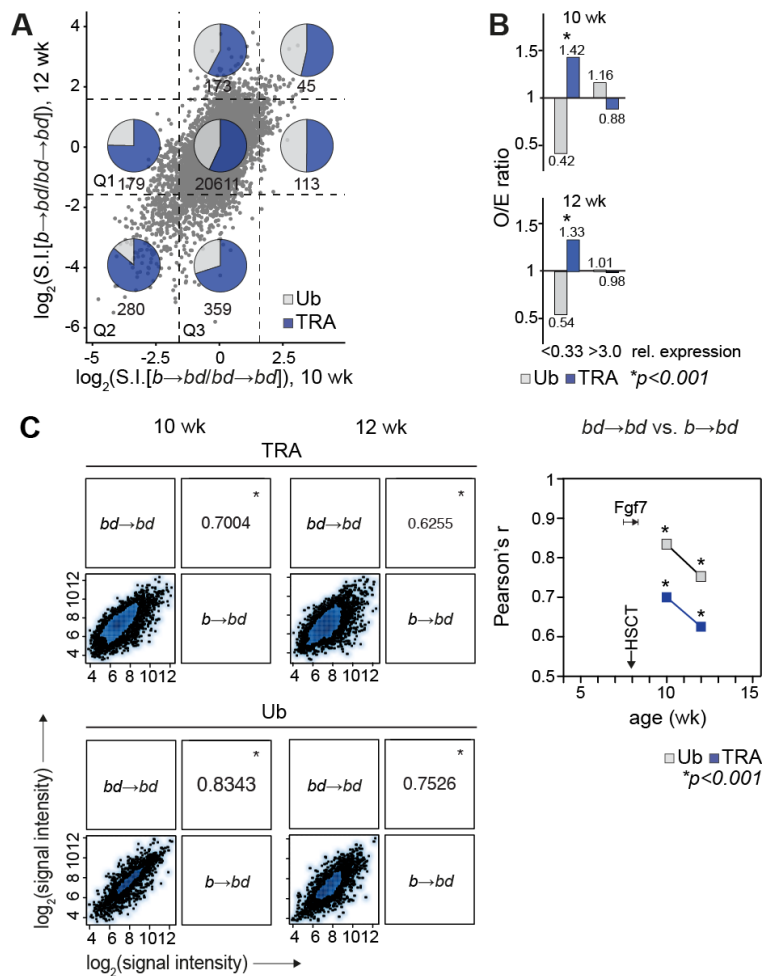


**Figure 17. Acute GVHD alters gene expression.** Global gene expression was analysed in entire residual mTEC<sup>high</sup> cell pools isolated from individual recipients at 10, 12, and 15 weeks of age (i.e. 2, 4, and 7 weeks after transplantation). The figure reflects data from 5 independent experiments, with 2 to 4 mice per group and experiment. (A) Gene expression profiling of mTEC<sup>high</sup> in transplant recipients using Mouse Gene 1.0 ST arrays (Affymetrix). The x- and y-axes represent relative expression of individual genes (given as  $\log_2$  values of signal intensity ratios, S.I.) in mice with acute GVHD ( $b \rightarrow bd$ ) vs. syngeneically transplanted

recipients without disease ( $bd \rightarrow bd$ ). Data is plotted as a function of recipient age (10 vs. 12 weeks). Genes whose expression levels are enhanced or decreased more than 3-fold relative to the control group (corresponding to relative expression values given by the S.I. ratios of  $<0.33$  and  $>3.0$ , respectively, or  $<-1.6$  and  $>+1.6$  on the  $\log_2$  scale) are considered to be significantly altered in consequence of acute GVHD (threshold is indicated by dashed lines). Q2 is the lower left quadrant, denoting genes whose expression levels are depressed at both 2 and 4 weeks after allogeneic HSCT (10- and 12-week old recipients). Q1 denotes transcripts whose expression levels are depressed at 2 but not at 4 weeks after allogeneic HSCT and Q3 denotes genes that are decreased only at 4 weeks. The inserted numbers denote the absolute numbers of genes in the respective quadrants. Transcripts from a total of 21759 genes are analysed. Ub (ubiquitously expressed genes, grey segment) and TRA (dark blue segment). (B) O/E performance analysis (O, observed number of events; E, expected number of events) of the presence of TRA vs. Ub among the genes with relative expression  $<0.33$  and  $>3.0$ . O/E ratio  $>1.0$  for TRA and  $<1.0$  for Ub;  $*p < 0.001$  using hypergeometric statistical analysis. (C) Analysis of linear relationship of global gene expression between no GVHD ( $bd \rightarrow bd$ ) and GVHD ( $b \rightarrow bd$ ) experimental groups for TRA (upper panel) and ubiquitously expressed transcripts, Ub (lower panel). In a correlation matrix analysis, signal intensities ( $\log_2$ ) of individual transcripts are plotted and the Pearson's correlation coefficient  $r$  between two variables is individually calculated as a function of recipient age. Numbers in each quadrant indicate Pearson's  $r$  values between the two groups tested. The asterisk (\*) symbol indicates a  $p < 0.001$  value for the quality of any measured Pearson's  $r$  at the given time point for TRA or Ub. Right panel: Pearson's correlation coefficient  $r$  is shown as a function of age and time after transplantation for Ub (grey squares) and TRA (blue squares).  $*p < 0.001$  of Pearson's  $r$ .

Here, the variation of each gene was calculated using the inter quartile range (IQR), a measure of statistical dispersion. Only 50% of the genes that had an IQR higher than the median of the IQR values of all genes were included for calculation of the Pearson's correlation coefficient (Pearson's  $r$ ). A low strength of association of TRA expression between mice with acute GVHD ( $b \rightarrow bd$ ) and syngeneically transplanted mice without acute GVHD ( $bd \rightarrow bd$ ) was indicated by a Pearson's  $r = 0.7004$  and  $r = 0.6255$  in 10 and 12 week old recipients, respectively (Figure 17C). These low  $r$  values showed that many TRA differed in the presence of acute GVHD in their expression level from a physiological level. In contrast, a higher  $r$  value indicated that expression levels were closer to normal. This analysis was done for TRA and Ub according to their definition and demonstrated that  $r$  values for TRA were lower than for Ub at all time points and experimental conditions employed. Hence, the GVHD-induced alterations were not as pronounced for Ub as for TRA. I interpreted these data such that a contraction in TRA diversity during acute GVHD was caused by cellular

loss of mTEC<sup>high</sup>, in particular Aire-positive mTEC. This explanation was based on the fact that ectopic TRA expression is a stochastic process in which only a limited number of mTEC<sup>high</sup> express a given TRA.<sup>66,75,249</sup> A comprehensive coverage of TRA expression is therefore only achieved by a sufficiently large mTEC<sup>high</sup> pool, which is, however, missing under conditions of acute GVHD. Next, I was interested whether TRA with lowered expression levels in mTEC<sup>high</sup> during acute GVHD in 10- and 12-week-old recipients were Aire-dependent. I compared my gene expression profile with published data from gene expression in mTEC from Aire<sup>-/-</sup> deficient mice.<sup>72</sup> A fraction of the downregulated TRA belonged to the subset of Aire-dependent TRA (Figure 18A). Impaired Aire-dependent TRA included for example Scgb1a (secretoglobin), Csn1s2a (casein g), Mup1 (major urinary protein 1) and Spt1 (salivary protein 1). Expression profile data of selected genes obtained by microarray analysis was verified by quantitative PCR (qPCR) (Figure 18B). This analysis confirmed the acute GVHD-induced reduction in expression of the Aire-dependent TRA Spt1, Mup1 and Csn1s2a. Among TRA that remained unchanged in the presence of acute GVHD, around one third was specific for a chronic GVHD target tissue (Figure 18C, left pie chart). However, the most substantially reduced TRA were found to be enriched for genes that are characteristically expressed in tissues known to be targets of chronic GVHD (i.e. skin, liver, salivary gland, lung, eye and G.I. tract) (Figure 18C, right pie charts).<sup>147</sup> These data led me to propose that a defect in the ectopic expression of a particular TRA during acute GVHD may result in the failure to negatively select TCR specific for this TRA and hence to the emergence of autoreactive T cells, a feature typical for GVHD. This hypothesis was tested in the work described in chapter 4.2.



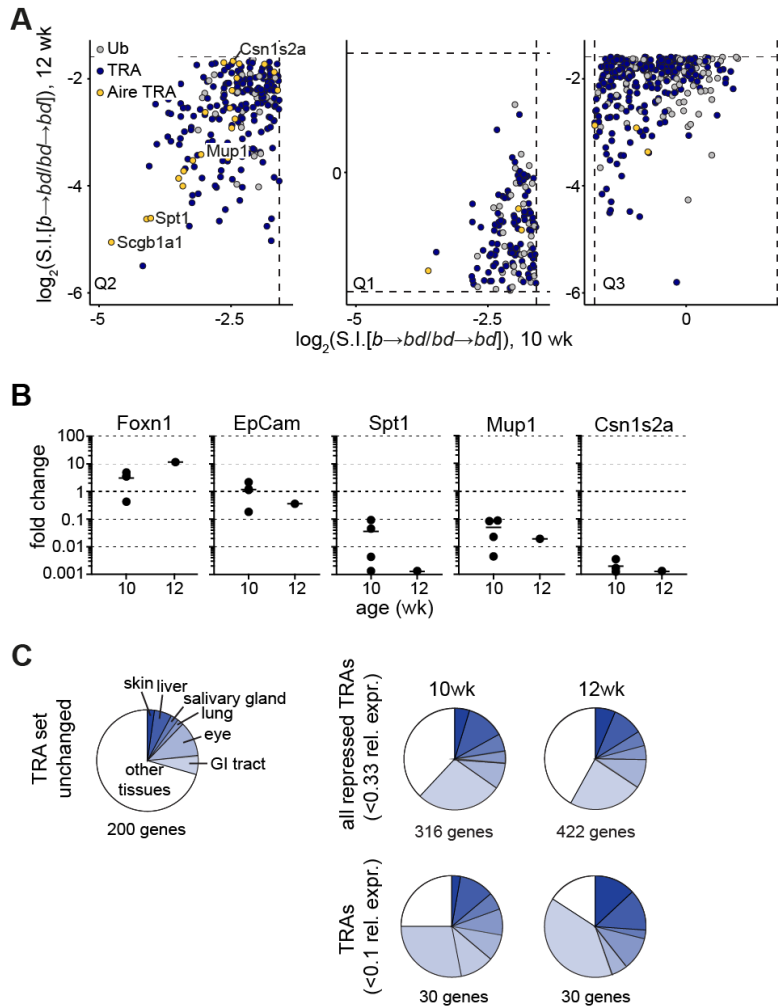


**Figure 18. Altered TRA are dependent on Aire and specific for chronic GVHD target tissues.** (A) Aire dependency of TRA with lowered expression levels in mTEC<sup>high</sup> during acute GVHD in 10- and/or 12-week old recipients (the axes are the same as in Figure 17A). Examples shown are the following: Scgb1a1, secretoglobin; Csn1s2a, casein g; Mup1, major urinary protein 1; Spt1, salivary protein 1. Aire-dependent TRA (yellow circles), Aire-independent TRA (dark blue circles), and Ub (grey circles). (B) Microarray data of selected genes is verified by quantitative PCR (qPCR). Expression in syngeneically transplanted recipients is set as 1 (thick, dashed line) and used as a control. Expression in allogeneically transplanted recipients is shown as x-fold change over controls as a function of recipient's age. Foxn1, forkhead box N1; EpCam, epithelial cell adhesion molecule; Spt1, salivary protein 1; Mup1, major urinary protein 1; Csn1s2a, casein alpha s2-like A (casein g). n.d., not done. (C) Tissue representation of TRA reduced during acute GVHD (<0.1 and <0.33 relative expression, respectively, vs. mice without acute GVHD at 10 and 12 weeks of age). As control, a random set of 200 TRA is used that remained unchanged in the course of acute GVHD (relative expression ~1).

**Table 2.**

(A) Genes downregulated during acute GVHD (relative expression &lt;0.125)

| Gene                          | Accession #  | Name   | Rel. Expression $b \rightarrow bd$ vs. $bd \rightarrow bd$ |       |
|-------------------------------|--------------|--|--|-------|
|                               |              |  | 10 wk  | 12 wk |
| <i>TRA are shaded in grey</i> |              |  |  |       |
| Scgb1a1                       | NM_011681    | secretoglobin, family 1A, member 1, lung                   | 0.037  | 0.030 |
| Rgs13                         | NM_153171    | regulator of G-protein signaling 13, tonsil, intestine     | 0.055  | 0.022 |
| Olf461                        | NM_146382    | olfactory receptor 461, sensory system                     | 0.058  | 0.193 |
| Fabp2                         | NM_007980    | fatty acid binding protein 2, intestine                    | 0.058  | 0.041 |
| Fabp1                         | NM_017399    | fatty acid binding protein 1, liver, intestine             | 0.060  | 0.081 |
| Spt1                          | NM_009267    | salivary protein 1, salivary gland                         | 0.062  | 0.041 |
| Defb3                         | NM_013756    | defensin beta 3, intestine, lung, other                    | 0.066  | 0.180 |
| Retnla                        | NM_020509    | resistin like alpha, mammary, adipose tissue, other        | 0.067  | 0.107 |
| Gnat3                         | NM_001081143 | guanine nucleotide binding protein, gustatory system       | 0.076  | 0.032 |
| Tm4sf20                       | NM_025453    | transmembrane 4 L six family member 20, intestine          | 0.077  | 0.118 |
| 1700026D08Rik                 | NM_029335    | RIKEN cDNA 1700026D08 gene, testis, other                  | 0.078  | 0.192 |
| Saa1                          | NM_009117    | serum amyloid A 1, intestine, liver, intestine             | 0.078  | 0.161 |
| Ttr                           | NM_013697    | transthyretin, liver, lung, placenta, eye                  | 0.080  | 0.159 |
| Lgals2                        | NM_025622    | lectin, galactose-binding, soluble 2, intestine, stomach   | 0.080  | 0.111 |
| Reg3b                         | NM_011036    | regenerating islet-derived 3 beta, pancreas, intestine     | 0.081  | 0.404 |
| Ctrb1                         | NM_025583    | chymotrypsinogen B1, pancreas, other                       | 0.084  | 0.252 |
| Mup2                          | NM_008647    | major urinary protein 2, liver, lung                       | 0.089  | 0.069 |
| Bmx                           | NM_009759    | BMX non-receptor tyrosine kinase                           | 0.090  | 0.107 |
| Gpr50                         | NM_010340    | G-protein-coupled receptor 50, placenta, other             | 0.090  | 0.480 |
| Lipn                          | NM_027340    | lipase, family member N, adipocytes, other                 | 0.091  | 0.115 |
| Calb1                         | NM_009788    | calbindin 1, brain, kidney, other                          | 0.091  | 0.182 |
| Svs4                          | NM_009300    | seminal vesicle secretory protein 4, prostate              | 0.091  | 0.234 |
| Dynlrb2                       | NM_029297    | dynein light chain roadblock-type 2, lung, testis, adipose | 0.091  | 0.154 |
| Mup7                          | NM_001134675 | major urinary protein 7, lung, mammary gland               | 0.094  | 0.062 |
| Pf4                           | NM_019932    | platelet factor 4, platelets, other                        | 0.094  | 0.172 |
| Mup11                         | NM_001164526 | major urinary protein 11, genital tract, other             | 0.095  | 0.076 |
| Vnn3                          | NM_011979    | vanin 3, liver   | 0.096  | 0.126 |

|               |                  |  |       |       |
|---------------|------------------|--|-------|-------|
| Abp1          | NM_029638        | amiloride binding protein 1, intestine   | 0.097 | 0.078 |
| Chi3l4        | NM_145126        | chitinase 3-like 4, intestine  | 0.100 | 0.172 |
| Tcfap2b       | NM_009334        | transcription factor AP-2 beta, skin, salivary, eye  | 0.100 | 0.088 |
| Hsd17b6       | NM_013786        | hydroxysteroid (17-beta) dehydrogenase 6, liver, intest.                                     | 0.102 | 0.037 |
| Reg1          | NM_009042        | regenerating islet-derived 1, intestine  | 0.105 | 0.129 |
| Anxa13        | NM_027211        | annexin A13, intestine   | 0.105 | 0.134 |
| Apoa4         | NM_007468        | apolipoprotein A-IV, intestine   | 0.106 | 0.050 |
| 2210415F13Rik | NM_001083<br>884 | RIKEN cDNA 2210415F13 gene, intestine  | 0.107 | 0.055 |
| Mup19         | NM_001135<br>127 | major urinary protein 19, liver, lung  | 0.107 | 0.087 |
| Cst10         | NM_021405        | cystatin 10, eye   | 0.108 | 0.154 |
| Klk1b11       | NM_010640        | kallikrein 1-related peptidase b11, salivary gland   | 0.109 | 0.080 |
| Serpina7      | NM_177920        | serine (or cysteine) peptidase inhibitor, liver  | 0.115 | 0.056 |
| Nts           | NM_024435        | neurotensin, intestine   | 0.118 | 0.168 |
| Sis           | NM_001081<br>137 | sucrase isomaltase, intestine  | 0.119 | 0.220 |
| Mup1          | NM_001163<br>011 | major urinary protein 1, liver, lung   | 0.119 | 0.094 |
| Mctp1         | NM_030174        | multiple C2 domains, transmembrane 1, brain eosinophil-associated, ribonuclease A family, 11 | 0.121 | 0.069 |
| Ear11         | NM_053113        |  | 0.121 | 0.196 |
| Prap1         | NM_009475        | proline-rich acidic protein 1, intestine   | 0.123 | 0.256 |
| Gpr128        | NM_172825        | G protein-coupled receptor 128   | 0.124 | 0.082 |

(B) Genes upregulated during acute GVHD (relative expression >4.0)

| Gene                          | Accession #      | Name                                       | Rel. Expression $b \rightarrow bd$ vs. $bd \rightarrow bd$ |       |
|-------------------------------|------------------|--|--|-------|
|                               |                  |  | 10 wk  | 12 wk |
| <i>TRA are shaded in grey</i> |                  |  |  |       |
| Gbp5                          | NM_153564        | guanylate binding protein 5, IFN-regulated | 9.36   | 3.62  |
| Myl9                          | NM_172118        | myosin, light polypeptide 9, regulatory    | 8.54   | 10.36 |
| Gbp2                          | NM_010260        | guanylate binding protein 2, IFN-regulated | 8.10   | 3.35  |
| C1s                           | NM_144938        | complement component 1, IFN-regulated      | 7.76   | 2.49  |
| Casp12                        | NM_009808        | caspase 12, inflammation, apoptosis        | 7.50   | 4.74  |
| Mpeg1                         | NM_010821        | macrophage expressed gene 1                | 7.26   | 2.84  |
| Gm12250                       | NM_001135<br>115 | predicted gene 12250                       | 6.88   | 4.33  |

|          |                  |   |      |      |
|----------|------------------|---|------|------|
| Nfib     | NM_001113<br>209 | nuclear factor I/B                                    | 6.73 | 9.56 |
| Gbp3     | NM_018734        | guanylate binding protein 3                           | 6.60 | 4.05 |
| Gbp6     | NM_145545        | guanylate binding protein 6                           | 6.52 | 2.07 |
| Apol10b  | NM_177820        | apolipoprotein L 10b                                  | 6.42 | 1.18 |
| Lifr     | NM_013584        | leukemia inhibitory factor receptor                   | 5.87 | 4.20 |
| Art2b    | NM_019915        | ADP-ribosyltransferase 2b                             | 5.70 | 2.79 |
| Mpzl2    | NM_007962        | myelin protein zero-like 2                            | 5.29 | 1.92 |
| Kitl     | NM_013598        | kit ligand  | 5.26 | 3.95 |
| Snord16a | NR_028548        | small nucleolar RNA, C/D box 16A                      | 5.25 | 1.46 |
| Cxcl12   | NM_001012<br>477 | chemokine (C-X-C motif) ligand 12                     | 5.23 | 2.69 |
| Sulf1    | NM_001198<br>565 | sulfatase 1   | 5.20 | 4.94 |
| Rad51    | NM_011234        | RAD51 homolog   | 5.15 | 4.74 |
| Dcn      | NM_007833        | decorin   | 5.09 | 4.84 |
| Pros1    | NM_011173        | protein S (alpha)                                     | 5.04 | 5.08 |
| Myadm    | NM_001093<br>765 | myeloid-associated differentiation marker             | 4.92 | 1.70 |
| Clca5    | NM_178697        | chloride channel calcium activated 5                  | 4.89 | 1.61 |
| Ptn      | NM_008973        | pleiotrophin  | 4.87 | 1.86 |
| Prss16   | NM_019429        | protease, serine, 16 (thymus)                         | 4.84 | 1.95 |
| Flna     | NM_010227        | filamin, alpha  | 4.78 | 3.73 |
| Irgm1    | NM_008326        | immunity-related GTPase family M member 1             | 4.72 | 3.92 |
| Pgm5     | NM_175013        | phosphoglucomutase 5                                  | 4.56 | 4.15 |
| Hey1     | NM_010423        | hairy/enhancer-of-split related with YRPW motif 1     | 4.56 | 3.18 |
| P4ha3    | NM_177161        | procollagen-proline, 2-oxoglutarate 4-dioxygenase     | 4.49 | 2.90 |
| Olfml1   | NM_172907        | olfactomedin-like 1                                   | 4.38 | 1.61 |
| Tnfsf10  | NM_009425        | tumor necrosis factor (ligand) superfamily, member 10 | 4.37 | 0.36 |
| Hmmr     | NM_013552        | hyaluronan mediated motility receptor                 | 4.30 | 1.55 |
| Lrrc17   | NM_028977        | leucine rich repeat containing 17                     | 4.26 | 1.36 |
| Fgfr2    | NM_010207        | fibroblast growth factor receptor 2                   | 4.16 | 2.28 |
| Osmr     | NM_011019        | oncostatin M receptor                                 | 4.15 | 5.12 |
| Ccnb1    | NM_172301        | cyclin B1   | 4.13 | 1.38 |
| Mtss1l   | NM_198625        | metastasis suppressor 1-like                          | 4.08 | 1.86 |
| Prc1     | NM_145150        | protein regulator of cytokinesis 1                    | 4.03 | 1.43 |
| Scn1a    | NM_018733        | sodium channel, voltage-gated, type I, alpha          | 4.02 | 4.05 |
| Acta2    | NM_007392        | actin, alpha 2, smooth muscle, aorta                  | 4.02 | 1.76 |

|       |           |                |      |      |
|-------|-----------|----------------|------|------|
| Slfn5 | NM_183201 | schlafen 5     | 4.00 | 4.07 |
| Il15  | NM_008357 | interleukin 15 | 4.00 | 2.66 |

## 4.2 Impaired thymic expression of tissue-restricted antigens licenses the *de novo* generation of autoreactive CD4<sup>+</sup> T cells during murine acute GVHD

### 4.2.1 A transgenic model to study generation of thymus-dependent autoreactive T cells during acute GVHD

Because thymic negative selection is sensitive to small changes in TRA expression,<sup>73</sup> a reduction in mTEC compartment size and hence TRA expression may lead to the emergence of thymus-dependent autoreactive T cells in the context of acute GVHD.<sup>180</sup> The *de novo* generation of autoreactive T cells from donor HSC is a hallmark of murine acute GVHD.<sup>177,178</sup> These autoreactive clones can mediate the transition from acute to chronic GVHD in different mouse models of alloHSCT.<sup>179-181,224</sup> There is now much experimental evidence that the thymic epithelium is a target of donor alloimmunity,<sup>162,223,224</sup> and that thymic acute GVHD interferes with the capacity of Aire-expressing mTEC<sup>high</sup> to sustain TRA diversity in the course of disease.<sup>225</sup> However, a direct link between the weakened platform for central tolerance and the emergence of autoreactive T cells during acute GVHD, and ultimately the development of an autoimmune syndrome during chronic GVHD, has not yet been proven. I decided to study the *de novo* production of TRA-specific T cells in the thymus during acute GVHD by using a transgenic mouse allogeneic HSCT model (Figure 19). Here, membrane-bound ovalbumin (mOVA) is expressed in transgenic mice under the rat insulin promoter (RIP) as a model neo-self-antigen not only in the pancreas but also in the thymus by both mature and immature mTEC. This model provided the tool to investigate tolerance

induction to a known antigen during acute GVHD, thus overcoming the lack of knowledge with regard to the specificities of the autoreactive effector T cells in chronic GVHD.<sup>146,184</sup> I chose the OT-II→RIP-mOVA system because (1) thymic mOVA expression is restricted to mTEC, (2) TCR selection against mOVA recapitulates physiological tolerance induction to TRA in the thymus medulla,<sup>71,72,76,98,250,251</sup> and (3) a reduction in mOVA mRNA in mTEC by as little as 30% suffices for the lack of deletion of OT-II cells in RIP-mOVA mice.<sup>252</sup>

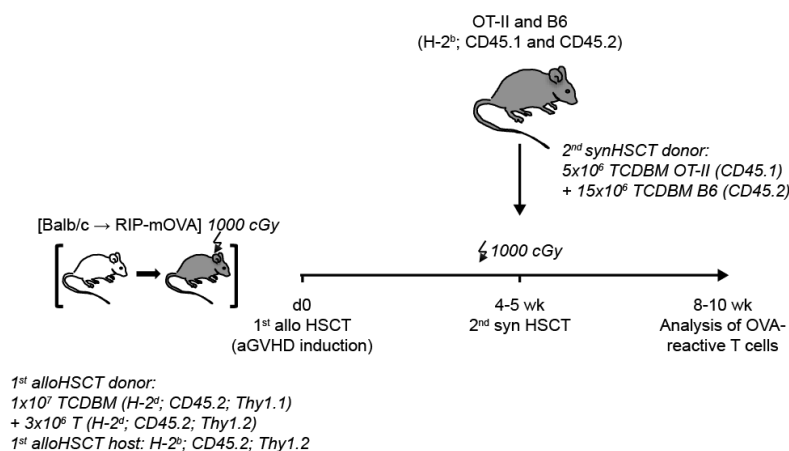


**Figure 19. A model to study generation of thymus-dependent autoreactive T cells during acute GVHD.** Balb/c-Thy1.1<sup>+</sup> TCD bone marrow replete with Balb/c splenic T cells was grafted into lethally irradiated RIP-mOVA recipients generating [Balb/c→RIP-mOVA] chimeric mice with thymic acute GVHD. Non-GVHD control mice received Balb/c-Thy1.1<sup>+</sup> TCD bone marrow only. Four to five weeks after first allogeneic HSCT (=GVHD induction), recipients were lethally re-irradiated and transplanted in a second syngeneic HSCT with TCD bone marrow from CD45.1<sup>+</sup> OT-II (H-2<sup>b</sup>) and wildtype B6 mice (H-2<sup>b</sup>). Four to five weeks after OT-II TCD bone marrow transfer, thymi, spleen and lymph nodes were isolated from RIP-mOVA recipients and OVA-reactive T cell clones analysed (congenically marked CD45.1<sup>+</sup>; Vα2<sup>+</sup> Vβ5<sup>+</sup>).

#### 4.2.2 Thymic GVHD induction in RIP-mOVA recipients

I first investigated whether impaired thymic function was a hallmark of acute GVHD in lethally irradiated RIP-mOVA recipients of fully MHC-mismatched HSCT (H-2<sup>d</sup>→H-2<sup>b</sup>). To this end, 8-week old

lethally irradiated RIP-mOVA mice (H-2<sup>b</sup>; 1000 cGy) were transplanted with  $3 \times 10^6$  Balb/c (H-2<sup>d</sup>) splenic T cells and  $10 \times 10^6$  Balb/c-Thy1a TCD bone marrow cells (Balb/c $\rightarrow$ RIP-mOVA; H-2<sup>d</sup> $\rightarrow$ H-2<sup>b</sup>; TCD+T group). Control mice without disease received TCD bone marrow alone (TCD group). Two weeks after transplantation, total thymic cellularity was severely diminished in both B6 and RIP-mOVA recipients from  $\geq 6 \times 10^7$  to  $< 5 \times 10^6$  cells in the presence of acute GVHD (Figure 20A, C). This reduced cellularity was reflected by aberrant thymopoiesis in mice suffering from acute GVHD. Frequencies of CD4<sup>+</sup>CD8<sup>+</sup> DP thymocytes were decreased from ~90% to ~30% in both, non-transgenic and transgenic mice, whereas increased frequencies of SP populations were detected (Figure 20B, D, left panel). This defect was related to alloreactive donor T cells (H-2<sup>d+</sup> Thy1.1<sup>-</sup>) infiltrating the thymus. Four weeks after allogeneic HSCt, RIP-mOVA recipients with or without acute GVHD showed >80% donor chimerism in thymi (Figure 20B, D, middle panel). Donor bone marrow derived cells were defined as H-2<sup>b</sup> H-2<sup>d+</sup> Thy1.1<sup>+</sup>. Due to the persistent presence of alloreactive donor T cells (splenic T cells; H-2<sup>b</sup> H-2<sup>d+</sup> Thy1.1<sup>-</sup>), donor bone marrow-derived T-cell development (H-2<sup>b</sup> H-2<sup>d+</sup> Thy1.1<sup>+</sup>; Figure 20B, D, right panel) remained impaired. In total, the experiments demonstrated that the induction of thymic acute GVHD in transgenic RIP-mOVA mice did not differ from a non-transgenic fully MHC-mismatched transplantation model.

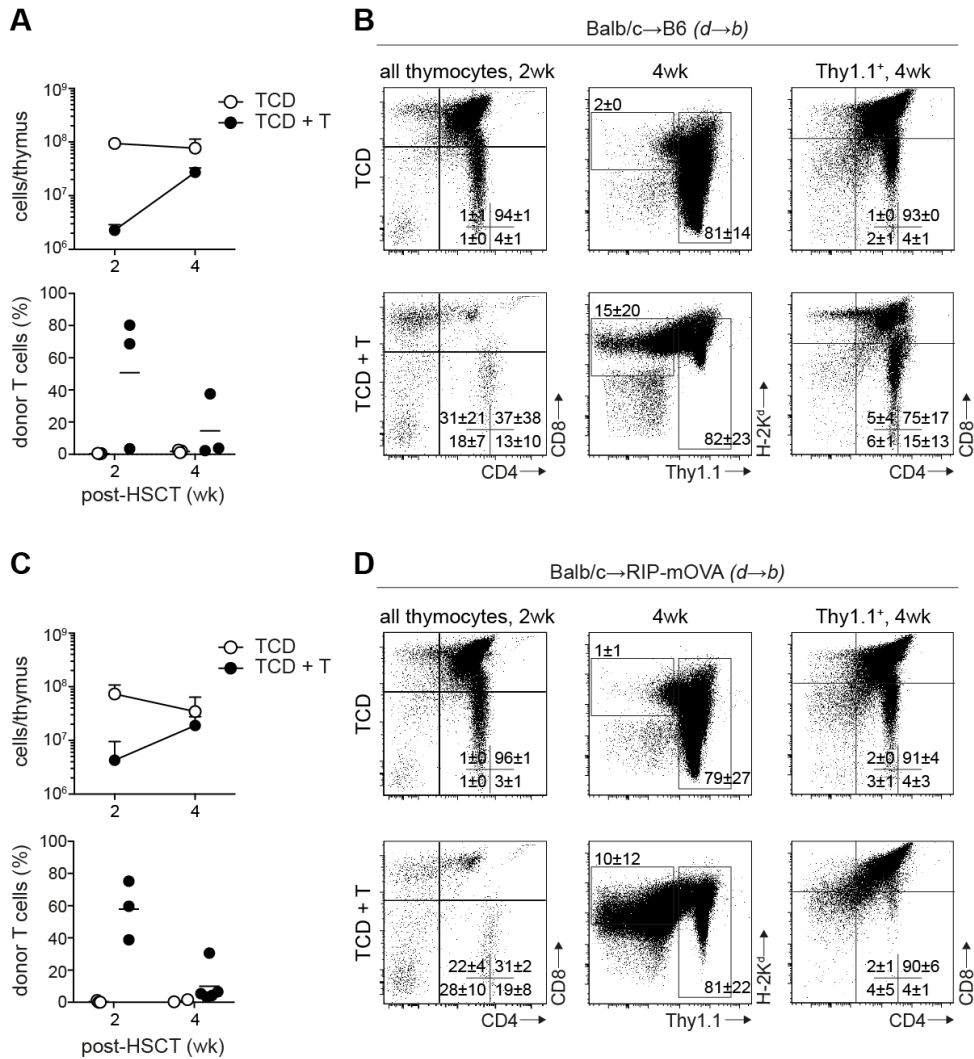


**Figure 20. Induction of thymic acute GVHD in RIP-mOVA mice.** In a fully MHC-mismatched transgenic and non-transgenic transplantation model, thymic acute GVHD was induced in 8-9 week old lethally irradiated RIP-mOVA and B6 mice ( $H-2^b$ ), respectively, by i.v. co-injection of Balb/c-Thy1.1<sup>+</sup> TCD bone marrow and Balb/c splenic T cells. Control animals without disease received Balb/c-Thy1.1<sup>+</sup> TCD bone marrow only. (A) Thymic cellularity in B6 recipients is analysed as a function of time post-HSCT (total cells per thymus) in mice without (TCD group, ○) and with acute GVHD (TCD+T group, ●). Donor T cell infiltration is given as percentages of H-2K<sup>d</sup>Thy1.1<sup>+</sup> T cells among total thymic cells (mean ± SD). (B) Donor bone marrow engraftment and the development of thymic acute GVHD was assessed by flow cytometric analysis. Left column: The flow cytometry dot plots depict surface expression of CD4 and CD8 on total thymocytes at 2 weeks post-transplantation. Middle and right columns: The flow cytometry dot plots depict surface expression of H-2K<sup>b</sup> and Thy1.1 on total thymocytes and CD4 and CD8 expression on donor bone marrow derived thymocytes at 4 weeks post-transplantation. Cell analysis was restricted to live thymocytes as defined by Dapi<sup>i</sup> staining. The numbers shown in each quadrant represent frequencies (% of the respective populations, mean ± SD). (C-D)



Transgenic RIP-mOVA mice were used as recipients of a fully MHC-disparate transplantation model. Acute GVHD was induced as in panel A and the same analysis was performed as in panels A and B. The figure represents combined data from three separate experiments with  $\geq 3$  mice analysed per group. \* $p < 0.05$ , Mann-Whitney U-test.

Next, I intended to corroborate that reduction in mTEC compartment size - proved to be a universal manifestation of thymic acute GVHD (Figures 14 and 15 of this thesis, and Dertschnig *et al.*<sup>225</sup>) - was also a hallmark of acute GVHD when transgenic HSCT recipients were used. The transfer of allogeneic T cells into RIP-mOVA mice indeed reduced total mTEC<sup>high</sup> numbers from  $\sim 5000$  (no GVHD) to  $< 1000$  (GVHD) cells/mouse after 2 and from  $\sim 2000$  (no GVHD) to  $< 200$  (GVHD) cells/mouse after 4 weeks (Figure 21). Two weeks after allo-HSCT total mTEC<sup>low</sup> numbers were reduced by approximately 50% when compared to mice without acute GVHD. This reduction was more pronounced at four weeks after allo-HSCT. Here, the presence of acute GVHD reduced total mTEC<sup>low</sup> numbers in RIP-mOVA mice from  $\sim 5000$  to  $< 500$  cells/mouse in a manner similar to non-transgenic recipients. In the haploidentical acute GVHD model ( $b \rightarrow bd$ ) described in chapter 4.1, the loss of mTEC<sup>high</sup> cells was associated with a reduction among mTEC<sup>high</sup> expressing Aire (Aire<sup>+</sup>mTEC<sup>high</sup>). In the absence of Aire expression, clonal deletion of OVA-specific CD4 T cells (OT-II) in RIP-mOVA mice is compromised,<sup>76,252,253</sup> hence I compared Aire expression in thymi isolated from RIP-mOVA mice with and without acute GVHD. In thymi of recipients of TCD bone marrow Aire<sup>+</sup> cells were as expected localised exclusively in the thymic medulla (Figure 22). Transgenic RIP-mOVA recipients did not differ from age-matched non-transgenic B6 recipients (Figure 22; panel i). However, in the presence of acute GVHD (TCD+T), Aire-expressing mTEC were neither detectable in non-transgenic (B6) nor in transgenic (RIP-mOVA) recipients (Figure 22; panels ii and iv). Taken together, the data presented in this chapter confirmed that acute thymic GVHD could be elicited in RIP-mOVA recipients as expected. With respect to impaired thymopoiesis and the defect in the Aire<sup>+</sup>mTEC<sup>high</sup> cell compartment these GVHD-induced changes were not different from non-transgenic HSCT systems.

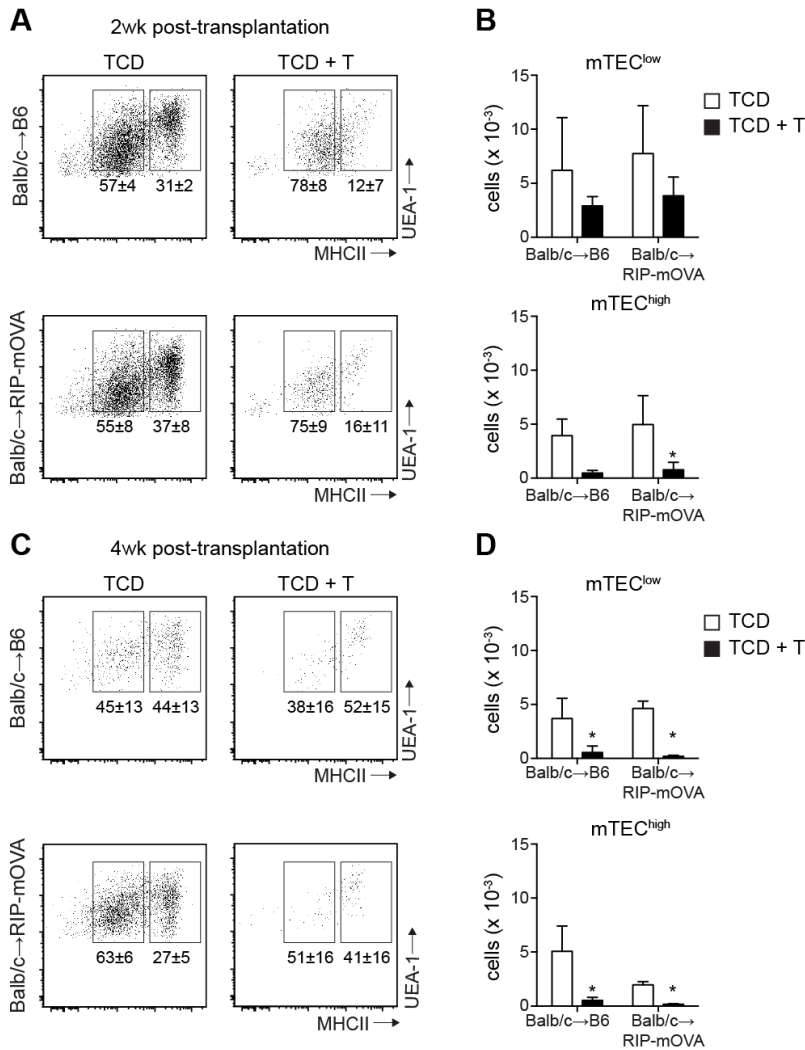


**Figure 21. Acute GVHD causes mTEC defects in RIP-mOVA mice.** mTEC<sup>high</sup> and mTEC<sup>low</sup> were analysed by flow cytometry as described in Figure 11. (A) Flow cytometry analysis identifying mTEC<sup>low</sup> and mTEC<sup>high</sup> in B6 (top panel) and RIP-mOVA (bottom panel) recipients in the presence and absence of acute GVHD 2 weeks post-transplantation. The numbers shown in each flow cytometry dot plot represent frequency (% mean ± SD) of the respective population among total mTEC. (B) Absolute cell numbers of mTEC<sup>low</sup> and mTEC<sup>high</sup> were calculated at 2 weeks post-HSCT for B6 and RIP-mOVA recipients. (C-D) The same analysis as in panels A and B was performed 4 weeks post-transplantation. The figure represents combined data from 3 independent experiments with ≥3 mice per group analysed. \**p* < 0.05, 2-way ANOVA, Sidak's multiple comparison test.

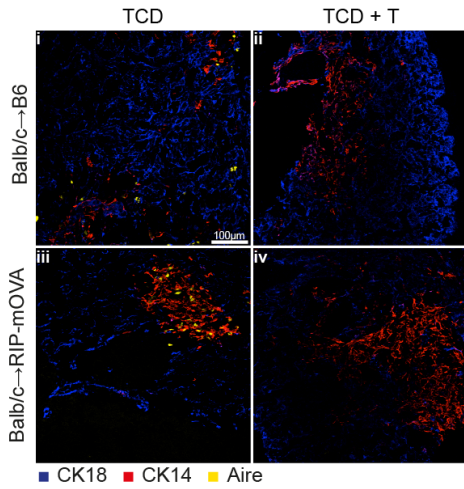


**Figure 22. Aire expression is lost in RIP-mOVA mice with acute GVHD.** Immunohistochemistry and confocal microscope analysis was performed on thymic frozen section taken from B6 and RIP-mOVA transplant recipients 2 weeks after HSCT. i) TCD Balb/c→B6; no GVHD, ii) TCD + T Balb/c→B6; acute GVHD, iii) TCD Balb/c→RIP-mOVA; no GVHD, iv) TCD + T Balb/c→RIP-mOVA; acute GVHD. Cytokeratin-18 (CK18, blue) and CK14-positive cells (red) define cTEC and mTEC, respectively. Aire<sup>+</sup> cells are shown in yellow and localise to the thymus medulla.

### 4.2.3 Acute GVHD reduces the thymic ectopic expression of the neo-self-antigen ovalbumin

Given the importance of OVA expression in mTEC for the efficacy of thymic negative selection of OVA-specific TCR,<sup>71,72,98,250,252</sup> I next determined whether acute GVHD interfered with global thymic OVA gene expression in mTEC<sup>low</sup> and mTEC<sup>high</sup>. As expected, there was no OVA expression detected in non-transgenic B6 mice, neither in mTEC<sup>low</sup>, nor in mTEC<sup>high</sup>. In allogeneically transplanted RIP-mOVA mice without disease (TCD) OVA expression was detected to the same extent in mTEC<sup>low</sup> and mTEC<sup>high</sup> (Figure 23A). These data argued for an Aire-independent regulation of OVA, since Aire expression was as expected only present in mTEC<sup>high</sup> (Figure 23B). In allogeneically transplanted RIP-mOVA mice with acute GVHD (TCD+T) the quantitative PCR data indicated that OVA mRNA levels were reduced in both mTEC<sup>low</sup> and mTEC<sup>high</sup> compared to the TCD group (Figure 23A). Aire expression was reduced at 2, but not at 4, weeks post-transplantation in mice with acute GVHD. Taken together, the data presented in this and the previous chapter demonstrated that reduced OVA expression was due to loss of OVA-expressing mTEC during acute GVHD.

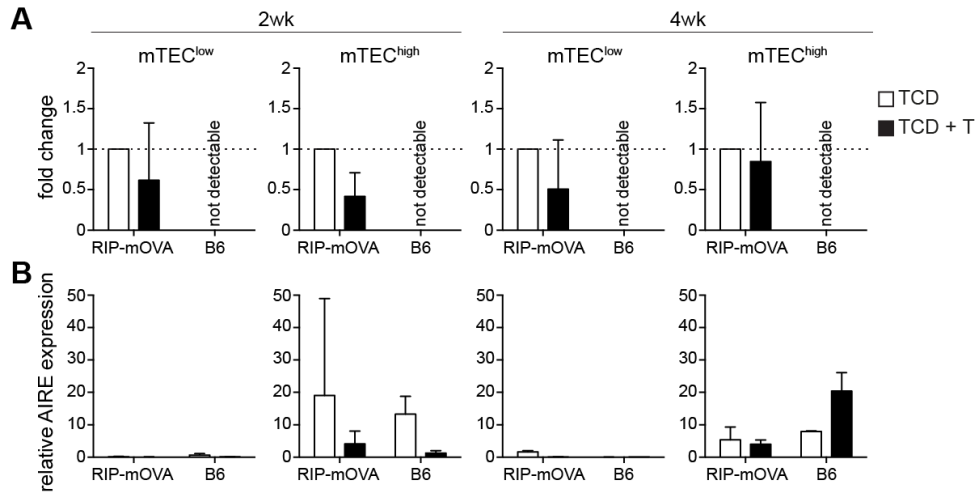


**Figure 23. OVA mRNA is decreased in acute GVHD.** Expression of OVA and Aire mRNA was determined by quantitative PCR in sorted mTEC<sup>low</sup> and mTEC<sup>high</sup> in B6 and RIP-mOVA recipients with (black bars) and without (white bars) acute GVHD. (A) OVA expression in RIP-mOVA recipients without acute GVHD is set as 1 and used as a control. Expression in RIP-mOVA recipients with acute GVHD and in B6 recipients is depicted as fold change over control. (B) Aire expression is shown as relative expression normalised to GAPDH. Analysis was done at 2 and 4 weeks post-transplantation.

#### 4.2.4 OVA-specific T cell clones escape negative selection during acute GVHD

Since efficient central tolerance induction requires adequate intrathymic OVA expression levels, the above results suggested that acute GVHD may affect negative selection of OVA-specific T cells. To directly test this hypothesis, RIP-mOVA recipients with acute GVHD were lethally re-irradiated 4-5 weeks after allogeneic HSCT (Balb/c→RIP-mOVA; H-2<sup>d</sup>→H-2<sup>b</sup>) and transplanted in a second syngeneic HSCT with TCD bone marrow mixture from CD45.1<sup>+</sup> OT-II (H-2<sup>b</sup>) and CD45.2<sup>+</sup> B6 mice (H-2<sup>b</sup>) (Figure 19). As controls, RIP-mOVA recipients without acute GVHD and non-transgenic B6 mice were used. In these OT-II→[Balb/c→RIP-mOVA] mice (H-2<sup>b</sup>→[H-2<sup>d</sup>→H-2<sup>b</sup>]) the hematopoietic system was fully replaced with cells stemming from OT-II and wt B6 donor HSC. Except in lymph nodes of RIP-mOVA mice with acute GVHD, donor chimerism in all cell lineages was >80% in thymus, spleen and lymph nodes of all experimental groups (Figure 24).

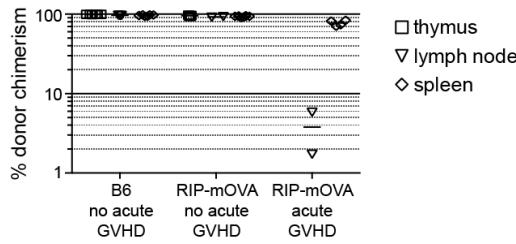


**Figure 24. Haematopoietic system is replaced by donor bone marrow.** Donor chimerism was analysed after second syngeneic HSCT (OT-II + B6→[Balb/c→RIP-mOVA]) as percentages of H-2K<sup>b+</sup> H-2K<sup>d-</sup> Thy1.1<sup>-</sup> cells among total cells in thymus, lymph node and spleen. n.d., not done. N ≥ 2

As expected, OVA-specific T cells expressing the TCR V $\alpha$ 2 V $\beta$ 5 chains and the congenic marker CD45.1 were not deleted in thymi of B6 mice without OVA expression. In these mice, CD45.1<sup>+</sup> CD4 T cells were detected at significantly higher frequencies than in RIP-mOVA mice without disease (Figure 25; 14 vs. 2%, 8 vs. 1%, and 8 vs. 3% in thymus, lymph nodes and spleen, respectively). In the latter group, adequate clonal deletion of OVA-reactive T cells resulted from normal levels of thymic OVA expression. In the absence of thymic OVA expression (OT-II→[Balb/c→B6]), CD45.1<sup>+</sup> CD4 OVA-specific T cells were not deleted in the thymus (10%) however and emerged in the periphery where they were detected in lymph nodes and spleen (Figure 25; 7 and 14%, respectively). Hence, the acute GVHD-dependent loss of OVA expression in OT-II→[Balb/c→RIP-mOVA] mice was sufficient to prevent effective negative selection of OT-II TCR and allowed the *de novo* generation of TCR V $\alpha$ 2<sup>+</sup> V $\beta$ 5<sup>+</sup> CD4 SP thymocytes (CD45.1<sup>+</sup>).

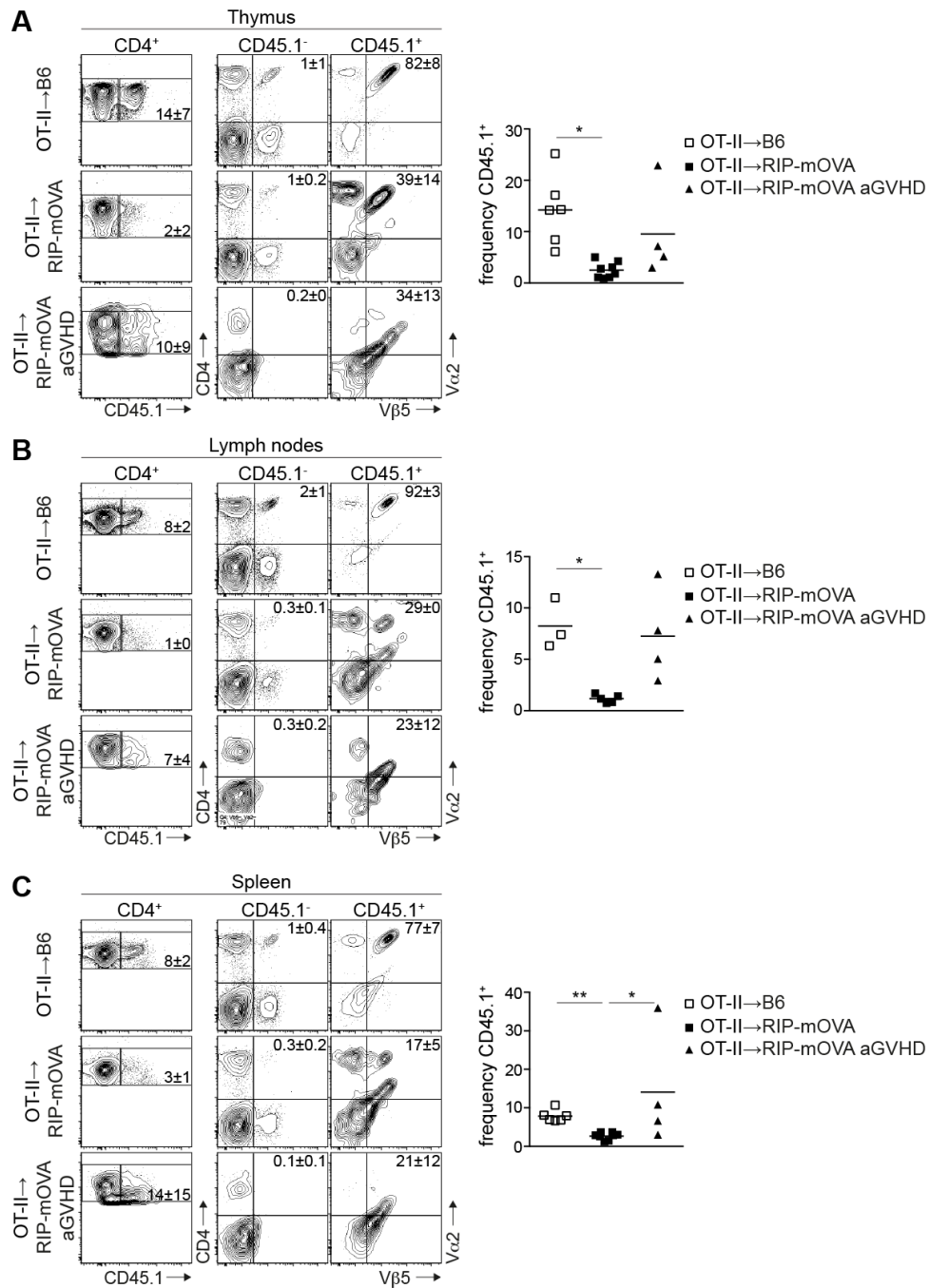


**Figure 25. OVA-specific T cells are not negatively selected during acute GVHD.**

(A) Flow cytometric analysis of thymocytes of B6, RIP-mOVA without acute GVHD and RIP-mOVA with acute GVHD transplanted with OT-II TCD bone marrow. Flow cytometry plots depict surface expression of CD4, CD45.1, V $\alpha$ 2 and V $\beta$ 5. The numbers shown in each quadrant represent frequency (mean  $\pm$  SD) of CD4<sup>+</sup> CD45.1<sup>+</sup> T cells among total CD4<sup>+</sup> SP thymocytes (left column). The numbers in the flow cytometry plots on the right represent

frequencies (mean  $\pm$  SD) of V $\alpha$ 2V $\beta$ 5 double positive thymocytes among CD45.1<sup>-</sup>CD4<sup>+</sup> and CD45.1<sup>+</sup>CD4<sup>+</sup> thymocytes, respectively. Cell analysis is restricted to live thymocytes as defined by Dapi staining. The frequencies of CD4<sup>+</sup>CD45.1<sup>+</sup> thymocytes in all three groups are summarised in a dot plot (right). The same analysis was performed in (B) lymph nodes and (C) spleen. The figure represents combined data of two independent experiments with  $\geq 3$  mice analysed per group. \* $p < 0.05$ , ANOVA.

#### 4.2.5 *De novo* generated OT-II T cells display a non-tolerant effector phenotype

To test whether OVA-specific T cells that were not negatively selected were functional and non-tolerant, expression of folate receptor 4 (FR4) and CD73 was measured on peripheral T cells. I chose to study these cell surface proteins since their expression is known to be low on non-nergic CD4<sup>+</sup> T cells.<sup>254</sup> Non-OVA-specific CD4<sup>+</sup> T cells expressed FR4 and CD73 at low levels, indicating a non-nergic phenotype in RIP-mOVA mice either with or without acute GVHD. Because expression of FR4 and CD73 was previously reported on CD4<sup>+</sup> regulatory T cells (T<sub>reg</sub>),<sup>255,256</sup> I also included Foxp3 as a marker for T<sub>reg</sub> in the analysis. The ratio T<sub>eff</sub>:T<sub>reg</sub> was increased from  $\sim 2.5$  to  $\sim 17$  in RIP-mOVA mice suffering from acute GVHD and then re-transplanted with TCD OT-II bone marrow when compared to RIP-mOVA mice without disease (Figure 26A). Thus, the frequency of T<sub>reg</sub> was diminished among the whole CD4<sup>+</sup> T cell pool in the spleen in the presence of disease (Figure 26A). OT-II T cells detected in the periphery of RIP-mOVA mice suffering from acute GVHD did not convert into T<sub>reg</sub> and displayed a FR4<sup>-</sup>CD73<sup>-</sup> non-tolerant effector phenotype (Figure 26B). These data strongly suggested - but did not finally prove - that responsiveness to self-antigen may have been sustained. The OT-II T cells had increased CD44 expression (Ag-experienced phenotype) and are larger in size, suggesting that they were capable of responding to self-peptide/MHC complexes (Figure 27).<sup>254</sup> These data suggested that OVA-specific T cells that were not negatively selected were non-nergic.

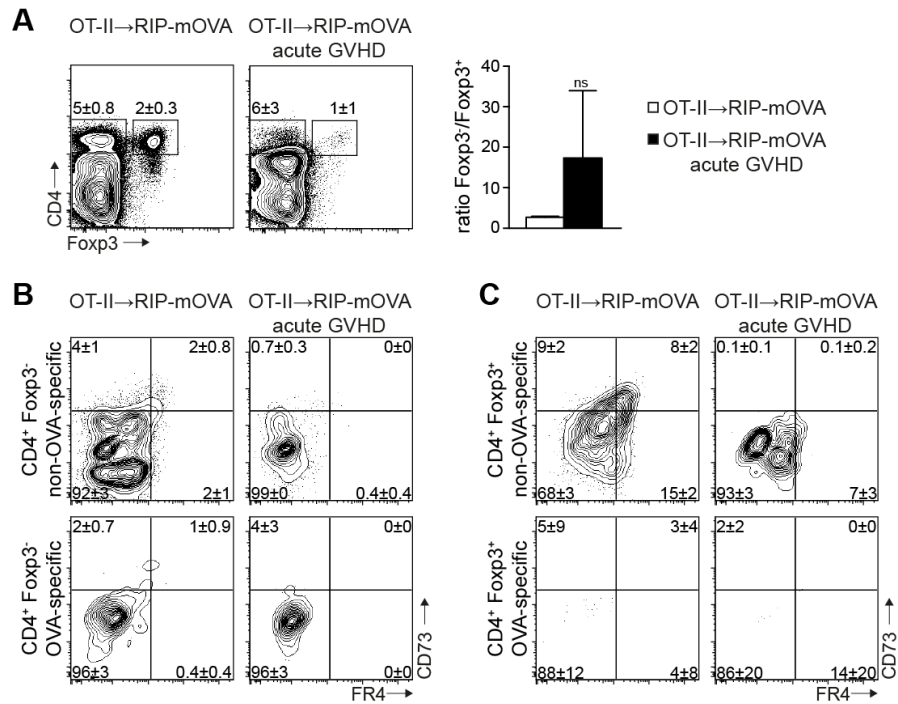


**Figure 26. OT-II T cells are non-nergic and represent non-T<sub>reg</sub> cells.** (A) Intracellular Fxp3 expression was analysed in total splenocytes in recipients without (left) and with (right) acute GVHD 4 weeks after the second syngeneic HSCT (OT-II→[Balb/c→RIP-mOVA]). Flow cytometry plots depict surface expression of CD4 versus intracellular expression of Fxp3. The numbers shown are frequencies of CD4<sup>+</sup> Fxp3<sup>-</sup> and CD4<sup>+</sup> Fxp3<sup>+</sup> cells, respectively. Bar graph shows ratio of Fxp3<sup>-</sup> versus Fxp3<sup>+</sup> CD4 T cells in RIP-mOVA mice in the presence (black) and absence (white) of acute GVHD. \**p*<0.05, Mann-Whitney U-Test. Surface expression of folate receptor 4 (FR4) and CD73 was analysed in (B) OVA-specific and non specific splenic CD4<sup>+</sup> Fxp3<sup>-</sup> T cells, and (C) in OVA-specific and non specific splenic CD4<sup>+</sup> Fxp3<sup>+</sup> T<sub>reg</sub> cells. The numbers shown represent frequencies of respective population (mean ± SD). The figure represents data from one experiment with ≥2 mice analysed per group.



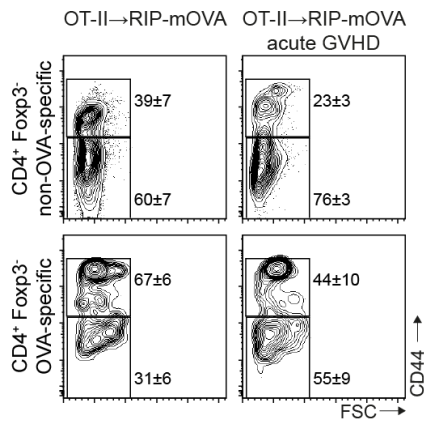


**Figure 27. OT-II cells show activated phenotype.** OVA-specific (bottom) and non-specific (top) CD4<sup>+</sup> splenic T cells were analysed for their CD44 expression. Splenocytes were isolated four 4 weeks after second syngeneic HSCT (OT-II→[Balb/c→RIP-mOVA]) from RIP-mOVA recipients with (right) and without (left) acute GVHD. The flow cytometry plots depict surface CD44 expression versus forward scatter profile. Numbers in the plots indicate frequencies (mean ± SD) of CD44<sup>low</sup> and CD44<sup>high</sup> populations among the indicated T cell population. The figure represents data from one experiment with ≥2 mice analysed per group.

In summary, the data shown in part two of the results provided a mechanism for how autoimmunity may develop in the context of acute GVHD. In the presence of disease, a reduction in mTEC pool size causes loss of an individual TRA that results in a failure to establish central tolerance to this TRA. In consequence TRA-reactive T cells can be exported to the periphery of allo-HSCT recipients.

### **4.3 Epithelial cytoprotection with fibroblast growth factor-7 (Fgf7) sustains ectopic expression of tissue-restricted antigens in the thymus during murine acute GVHD**

#### **4.3.1 Fgf7 sustains the thymic mTEC<sup>high</sup> compartment including Aire expression**

Given my observations above, approaches for mTEC cytoprotection may increase thymus-dependent T-cell production and may also prevent the emergence of thymus-dependent autoreactive T cells<sup>180</sup> and thus alter autoimmune outcome. Since previous studies by Rossi et al.<sup>216,239</sup> described that administration of the epithelial growth factor Fgf7 acts directly on TEC and results in increased thymopoiesis, I chose to study the role of Fgf7 on mTEC<sup>high</sup> in the course of acute GVHD. Because efficient central tolerance requires the full scope of TRA, which is only ensured by a sufficient large enough mTEC<sup>high</sup> cell pool, I asked whether the mTEC<sup>high</sup> compartment size and heterogeneity were sustained by using Fgf7 as a strategy for epithelial cytoprotection. First, Fgf7's effect on thymus size and structure and T cell development was assessed to confirm the previous findings.<sup>216</sup> Fgf7 was administered in a peritransplant manner (i.p. 5 mg/kg/day from day -3 to 3 after allogeneic HSCT) in recipients of allogeneic HSCT (*b*→*bd* +Fgf7) as described.<sup>216,239</sup> Confirming previous data, thymus size was increased in Fgf7 treated mice with acute GVHD compared to untreated animals (Figure 28A).<sup>216</sup> Furthermore, structural organisation and thymic T-cell development was normal in those mice, despite the continued presence of acute GVHD in other target organs. The protective effect of Fgf7 was independent of the presence of donor T cells, as suggested previously,<sup>216</sup> since the absolute numbers of thymus-infiltrating donor T cells were comparable to untreated recipient with acute GVHD (Figure 28B).

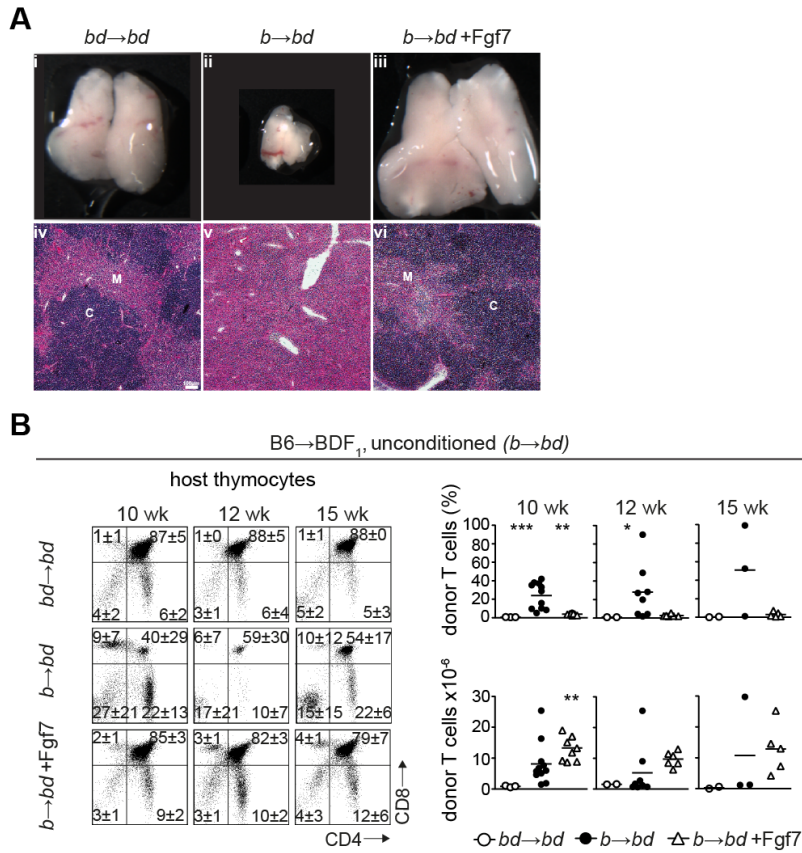


**Figure 28. Fgf7 boosts thymopoiesis and restores thymic architecture.** Acute GVHD was induced by the transfer of B6.CD45.1 splenic T cells to unirradiated BDF<sub>1</sub> recipients (*b*→*bd*; ●). Syngeneically transplanted BDF<sub>1</sub> mice serve as controls without disease (*bd*→*bd*; ○). Fgf7 was i.p. injected into one group of BDF<sub>1</sub> recipients that underwent allogeneic transplantation (*b*→*bd*+Fgf7; △). (A) Photographic pictures of thymi without acute GVHD (i; *bd*→*bd*), with acute GVHD (ii; *b*→*bd*) and with acute GVHD but after Fgf7 treatment (iii; *b*→*bd*+Fgf7) (top row). Histopathology of thymic section was analysed by H&E staining at 2 weeks after transplantation (iv; *bd*→*bd*, v; *b*→*bd*, vi; *b*→*bd*+Fgf7). M, medulla; C, cortex. (B) The flow cytometry dot plots depict surface expression of CD4 and CD8 on host thymocytes. Cell analysis is restricted to live thymocytes as defined by forward/side scatter and exclusion of cells staining positive for propidium iodide. The numbers shown in each quadrant represent frequencies (% of the respective populations, mean ± SD). The figure represents combined data from four separate experiments; with an aggregate of 11 mice analysed for each group. Infiltration of donor-derived CD45.1<sup>+</sup> T cells into host thymi is given as frequency (% among total thymic cells) and absolute cell numbers (x 10<sup>6</sup>, mean ± SD). \**p*<0.05, Mann-Whitney U-test.

The TEC compartment was analysed in 8, 10, 12 and 15 week old recipients (4 days, 2, 4 and 7 weeks post-transplantation). Fgf7 failed to prevent initial mTEC<sup>high</sup> cell loss in  $b \rightarrow bd$  recipients (Figure 29). However, Fgf7 maintained stable numbers of mTEC<sup>high</sup> ( $\geq 4 \times 10^3$  cells/mouse) which were significantly higher compared to  $b \rightarrow bd$  recipients not treated with Fgf7 ( $\leq 10^3$  cells/mouse) for the whole observation time (Figure 29).

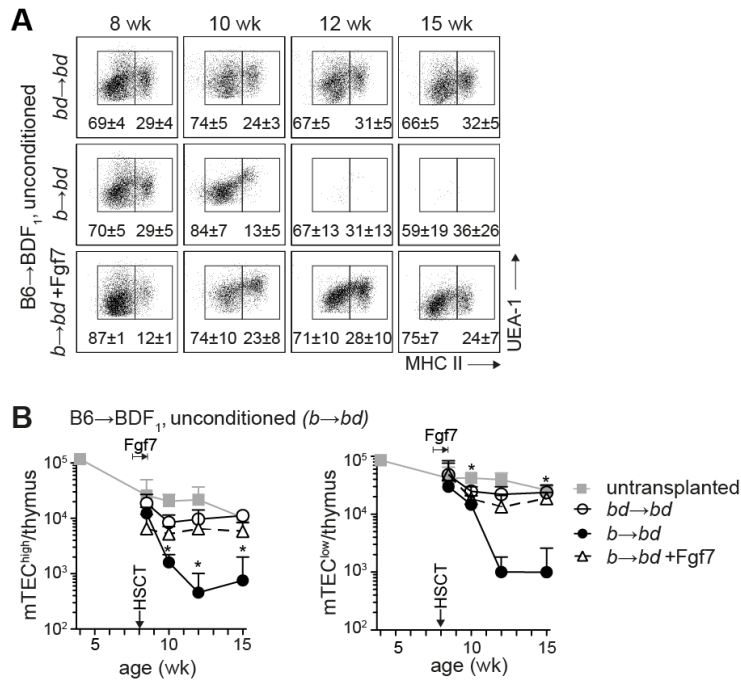


**Figure 29. Fgf7 sustains mTEC compartment size.** The mTEC compartment was analysed after Fgf7 administration (i.p. 5 mg/kg/day; day -3 to day +3 after allogeneic HSCT). (A) mTEC<sup>high</sup> and mTEC<sup>low</sup> were analysed by flow cytometry as a function of age using the strategy described in Figure 11. Bottom row depicts flow cytometry plot of allogeneically transplanted BDF<sub>1</sub> recipients that underwent Fgf7 treatment ( $b \rightarrow bd + Fgf7$ ). The numbers shown in each flow cytometry dot plot represent frequency (% mean  $\pm$  SD) of the respective population among total mTEC. The figure represents combined data of individual mice from 6 separate experiments.  $bd \rightarrow bd$ ; syngeneic controls, no acute GVHD.  $b \rightarrow bd$ ; allogeneic HSCT, acute GVHD. (B) Absolute numbers of mTEC<sup>high</sup> (left) and mTEC<sup>low</sup> are analysed as a function of recipient age in three groups of a haploidentical transplantation model. Acute GVHD was induced in 8-week old unconditioned BDF<sub>1</sub> recipients ( $b \rightarrow bd$ , black circles). Cell numbers in allogeneic recipients that were injected with Fgf7 are depicted as white triangles. Untransplanted BDF<sub>1</sub> mice (grey squares) or syngeneically transplanted mice ( $bd \rightarrow bd$ , open circles) serve as controls. A total of 6 experiments were performed, with 3 to 5 mice per group and experiment. \* $p < 0.05$ , analysis of variance (ANOVA).

Cell numbers were comparable to syngeneically transplanted control animals and to untransplanted, age-matched naïve mice. Furthermore, normal cell numbers of mTEC<sup>low</sup> were present in mice with acute GVHD but treated with Fgf7 ( $\geq 10^4$  cells/mouse and  $\leq 10^3$  cells mouse with and without treatment, respectively). Upon Fgf7 treatment the mTEC<sup>high</sup> subset expressing Aire was preserved at  $\sim 3000$  cells/mouse during acute GVHD, which contrasted the depletion of these cells to numbers as low as 300 cells/mouse in untreated animals with acute GVHD (Figure 30).

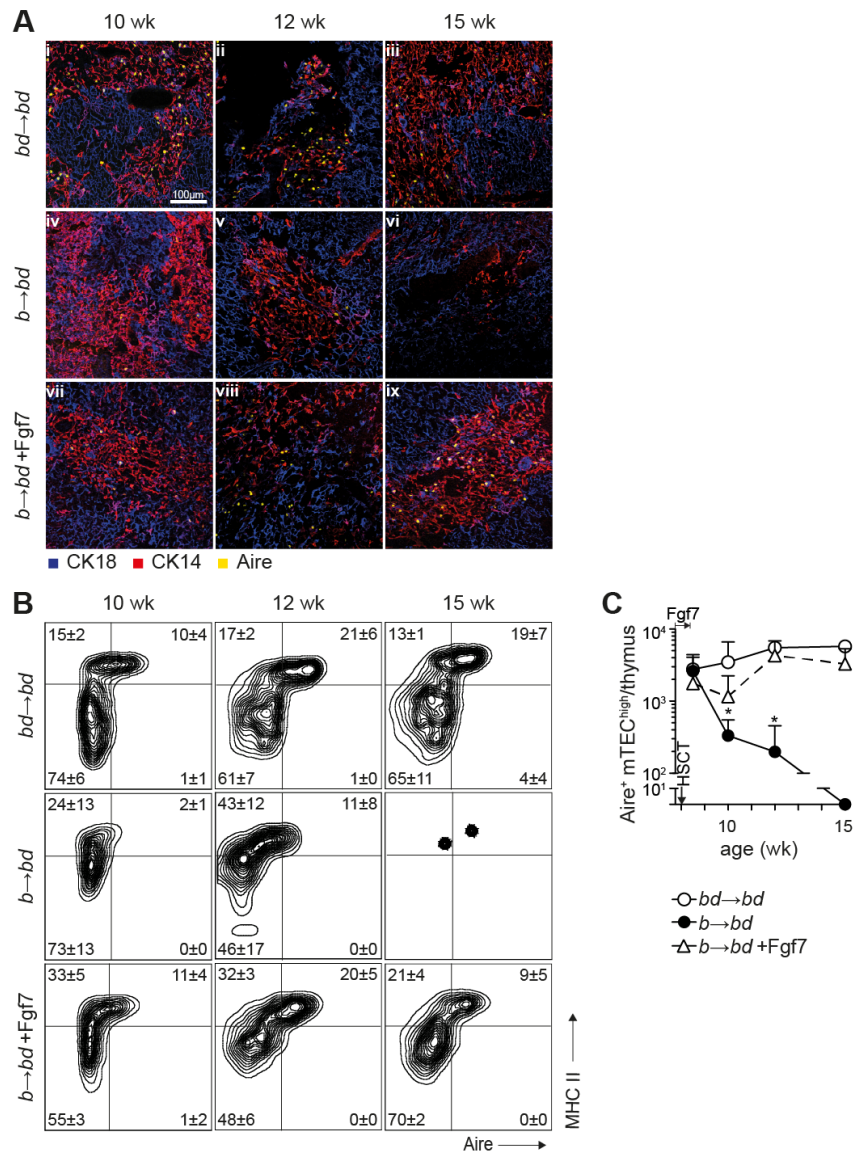


**Figure 30. Fgf7 rescues Aire expressing mTEC.** Aire expression was qualitatively and quantitatively analysed in recipients' thymi. (A) OCT embedded thymi from unconditioned transplant recipients at ages 10, 12, and 15 weeks (i.e. 2, 4, and 7 weeks after transplantation) were cut in sections and analysed by confocal microscope. Sections were stained for Cytokeratin-18 (CK18, blue; cortex), CK14 (red; medulla) and Aire (yellow). Analyses of allogeneically transplanted mice with Fgf7 treatment are shown in the bottom row. [i-iii] *bd*→*bd*, [iv-vi] *b*→*bd*, [vii-ix] *b*→*bd* + Fgf7. (B) The flow cytometry plots display intracellular Aire and surface MHC class II expression of DAPI<sup>+</sup>CD45<sup>+</sup>EpCam<sup>+</sup>Ly51<sup>+</sup>UEA-1<sup>+</sup> mTEC. Numbers represent frequencies (%) of cells (mean ± SD). Bottom row shows data of *b*→*bd* + Fgf7 recipients. (C) Based on flow cytometry data absolute numbers of Aire<sup>+</sup>mTEC<sup>high</sup> were calculated per individual recipient mouse (mean ± SD). Syngeneic HSCT, *bd*→*bd*, open circles; allogeneic HSCT, *b*→*bd*, black circles; allogeneic HSCT + Fgf7

treatment,  $b \rightarrow bd$  +Fgf7, open triangles. A total of 5 experiments were performed with 3 to 5 mice per group.  $*p < 0.05$ , ANOVA.

To investigate if increased cell numbers upon Fgf7 treatment were due to enhanced proliferation within the mTEC compartment, I analysed BrdU incorporation. I first analysed BrdU incorporation and cell cycle during a short time window 2 weeks after transplantation. To this end, recipient mice were intraperitoneally (i.p.) injected with BrdU and analysed 16 hours afterwards. 11% of mTEC<sup>high</sup> cells were proliferating (in S phase) in syngeneically transplanted mice, whereas frequency for mTEC<sup>low</sup> cells was slightly lower (9%) (Figure 31A, left panel). This observation was consistent with published data from normal mice.<sup>57</sup> Treatment with the mitogenic agent Fgf7 did not result in increased proliferation rates of mTEC<sup>high</sup>. In mice suffering from acute GVHD without Fgf7 treatment, 26% of mTEC<sup>high</sup> were in S phase, whereas prior Fgf7 administration resulted in only 16% proliferating mTEC<sup>high</sup> (Figure 31A, middle and right panel). The same observation was made for mTEC<sup>low</sup> cells. The frequency of proliferating mTEC<sup>low</sup> in untreated mice with acute GVHD was twice as high as in GVHD-positive animals that underwent Fgf7 treatment (Figure 31A, middle and right panel; 11 vs. 5%). This snapshot analysis revealed that 2 weeks after transplantation, the mitogenic effect of earlier Fgf7 treatment was not existent. To analyse kinetics of cell proliferation and to test whether higher turnover within the mTEC compartment was present earlier, a pulse chase experiment was performed. Here, mice were fed from day -3 to 3 after HSCT with drinking water supplemented with BrdU (0.8 mg/ml). The time period of BrdU feeding corresponded to the time frame of Fgf7 therapy. BrdU incorporation into mTEC was analysed at 8.5, 10 and 12 weeks of age (4 days, 2, 4 weeks post-transplantation, respectively). Consistent with reports that mTEC are continuously replaced in adulthood,<sup>57,66</sup> ~5% of mTEC underwent cell division within 1 week in the  $b \rightarrow bd$  and  $bd \rightarrow bd$  transplant groups (Figure 31B). This frequency increased to ~15% in mice with acute GVHD but that were treated with Fgf7. Label retention analyses indicated high turnover of mTEC in response to Fgf7 in  $b \rightarrow bd$  recipients as BrdU concentration declined to <10% in 12 week old recipients. This analysis of proliferation history showed that rescue of mTEC<sup>high</sup> numbers was therefore the consequence of enhanced proliferation within the entire mTEC compartment.

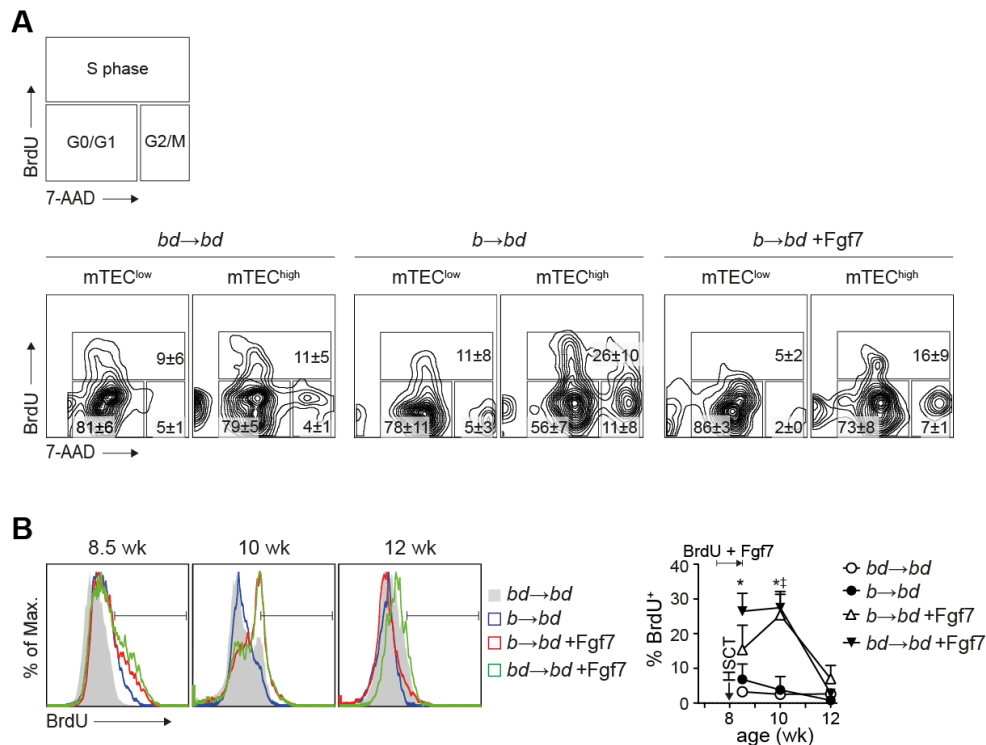


**Figure 31. Fgf7 enhances proliferation of the mTEC compartment.** Analysis of BrdU incorporation. (A) Cell cycle analysis of mTEC<sup>low</sup> and mTEC<sup>high</sup> 2 weeks after GVHD induction. BrdU was i.p. injected 16 hours prior to analysis in syngeneically recipients and untreated or Fgf7-treated allogeneically recipients. Flow cytometry plots depict intracellular expression of BrdU and 7-AAD (7-Aminoactinomycin D), which marks the DNA. The numbers represent frequencies of cells in G<sub>0</sub>/G<sub>1</sub> (BrdU<sup>-</sup> 7-AAD<sup>-</sup>), S (BrdU<sup>+</sup> 7-AAD<sup>-/+</sup>) and G<sub>2</sub>/M phase (BrdU<sup>-</sup> 7-AAD<sup>+</sup>). (B) Analysis of mTEC proliferation in response to Fgf7. Eight-week-old BDF<sub>1</sub> mice were left untreated or were treated with Fgf7 from days -3 to +3 after allogeneic HSCT. All mice simultaneously received 0.8 mg/ml BrdU in their drinking water. mTEC were analysed for BrdU incorporation at the indicated ages after transplantation. Left: flow cytometry histogram. Right: BrdU<sup>+</sup> cells (%) ±SD, \**p*<0.001, ANOVA, acute GVHD vs. mice without acute GVHD.

#### 4.3.2 Fgf7 administration sustains a more diverse TRA transcriptome in mTEC<sup>high</sup> during acute GVHD

Because treatment of mice suffering from acute GVHD with Fgf7 restored the mTEC<sup>high</sup> compartment including Aire-expression, I next asked whether Fgf7 also sustained the heterogeneity of TRA expression by



mTEC<sup>high</sup> (Table 3). To quantify changes of global gene expression patterns in response to Fgf7, a correlation matrix analysis was performed (see section 4.1.5). During early acute GVHD, the TRA spectrum was not preserved by Fgf7 indicated by a Pearson's  $r = 0.635$  versus  $bd \rightarrow bd$  mice. However, a broader array of TRA was expressed by 4 and 7 weeks after allogeneic HSCT as indicated by an expression profile that was closer to that of age-matched  $bd \rightarrow bd$  controls (Pearson's  $r = 0.722$  and  $0.807$ , respectively) (Figure 32A, C). Hence, peritransplant administration of Fgf7 sustained a more diverse TRA transcriptome during acute GVHD. Furthermore, the Ub expression spectrum was maintained by Fgf7 shown by higher Pearson's  $r$  values than without treatment (Pearson's  $r = 0.8242$  for  $bd \rightarrow bd$  versus  $b \rightarrow bd$  +Fgf7; Pearson's  $r = 0.7526$  for  $bd \rightarrow bd$  versus  $b \rightarrow bd$  +Fgf7) (Figure 32B, C). Expression levels of a selection of genes that were altered by acute GVHD were plotted as a heatmap to illustrate the effect of Fgf7 (Figure 33). Individual TRA expression patterns were differentially affected by acute GVHD and Fgf7 as some but not all Aire-dependent TRA returned to nearly normal expression in the observation period. An increase in gene expression of three Aire-dependent TRA (Spt1, Mup1 and Csn1s2a) was detected in  $b \rightarrow bd$  +Fgf7 mice by qPCR (Figure 34). Epithelial cell adhesion molecule (EpCam), which is specifically expressed in epithelial tissues<sup>257</sup>, and forkhead box N1 (Foxn1), whose expression characterises the thymic epithelial lineage,<sup>258</sup> served as controls. EpCam and Foxn1 expression was neither downregulated by acute GVHD, nor increased due to Fgf7 treatment.

**Table 3.**

(A) Genes upregulated in response to Fgf7 during acute GVHD (&gt;5-fold)

| Gene                          | Accession#   | Name   | Fold change<br><i>b</i> → <i>bd</i> + Fgf7, 15 wk<br>vs. <i>b</i> → <i>bd</i> , 12 wk<br>(rel. expression) |   |       |
|-------------------------------|--------------|--|--|---|-------|
|                               |              |  | rel.<br>expr.  | <i>b</i> → <i>bd</i> vs.<br><i>bd</i> → <i>bd</i><br>10wk 12 wk |       |
| <i>TRA are shaded in grey</i> |              |  |  |   |       |
| Gsta1                         | NM_008181    | glutathione S-transferase, alpha 1           | <b>24.07</b>   | 0.302   | 0.028 |
| Mzt1                          | NM_175245    | testis-specific serine kinase 3              | <b>17.39</b>   | 0.972   | 0.421 |
| Tac1                          | NM_009311    | tachykinin 1                                 | <b>16.24</b>   | 0.509   | 0.045 |
| Gsta2                         | NM_008182    | glutathione S-transferase, alpha 2           | <b>16.06</b>   | 0.301   | 0.041 |
| Gmnn                          | AF068780     | serine (or cysteine) peptidase inhibitor     | <b>14.63</b>   | 1.459   | 0.252 |
| Gm10639                       | NM_001122660 | predicted gene 10639                         | <b>13.84</b>   | 0.291   | 0.047 |
| Cyb5d1                        | NM_001045525 | cytochrome b5 domain containing 1            | <b>13.04</b>   | 0.897   | 0.404 |
| 4930420K17Rik                 | BC147127     | ribosomal protein L34                        | <b>12.76</b>   | 1.024   | 0.052 |
| Spink5                        | NM_001081180 | SRY-box containing gene 8                    | <b>11.60</b>   | 0.893   | 0.018 |
| Apool                         | NM_026565    | apolipoprotein L 7e                          | <b>11.59</b>   | 0.991   | 0.118 |
| Fam175b                       | NM_198017    | gap junction protein, delta 3                | <b>11.26</b>   | 1.114   | 0.106 |
| Taf1d                         | AK161656     | TATA box binding protein (Tbp) assoc. factor | <b>10.96</b>   | 0.455   | 0.322 |
| Ddah1                         | NM_026993    | dimethylarginine dimethylaminohydrolase 1    | <b>10.53</b>   | 0.765   | 0.341 |
| LOC672291                     | BC128281     | similar to Ig kappa chain V-V region MOPC    | <b>9.85</b>  | 0.507   | 0.915 |
| Ccdc58                        | NM_198645    | transmembrane protein 167B                   | <b>9.69</b>  | 1.055   | 0.139 |
| Calml4                        | NM_138304    | calmodulin-like 4                            | <b>9.65</b>  | 0.198   | 0.052 |
| Defb5                         | NM_030734    | defensin beta 5                              | <b>9.51</b>  | 0.145   | 0.749 |
| 1110032A03Rik                 | NM_023483    | RIKEN cDNA 1110032A03 gene                   | <b>8.94</b>  | 0.411   | 0.123 |
| D230041D01Rik                 | AK141161     | RIKEN cDNA D230041D01 gene                   | <b>8.94</b>  | 0.563   | 0.404 |
| Ccnc                          | NM_016746    | zinc finger, DHHC domain containing 11       | <b>8.40</b>  | 1.033   | 0.120 |
| Mir677                        | NR_030442    | predicted gene 9890                          | <b>8.39</b>  | 0.888   | 0.479 |
| Igf1                          | NM_010512    | insulin-like growth factor 1                 | <b>8.26</b>  | 0.311   | 0.070 |
| Tslp                          | NM_021367    | thymic stromal lymphopoietin                 | <b>8.25</b>  | 0.297   | 0.151 |

|               |               |   |             |              |              |
|---------------|---------------|---|-------------|--------------|--------------|
| Rock2         | ENSMUST116446 | scavenger receptor class A, member 3            | <b>7.64</b> | <i>1.391</i> | <i>0.403</i> |
| Gca           | NM_145523     | grancalcin                                      | <b>7.64</b> | <i>0.596</i> | <i>0.120</i> |
| Spink3        | NM_009258     | serine peptidase inhibitor                      | <b>7.32</b> | <i>0.152</i> | <i>0.040</i> |
| Ear1          | NM_007894     | eosinophil-associated, ribonuclease A family,1  | <b>7.07</b> | <i>0.300</i> | <i>0.031</i> |
| Apoa4         | NM_007468     | apolipoprotein A-IV                             | <b>6.99</b> | <i>0.106</i> | <i>0.050</i> |
| Fam19a1       | NM_182808     | family with sequence similarity 19 member A1    | <b>6.93</b> | <i>0.403</i> | <i>0.153</i> |
| Hnf4g         | NM_013920     | hepatocyte nuclear factor 4, gamma              | <b>6.89</b> | <i>0.333</i> | <i>0.067</i> |
| Retnla        | NM_020509     | resistin like alpha                             | <b>6.76</b> | <i>0.067</i> | <i>0.107</i> |
| Ucma          | NM_001113558  | upper zone of growth plate and cartilage matrix | <b>6.75</b> | <i>0.384</i> | <i>0.094</i> |
| Fabp7         | NM_021272     | fatty acid binding protein 7                    | <b>6.64</b> | <i>0.399</i> | <i>0.044</i> |
| 5730455O13Rik | NM_001081075  | RIKEN cDNA 2700078E11 gene                      | <b>6.52</b> | <i>1.082</i> | <i>0.207</i> |
| A630095E13Rik | NM_001033325  | RIKEN cDNA A630095E13 gene                      | <b>6.25</b> | <i>0.314</i> | <i>0.175</i> |
| Il1rl2        | NM_133193     | interleukin 1 receptor-like 2                   | <b>6.20</b> | <i>0.472</i> | <i>0.093</i> |
| Scgb1a1       | NM_011681     | secretoglobin, family 1A, member 1              | <b>6.19</b> | <i>0.037</i> | <i>0.030</i> |
| Fabp2         | NM_007980     | fatty acid binding protein 2                    | <b>6.03</b> | <i>0.058</i> | <i>0.041</i> |
| Ifi205        | NM_172648     | interferon activated gene 205                   | <b>6.01</b> | <i>2.099</i> | <i>0.380</i> |
| Fam126b       | NM_172513     | family with sequence similarity 126             | <b>5.91</b> | <i>0.759</i> | <i>0.154</i> |
| Rnf113a2      | NM_025525     | integrin alpha M                                | <b>5.86</b> | <i>0.843</i> | <i>0.158</i> |
| Polr2j        | NM_011293     | mediator of RNA polymerase I transcription,18   | <b>5.63</b> | <i>1.361</i> | <i>0.093</i> |
| Clec12b       | NM_027709     | C-type lectin domain family 12 member B         | <b>5.53</b> | <i>2.078</i> | <i>0.796</i> |
| Olfir98       | NM_146510     | dual adaptor for phosphotyrosine                | <b>5.52</b> | <i>1.396</i> | <i>0.463</i> |
| Thap6         | NR_028429     | THAP domain containing 6                        | <b>5.27</b> | <i>0.600</i> | <i>0.372</i> |
| Mir680-2      | NR_030448     | SH3 domain binding glutamic acid-rich p-like 3  | <b>5.23</b> | <i>0.713</i> | <i>0.237</i> |
| Igj           | NM_152839     | cryptochrome 2                                  | <b>5.22</b> | <i>1.196</i> | <i>0.760</i> |
| Fabp9         | NM_011598     | fatty acid binding protein 9                    | <b>5.14</b> | <i>0.268</i> | <i>0.085</i> |
| Uevld         | NM_001040695  | Ngg1 interacting factor 3-like 1                | <b>5.13</b> | <i>1.449</i> | <i>1.090</i> |
| C130021I20Rik | AK147796      | RIKEN cDNA 4930430A15 gene                      | <b>5.13</b> | <i>0.970</i> | <i>1.123</i> |
| Styx          | NM_019637     | smu-1 suppressor of mec-8 and unc-52 homol.     | <b>5.05</b> | <i>1.099</i> | <i>0.319</i> |

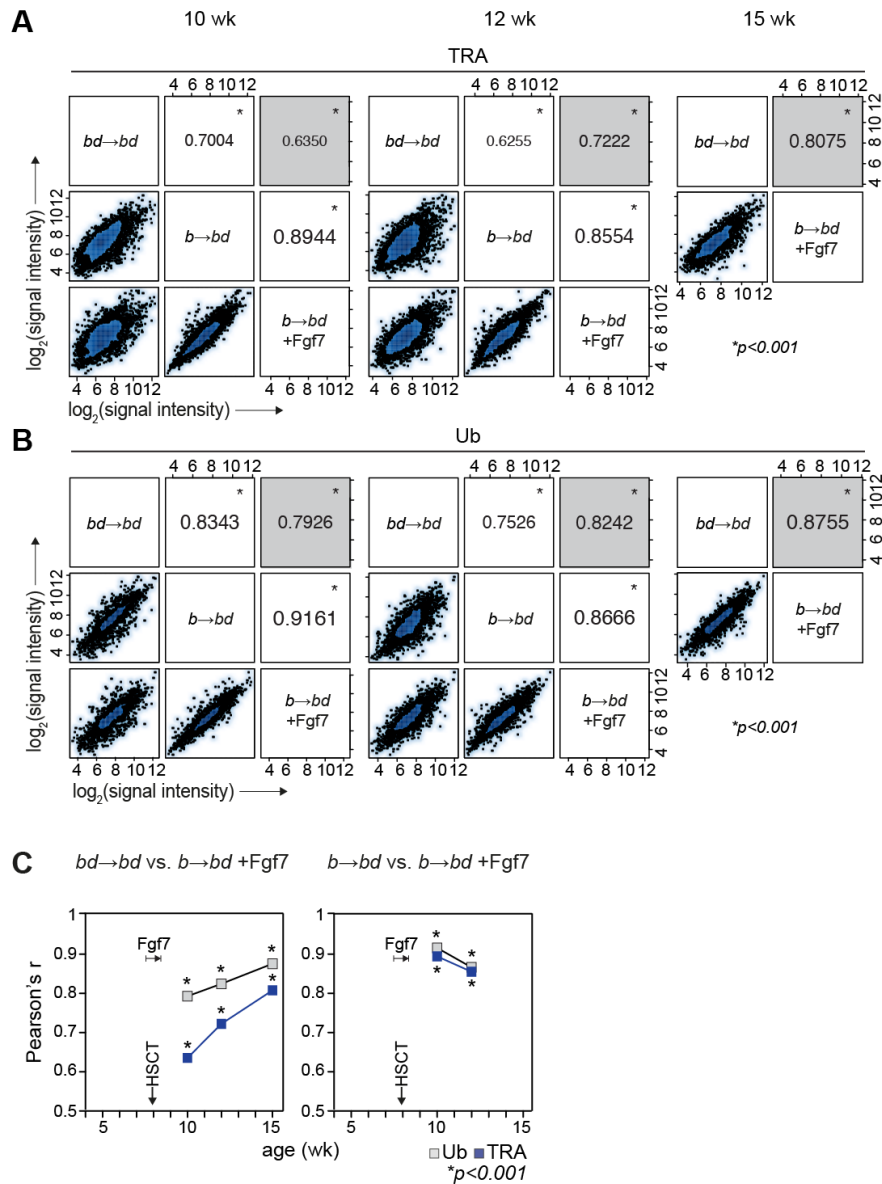


**Figure 32. Peritransplant administration of Fgf7 sustains a more diverse TRA transcriptome in mTEC<sup>high</sup> during acute GVHD.** The linear relationship of global gene expression between two experimental groups is tested independently for (A) TRA and (B) ubiquitously expressed transcripts, Ub. In a correlation matrix analysis, signal intensities ( $\log_2$ ) of individual transcripts are plotted and the Pearson's correlation coefficient  $r$  between two variables is individually calculated as a function of recipient age. Numbers in each quadrant (Fgf7 treatment is shaded in grey) indicate Pearson's  $r$  values between the two variables tested. The asterisk (\*) symbol indicates a  $p < 0.001$  value for the quality of any measured Pearson's  $r$  at the given time point for TRA or Ub. (C) Pearson's correlation coefficient  $r$  is shown as a function of age and time after transplantation for Ub (grey squares) and TRA (blue squares).  $*p < 0.001$  of Pearson's  $r$ .

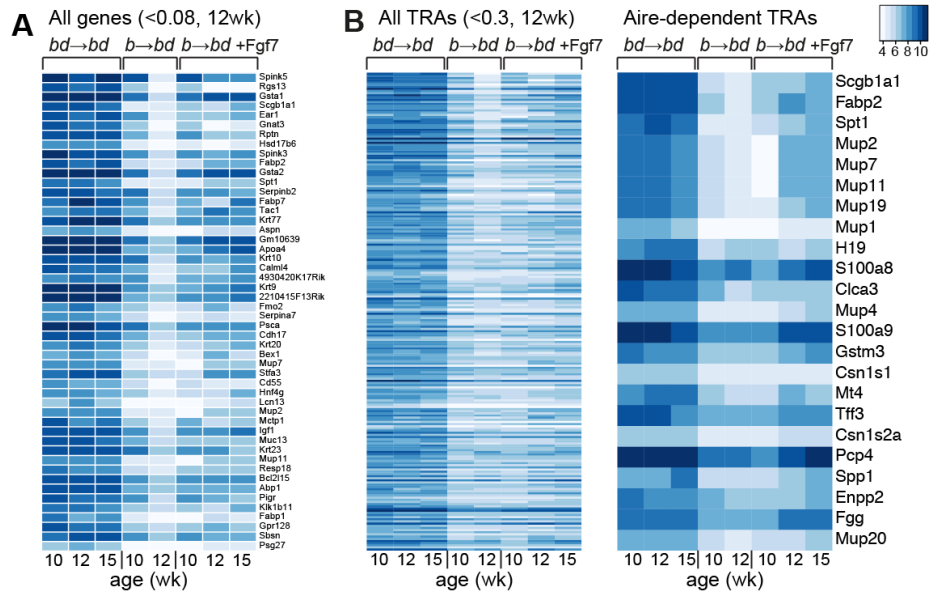


**Figure 33. Individual TRA expression patterns are differentially affected by acute GVHD and Fgf7.** Expression levels of individual genes expressed in mTEC<sup>high</sup> are given in a heatmap as colour coded log<sub>2</sub> value of signal intensities. (A) The map is sorted according to relative expression of genes in mTEC<sup>high</sup> (*b*→*bd* vs. *bd*→*bd* mice; 12 week old) and contains all TRA with a relative expression of <0.08 (which equals a 12.5-fold decrease in signal intensities of all genes) during acute GVHD in age-matched mice. (B) Left panel: The map is sorted according to relative expression of genes in mTEC<sup>high</sup> (*b*→*bd* vs. *bd*→*bd* mice; 12 week old) and contains all TRA with a relative expression of <0.3 (~3-fold decrease) during acute GVHD in age-matched mice. Enhancement of TRA expression in response to Fgf7 was detectable by higher signal intensities of individual genes. Right panel: Aire-dependent TRA were sorted as before.

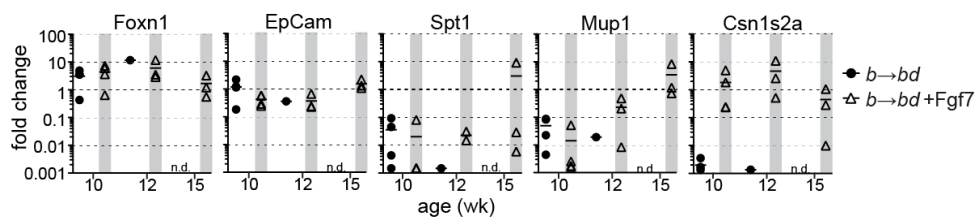


**Figure 34. Quantitative PCR confirms microarray data.** Microarray data of selected genes is verified by quantitative PCR (qPCR). Expression in syngeneically transplanted recipients was set as 1 (thick, dashed line) and used as a control. Expression in allogeneically transplanted recipients that were left untreated or treated with Fgf7 is shown as x-fold

change over controls as a function of recipient's age. Foxn1, forkhead box N1; EpCam, epithelial cell adhesion molecule; Spt1, salivary protein 1; Mup1, major urinary protein 1; Csn1s2a, casein alpha s2-like A (casein g). n.d., not done.

I hypothesised that Fgf7 restored TRA expression independently of their signal intensity and that treatment did not preferentially affect Aire-dependent TRA. To test this assumption, multidensity histogram analysis was performed (Figure 35). In this analysis signal intensities of individual transcripts of Ub, Aire-independent and Aire-dependent TRA were plotted against transcript frequencies. Only transcripts whose expression levels were decreased during acute GVHD by greater than 3-fold at 2 and 4 weeks after allogeneic HSCT (corresponding to genes in lower left quadrant Q2 of Figure 17A), were included in the analysis. The data demonstrated that signal intensity distribution was similar for all three gene pools in syngeneically transplanted mice ( $bd \rightarrow bd$ ; Figure 35, top panels). Since signal intensities did not differ between Ub, Aire-independent and Aire-dependent TRA, the finding of an enrichment of TRA among downregulated genes during acute GVHD was independent of signal intensities, but rather caused by a loss of  $mTEC^{high}$  (Figure 35, middle panels). Fgf7 treatment of  $b \rightarrow bd$  mice partially restored both Aire-dependent and Aire-independent TRA ( $b \rightarrow bd + Fgf7$ ; Figure 35 lower panels). Thus, no preference for restoration of Aire-dependent TRA by Fgf7 was observed. I interpreted this data as such that Fgf7 restored the whole  $mTEC^{high}$  compartment, and not only  $Aire^+mTEC^{high}$ . This resulted in Fgf7 being efficient to restore both, Aire-independent and Aire-dependent TRA.

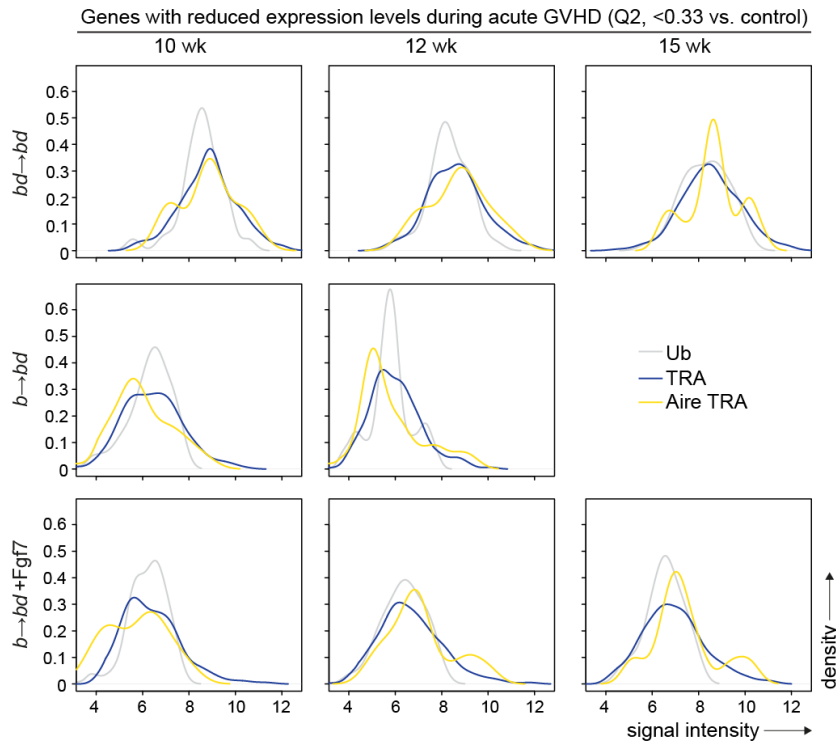


**Figure 35. Fgf7 administration alters thymic expression of TRA independently of their signal intensity.** Multidensity histogram analyses of TRA and Ub whose expression levels are decreased during acute GVHD by greater than 3-fold at 2 and 4 weeks after allogeneic HSCT (10 and 12-week old recipients, respectively). Data shown corresponds to quadrant Q2 of Figure 17 with a total of 280 tested transcripts. Signal intensities of individual transcripts in three different gene pools are plotted against transcript frequencies (density). Ub (grey), Aire-independent TRA (dark blue) and Aire-dependent TRA (yellow).

### 4.3.3 Fgf7 administration alters thymic expression of TRA independently of their tissue specificity and acute GVHD

Finally, based on the aforementioned results regarding the tissue specificity of downregulated TRA, I asked whether Fgf7 specifically affected TRA that were expressed mainly in chronic GVHD target tissues. Both the effects of Fgf7 on TRA in mice without disease ( $bd \rightarrow bd$ ) (Figure 36A) and with acute GVHD ( $b \rightarrow bd$ ) (Figure 36B) were analysed. The data clearly demonstrated that neither in the absence nor in the presence of disease an enrichment of genes that are typically expressed in tissues known to be

targets of chronic GVHD was present. Notably, analysis of tissue representation of TRA whose expression levels were lower during acute GVHD but normal in response to Fgf7 revealed that genes segregated at similar high frequencies for their tissue expression profiles as shown on page 52 (Figure 36C). These data demonstrated that the Fgf7 effect was not specific for genes that are expressed mainly in chronic GVHD target tissues.

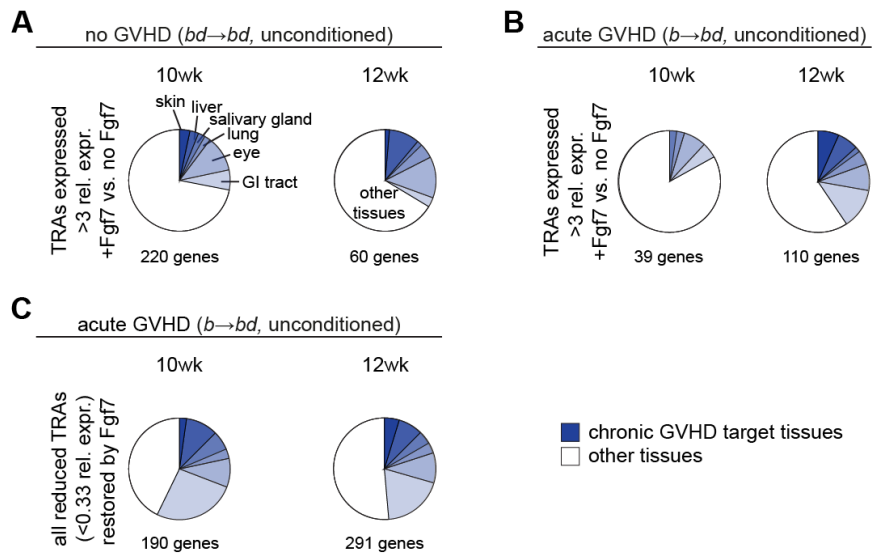


**Figure 36. Fgf7 administration alters thymic expression of TRA independently of their tissue specificity and acute GVHD.** (A) Effect of Fgf7 on TRA in mice without disease (syngeneic transplantation,  $bd \rightarrow bd$ ). The pie chart shows tissue representation of the 220 and 60 TRA whose expression levels are enhanced by >3-fold in response to Fgf7 at 10 and 12 weeks of age, respectively (2 and 4 weeks after syngeneic transplantation). (B) Effect of Fgf7 on TRA in mice with acute GVHD ( $b \rightarrow bd$ ). The pie chart shows tissue representation of the 39 and 110 TRA whose expression levels were enhanced by >3-fold in response to Fgf7 at 10 and 12 weeks of age, respectively (2 and 4 weeks after acute GVHD induction). (C) Effect of Fgf7 on TRA reduced during acute GVHD ( $b \rightarrow bd$ ). The pie chart shows tissue representation of the 190 and 291 TRA, respectively, whose expression levels are lower during acute GVHD but normal in response to Fgf7.

Taken together, the data demonstrated that mTEC cytoprotection by Fgf7 sustained the mTEC compartment in the course of acute GVHD and hence a more diverse TRA transcriptome could be achieved despite ongoing alloimmunity.



## 5. DISCUSSION

Despite advances in experimental and clinical HSCT, acute and chronic GVHD continue to be major causes of posttransplant mortality and morbidity.<sup>126</sup> Several clinical studies proved acute GVHD to be a risk factor for chronic GVHD; the latter of which is characterised by autoimmune manifestations.<sup>132,141,143</sup> In contrast to acute GVHD, the pathomechanism of chronic GVHD is less well understood. Moreover, clinical data for the mechanism of the transition from acute to chronic GVHD do not exist at present. From studies of animal models, four different mechanisms have been proposed that may alone or in combination contribute to the pathogenesis of chronic GVHD.<sup>147</sup> These propositions include 1) a deficiency in the  $T_{reg}$  compartment; 2) a role for B cells and autoantibodies; 3) activation of the TGF- $\beta$  pathway; and 4) thymic dysfunction resulting from prior acute GVHD. Since thymic dysfunction is a characteristic feature of both clinical and experimental acute GVHD,<sup>162,177-181</sup> understanding of the precise mechanism of thymic injury may prove to be crucial for the understanding of the transition from acute to chronic GVHD. Here, alterations in the mTEC compartment may serve as a possible explanation for the emergence of autoreactive T cells in the periphery following allogeneic HSCT.

The existence of a link between mTEC injury and the emergence of autoreactive T cells generated in the course of acute GVHD remained unknown at the start of this thesis project. My study was based on data that had established TEC as direct targets of allorecognition and, in response, their apoptosis during acute GVHD.<sup>162</sup> Moreover, acute GVHD-caused TEC injury was shown to impair intrathymic T-cell development and T-cell export to the periphery.<sup>213</sup> I therefore hypothesised that defects in mTEC function during acute GVHD result in impaired thymic negative selection and consequently in a peripheral T-cell repertoire that harbours autoreactive clones at higher levels than normal.

Within my thesis work, I demonstrated that mTEC injury is a universal event in different murine models of acute GVHD. Mature mTEC<sup>high</sup> were deleted in the course of disease which resulted in a reduced size of the entire mTEC compartment (Figure 15). The mTEC<sup>high</sup> compartment is essential for thymic negative selection, since it has the unique capacity to express a large array of peripheral self-antigens, which

are to a great extent controlled by the transcription factor Aire.<sup>87</sup> I found that within the mTEC compartment, the Aire<sup>+</sup>mTEC<sup>high</sup> cells were particularly affected by acute GVHD (Figure 16). In consequence, the diversity of TRA expression was significantly impaired (Figure 17). Using a transgenic transplantation model, I was able to demonstrate that loss of TRA had a biological effect. In this model, purging of an individual self-antigen (OVA) from the TRA pool failed to induce central tolerance induction against this specific TRA. OVA-specific CD4<sup>+</sup> T cells were present in the spleen and lymph nodes of mice with acute GVHD as a consequence of diminished OVA expression in mTEC (Figure 25). I also investigated the cytoprotective agent Fgf7 as a potent treatment to protect, repair, and enhance TEC function, resulting in improved thymic negative selection. Peritransplant administration of Fgf7 restored the mTEC compartment, including cells that expressed Aire. In consequence, TRA expression in mTEC<sup>high</sup> was sustained despite the presence of allogeneic donor T cells in the thymus (Figure 32).

### ***Loss of mTEC – a universal manifestation of acute GVHD***

The use of the non-ablative B6→BDF<sub>1</sub> transplantation model allowed me to distinguish pathogenic influences on TEC caused by acute GVHD from those that resulted from cytoreductive therapy. I confirmed previous data from this haploidentical model that the TEC compartment is affected by alloreactive T cells.<sup>162</sup> In this previous study, mostly cTEC were lost during acute GVHD. However, recent progress in the identification of TEC subsets provided the tool to investigate the thymic stroma in more detail.<sup>56,57,63-66</sup> I identified the mTEC compartment as the major target of allorecognition by donor T cells. Since I distinguished immature and mature mTEC by using detection of MHC class II, my data provides further details into thymic injury in the course of acute GVHD. The mature mTEC<sup>high</sup> cells were preferentially affected by acute GVHD as cell numbers were reduced to almost undetectable levels during the observation period. I could confirm these data in other models, including haploidentical, MHC-mismatched and MHC-matched transplantation systems that used TBI as cytoreductive conditioning. In these models, radiation therapy initially reduced mTEC<sup>high</sup> numbers independently of acute GVHD, but the presence

of acute GVHD pronounced this injury further. My data argue for a reduction of mTEC<sup>high</sup> compartment size as a universal manifestation, and radiation injury is not mandatory as suggested before.<sup>223</sup> None of the experimental models fully reflected the complexity of the clinical situation as individual experimental models are specifically designed to address only desired subsets of all the clinical parameters. Seeking to identify specific autoimmune mechanisms in a multifactorial pathology such as acute GVHD, a reductionist approach was, however, advantageous, which was then further strengthened by a comparison of data sets gained from distinct experimental models.

Both mTEC<sup>low</sup> and mTEC<sup>high</sup> numbers regenerated to normal values upon acute GVHD induction in the haploidentical transplantation model with TBI (Figure 15B). The reason for this observation was not addressed but a recent study suggests a role for cytokine-mediated thymic regeneration after TBI.<sup>259</sup> Here, radio-resistant DCs were shown to upregulate IL-23 following irradiation and subsequently induce IL-22 expression in thymic lymphoid tissue inducer cells. This mechanism resulted in IL-22-mediated regeneration of the thymic microenvironment. Hence, such a regenerative mechanism might apply for the haploidentical  $b \rightarrow bd$  +TBI model. Such a contention remains to be tested.

My conclusion that loss of mTEC is a universal manifestation of acute GVHD was consistent with a recent study where TBI treated Balb/c recipient were transplanted with B6 TCD bone marrow replete either with donor CD4<sup>+</sup> or CD8<sup>+</sup> T cells.<sup>224</sup> In this transplantation model CD8<sup>+</sup> T cells were more potent in mediating mTEC injury than CD4<sup>+</sup> T cells but both donor T cells caused a significant loss in mTEC numbers. In other experimental systems, mTEC were shown to be highly susceptible to chemotherapy.<sup>260</sup> Among all TEC subsets, mTEC<sup>high</sup> were ablated foremost as a consequence of chemotherapy, which mirrored my observation that acute GVHD mostly affects these tolerance inducing cells.

### ***Acute GVHD weakens the platform for central tolerance***

The above data suggested that negative selection is affected by acute GVHD, since mTEC provide the platform for central tolerance. I approached this issue by investigating in more detail the effect of acute

GVHD on mTEC<sup>high</sup> function. Contraction of the total mTEC<sup>high</sup> pool in unconditioned  $b \rightarrow bd$  recipients indeed corresponded to progressive decreases in the subset that expresses Aire. In other systems, e.g. systems that used ablation of Aire, the absence of Aire is associated with decreased TRA expression, which leads in turn to impaired negative selection.<sup>72,73,85,86</sup> Similar to these systems, gene expression analysis of isolated mTEC<sup>high</sup> indeed revealed that the development of thymic acute GVHD was associated with an overall decrease in TRA expression levels (Figure 17). Since signal intensities of TRA and ubiquitously expressed genes (Ub) did not differ from each other, the enrichment of TRA among the downregulated genes was independent of signal intensity but rather caused by a loss of mTEC<sup>high</sup>. Not all TRA were reduced to the same extent, however, and some were not affected at all. I also observed differences in the profiles of reduced TRA at 2 and 4 weeks post-transplantation but many TRA were affected by acute GVHD at both time points. This observation may have been due to the fact that ectopic TRA expression is a stochastic process.<sup>75,249</sup> Only a limited number of mTEC<sup>high</sup> (1-3%) express a particular TRA,<sup>66,75</sup> and a comprehensive coverage of TRA expression is hence only achieved by a sufficiently large mTEC<sup>high</sup> pool. The latter is, however, missing under conditions of acute GVHD.

Promiscuous gene expression by mTEC is independent of any spatial or temporal pattern control observed during regular tissue development and is typically representative of all organs. The size and complexity of this profile is highly conserved between mouse and man<sup>70</sup> thus underscoring the suitability of using experimental models to emulate the situation in clinical HSCT. Analysis of published data of TRA tissue representation in C57BL/6 mice from Kyewski *et al.*<sup>70</sup> revealed that approximately one third of TRA represent genes specifically expressed in the major targets of chronic GVHD such as the skin, liver, salivary glands, lung, eye, and gastrointestinal tract (Figure 37). This tissue distribution remained unchanged in age-matched recipients of syngeneic transplants. However, the most substantially downregulated TRA during acute GVHD were specific for these tissues that are target organs of human chronic GVHD. These data suggested the generation of autoreactive T cells specific for these chronic GVHD target tissues.

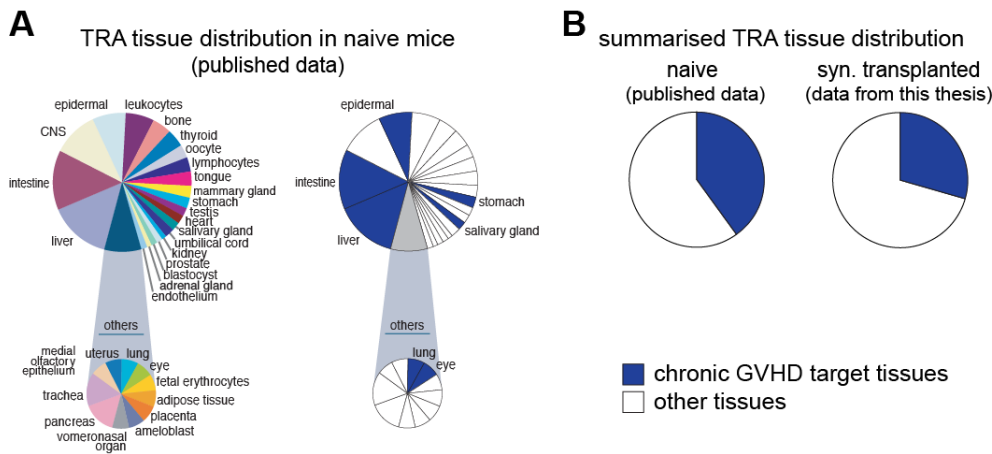


**Figure 37. TRA tissue distribution.** (A) Left pie chart: Data from *Kyewski et al. (2006)*<sup>70</sup> showing tissue distribution of TRA in mTEC<sup>high</sup> from naïve mice. Right pie chart: Dataset from naïve mice displaying only the TRA that are specifically expressed in the major target tissues of chronic GVHD. (B) Altered representation of panel A which combines these TRA in one area (left pie chart). TRA tissue representation in naïve mice was then compared to syngeneically transplanted mice (pie chart on the right).

### *Use of the RIP-mOVA system to study thymic negative selection in the presence of acute GVHD*

Having established that acute GVHD was associated with a defect in TRA expression, I intended to demonstrate whether there was a mechanistic link to the emergence of autoreactive T cells. Since the specificities of the autoreactive T cells in chronic GVHD remain unidentified, and since even the identification of such would not definitely prove a causal relationship with impaired thymic TRA expression, I decided to study ovalbumin (OVA), which can be introduced into the thymus as a neo-self-antigen. I took advantage of the well established OT-II→RIP-mOVA transplantation system.<sup>98</sup> This system is suitable to study thymic negative selection mediated by mTEC since firstly, thymic membrane-bound OVA (mOVA) expression under the RIP-promoter is restricted to mTEC; secondly, TCR selection against mOVA recapitulates physiological tolerance induction to TRA in the thymus medulla,<sup>71,72,76,98,250,251</sup> and thirdly, a reduction in the expression of mOVA mRNA by as little as 30% suffices for the failure deletion of OT-II T cells in RIP-mOVA mice.<sup>252</sup> Thymic

OVA expression was detected in the mTEC compartment in transgenic recipients without disease as expected. Unexpected was, however, that OVA was present in both mTEC<sup>low</sup> and mTEC<sup>high</sup>, which argued for OVA being regulated independently of Aire, since only mTEC<sup>high</sup> express Aire.<sup>72,76,77</sup> These data were not consistent with studies showing OVA expression to be Aire-dependent,<sup>252,261</sup> but they agreed with another study.<sup>76</sup> The first two studies determined OVA expression in total thymic stromal preparations, however, and not specifically in mTEC.

The induction of acute GVHD in RIP-mOVA mice led to mTEC injury. Both mTEC<sup>low</sup> and mTEC<sup>high</sup> were decreased in absolute cell numbers similar to the non-transgenic haploidentical transplantation model used above (Figure 21). In addition, Aire-expressing mTEC<sup>high</sup> were deleted in the presence of acute GVHD (Figure 22). However, Aire mRNA expression was not significantly affected by disease. The reason why acute GVHD only interferes with Aire protein expression, but not with Aire mRNA expression, remains to be elucidated. Possible mechanisms may include defects in mRNA translation, stability of protein, or degradation of the Aire protein. In summary, my data demonstrated that OVA-expressing mTEC were deleted during acute GVHD, and consequently thymic OVA expression was reduced. Under physiological conditions, i.e. mice without acute GVHD, OT-II T cells were efficiently deleted in a RIP-mOVA thymus and they accounted for frequencies of only 1-3% among all CD4<sup>+</sup> T cells in the periphery (Figure 25). However, acute GVHD allowed the emergence of OT-II T cells to the periphery due to diminished thymic OVA expression, which resembled the situation in non-transgenic wildtype mice (no thymic OVA expression). These data indicated that the loss of a single TRA licenses the *de novo* generation of autoreactive CD4<sup>+</sup> T cells during acute GVHD. Characterisation of OT-II T cells in the periphery with acute GVHD revealed that they were fully functional and did not acquire an anergic phenotype. Moreover, an activated phenotype was suggested based on larger cell size and higher CD44 expression (Figure 27). It is noteworthy that OT-II T cells detected in the periphery represented T<sub>effector</sub> cells, i.e. non-T<sub>reg</sub> cells, which was another indication that they were capable of responding to their antigen. It was, however, not surprising that T<sub>reg</sub> cells were found to be diminished in hosts in the presence of acute GVHD, since T<sub>reg</sub> development relies on a functional thymus.<sup>92</sup> Their absence was consistent with observations from clinical studies where peripheral blood

$T_{\text{reg}}$  numbers are reduced in patients suffering from acute GVHD.<sup>262</sup> This relationship thus provides a further explanation for the presence of an autoimmune syndrome following acute GVHD.

I did not test directly if OT-II T cells that escaped negative selection were capable of responding to OVA, a feature that would be required for effector function that leads to autoimmune disease. To test this,  $CD4^+$  OT-II T cells will have to be isolated directly from the thymus or periphery and cultured *in vitro* together with host-derived APCs pulsed with OVA peptide or protein. Proliferation of OT-II T cells will indicate their ability to respond to OVA. To test the OT-II response directly *in vivo*, the transfer of isolated  $CD4^+$  OT-II SP thymocytes in a secondary Rag-deficient recipient immunised with recombinant *Listeria monocytogenes* bacteria engineered to secrete chicken OVA might also be helpful.<sup>98</sup> Another *in vivo* system that might be useful to answer this question is the immunisation of the RIP-mOVA host itself.<sup>263</sup> RIP-mOVA mice allow the activation of OVA-reactive T cells in the pancreatic lymph node, which is the principal site for activation of diabetogenic T cells.<sup>97,263,264</sup> Primed OT-II T cells are able to infiltrate the pancreas and to attack the neo-self-antigen OVA, which results in the development of diabetes in these RIP-mOVA mice. The development of diabetes can be followed by blood glucose measurements. OT-II T cells that infiltrate the pancreas and cause insulinitis can be detected by histological analyses. It remains to be tested whether these functional assay systems are applicable and informative in the GVHD settings.

A caveat of the OT-II system is the unphysiological high frequency of OVA-specific precursors, which may alter the negative selection process.<sup>250</sup> To overcome this limitation, OT-II TCD bone marrow was transplanted together with B6 wild type TCD bone marrow at a 1:3 ratio. This strategy ensures proper negative selection of OVA-specific T cells as would be expected in normal T-cell development. In both, B6 and RIP-mOVA hosts without acute GVHD, B6 wild type T cells used the  $V\alpha 2$  and  $V\beta 5$  chain randomly at a frequency of 4% as would be expected from a normally selected diverse TCR repertoire. Interestingly, in RIP-mOVA hosts with acute GVHD, B6 wild type T cells did not use the  $V\beta 5$  chain. These data further evidenced that the loss in ectopic TRA expression is sufficient for the *de novo* generation and export of TRA-specific  $CD4^+$  T cells in mice.

### ***Potential mechanism of autoreactive T-cell neogenesis following allogeneic HSCT***

In summary, I propose an etiologic link between the alloreactivity of acute GVHD and the autoimmunity typically seen in chronic GVHD. Such a link may be based on an impaired size of the  $mTEC^{high}$  compartment as a result of acute GVHD. A potential mechanism how new T cells are generated following allogeneic HSCT from donor HSC in a thymus-dependent regenerative mechanism is shown in Figure 38. The top panel A shows normal thymus function, which is briefly summarised again. T-cell development requires the seeding of grafted HSCs and subsequent import of progenitor cells from the host bone marrow (blue symbols) via the blood circulation into the thymus cortex. In an intact host thymus the T-cell precursors mature and are positively selected in response to signals provided by  $cTEC$ . In parallel to their migration to the thymus medulla, T-cell precursors differentiate into  $CD4^+$  or  $CD8^+$  T cells which are then subjected to thymic negative selection. In such a process developing T cells are exposed to self-antigens, including TRA. An essential prerequisite for the negative selection of self-reactive T cells is the ability of  $Aire^+mTEC^{high}$  to build a reservoir of a large array of TRA. TRA are presented either by  $mTEC$  themselves, indirectly by thymic dendritic cells, or by both cell types in parallel. High-affinity TCR ligation of these TRA leads to clonal deletion (negative selection) of the responding T cells.  $Aire^+mTEC^{high}$  do not homogeneously express a large pool of TRA, however. Rather, the expression of individual antigens is restricted to a subset of  $mTEC^{high}$ , indicating a high level of heterogeneity between  $mTEC$  subpopulations. Hence,  $Aire^+mTEC^{high}$  compartment size contributes to TRA diversity. The stochastic process of ectopic TRA expression is symbolised in Figure 38 by the expression of a given TRA by only a limited number of  $mTEC^{high}$  (e.g. TRA1, 2, 3 in one  $mTEC^{high}$ , TRA3, 4, 6 in another, TRA1, 2, 4, 5 in a third and TRA7 in a fourth cell). It is believed on the basis of a very limited set of single cell analysis that a comprehensive mosaic of TRA is only achieved by the complete  $mTEC^{high}$  pool which is symbolised by expression of all TRA (1-7) by the total cell pool. This mechanism ensures an efficient deletion of a highly diverse self-reactive TCR repertoire (red symbols). The surviving mature T cells (blue symbols) are exported to peripheral lymphoid tissues where they constitute the pool of self-tolerant



but pathogen-specific naive T cells. In panel B of Figure 38 thymus function in recipients with acute GVHD is shown. In preclinical allogeneic HSCT models the activation of alloreactive donor T cells (black symbols) is linked to death of cells residing in the TEC compartment,<sup>36</sup> including those mTEC that express Aire. A decrease in the size of the Aire<sup>+</sup>mTEC<sup>high</sup> compartment results in the transcription of a smaller array of TRA. This mechanism is symbolised by the loss of TRA4, 5 and 6 in result from death of two mTEC<sup>high</sup> cells. It is postulated that such reduction in TRA diversity leads to an enhanced emergence of new T-cell clones that are reactive to TRA4, 5 and 6 in the periphery. My studies then also demonstrated that many of those thymic TRA whose expression levels were reduced as a consequence of acute GVHD represented proteins that are specifically expressed in known target tissues of chronic GVHD, including salivary and lacrimal glands (e.g. salivary protein), liver (e.g. urinary protein) and lung (e.g. secretoglobin) (Figure 18). This proposed mechanism agrees with a recently published study by Wu *et al.*<sup>224</sup> who showed that the mTEC compartment is disrupted by acute GVHD resulting in the emergence of host reactive T cells.

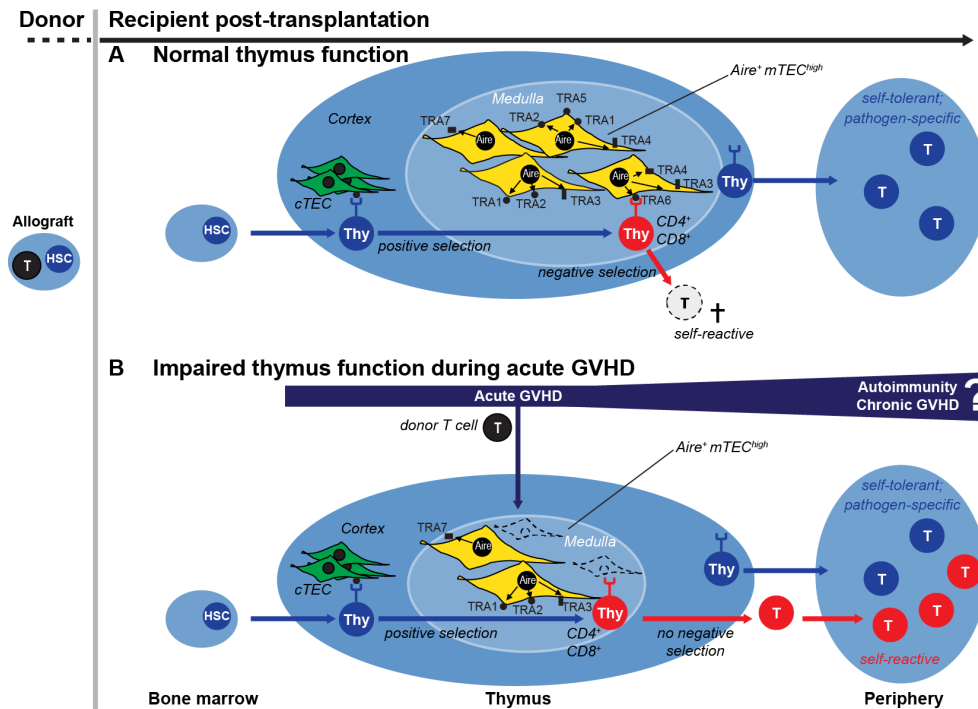


**Figure 38. Hypothesised mechanism of autoreactive T-cell neogenesis following allogeneic HSCT.** (A) Normal thymus function (B) Thymus function in recipients with acute GVHD (as described in the text)

While my data make the mechanism shown in Figure 38 highly plausible, it should be noted that the emergence of autoreactive T cells may not be sufficient to cause an autoimmune syndrome typical for chronic GVHD. This fact may be due to additional peripheral control mechanisms that regulate autoimmunity. For example, natural  $T_{reg}$  are generated in the thymus and prevent activation of peripheral autoreactive T cells.<sup>92,265</sup> Very recent data demonstrated that the medullary compartment provides a developmental niche for natural  $T_{reg}$ .<sup>94-96</sup> Since the mTEC compartment is affected by acute GVHD, it can be envisaged that there is not only a defect in T cell development and the essential selection processes, but also in the intrathymic generation of  $T_{reg}$  cells. If such a mechanism proves to be true, a 2-hit model for chronic GVHD will apply.<sup>266</sup> This model suggests the development of chronic GVHD being dependent on the emergence of

autoreactive T cells from the thymus to the periphery (Hit 1) in the context of peripheral deficiencies in thymic  $T_{\text{reg}}$  cells (Hit 2).

Nevertheless, chronic GVHD and its autoimmune manifestations can occur also without preceding acute GVHD.<sup>139,149</sup> Either thymic GVHD is present but not detectable by routine clinical analyses or thymic GVHD is indeed absent. The first possibility would not rule out a role for impaired thymic negative selection in the development of an autoimmune syndrome. In contrast to the tools available for the diagnosis of skin, gut, or liver acute GVHD (physical examination, biomarkers of inflammation, biopsy, endoscopy), routine diagnosis of acute GVHD of the thymus is not readily available. The development of minimally invasive tools for diagnosis of thymic GVHD (e.g. imaging or biomarker based) may be a methodologic necessity to assess thymic GVHD.<sup>226</sup> The second possibility implies that other mechanism than impaired thymic negative selection must exist that drive the development of an autoimmune syndrome. A recent study suggested that autoimmunity can occur in the absence of any defects in thymic negative selection and in the presence of a functional  $T_{\text{reg}}$  repertoire.<sup>267</sup> The authors showed in a novel transgenic mouse model that during an infection T cells responded to a neo-self-antigen that did not induce negative selection when promiscuously expressed in the thymus medulla. This study suggested that a mismatch between the threshold for negative selection and activation in the periphery during an infection allows low avidity T cells to emerge from the thymus to the periphery where they can cause autoimmunity upon restimulation. Other experimental systems suggested the thymus to be negligible for the generation of autoimmune-like chronic GVHD.<sup>146,183-185</sup> Rather mature donor T cells transferred in the graft are activated and expanded by alloimmune response and contribute to the development of chronic GVHD and its autoimmune manifestations. Furthermore, inappropriately low numbers of  $T_{\text{reg}}$  in acute GVHD have been defined as a major event that leads to the development of autoimmunity and consequently chronic GVHD.<sup>166</sup>

***Fgf7 restores the thymic mTEC<sup>high</sup> compartment and sustains the diversity of TRA expression***

To test if factors that foster epithelial cell proliferations and act directly on TEC are thus effective in restoring the mTEC compartment and consequently improving the diversity of TRA expression, I chose to study Fgf7. Fgf7 has before been reported to efficiently enhance the proliferation of the TEC compartment, and thus to increase intrathymic T cell development.<sup>239</sup> Murine studies of allogeneic HSCT showed that treatment with Fgf7 protects the host thymus<sup>239,241</sup> and one study was able to demonstrate a beneficial effect on central tolerance induction.<sup>180</sup>

The peritransplant administration of Fgf7 to allogeneically transplanted recipients did not affect the initial drop in mTEC<sup>high</sup> numbers (Figure 29). Nevertheless, stable cell numbers of mTEC<sup>high</sup> and Aire<sup>+</sup>mTEC<sup>high</sup> similar to mice without disease were reached later after GVHD induction and maintained over the whole observation period. This result was not consistent with a previous study that showed an increase in all TEC populations as early as 3 days after Fgf7 treatment.<sup>239</sup> These experiments were done in wild type mice without acute GVHD. These data suggested that Fgf7 could only partially compensate the loss of cells caused by acute GVHD at early time points. Fgf7 mediated its action by enhancing TEC proliferation early after administration, as shown by BrdU analyses (Figure 31). In the absence of exogenous Fgf7, 5% of mTEC underwent cell division within 1 week in the  $b \rightarrow bd$  and  $bd \rightarrow bd$  transplant group. These data are consistent with reports showing that mTEC are continuously replaced in adulthood.<sup>57,66</sup> In mice with acute GVHD but treated with Fgf7 the frequency of proliferating cells in the first week increased to 15%. High turnover of mTEC in response to Fgf7 was therefore responsible for the rescue of mTEC<sup>high</sup> numbers. However, it remains unknown how the stable cell population is maintained at later time points post treatment, since snap shot analysis of BrdU incorporation 2 weeks after Fgf7 administration and GVHD induction did not show increased proliferation compared to HBSS-treated recipients. This raises the question if Fgf7 has more a protective than a proliferative effect, a point that will need to be addressed. One possibility to test this issue will be to administrate Fgf7 before inducing acute GVHD. This prophylactic intervention may allow Fgf7 to firstly induce a protective effect before

alloreactive T cells can attack TEC. Another approach will be the long term follow up of recipients treated with Fgf7. Fgf7 has been shown to act on TEC progenitors by stimulating their proliferation and differentiation and on residual mTEC.<sup>239</sup> It remains, however, unclear what the contribution of these two populations to the recovery of mTEC<sup>high</sup> is. Interestingly, alloreactive donor T cells remained present in the host thymus despite Fgf7 administration. Given the fact that Fgf7's receptor Fgfr2IIIb is not expressed on T cells, it is not surprising that Fgf7 did not have a direct trophic or proliferative effect on thymus-infiltrating donor T cells. An explanation might be that the effect of Fgf7 on the TEC compartment overcomes the injury caused by alloreactive donor T cells. Gene expression data from mTEC<sup>high</sup> cells isolated from syngeneically transplanted mice treated with Fgf7 are available and will provide further information about the molecular mechanism how Fgf7 protects the thymic epithelium (microarray data generated during this thesis project). Preliminary analyses revealed that a number of genes, which were upregulated upon Fgf7 administration, are involved in cell cycle regulation and in the control of apoptosis. This work is in progress.

The presence of mTEC<sup>high</sup> and Aire<sup>+</sup>mTEC<sup>high</sup> cell numbers close to normal numbers observed in recipients without acute GVHD, suggest the recovery of TRA expression in response to Fgf7. Indeed, gene expression analysis revealed that peritransplant administration of Fgf7 sustained a more diverse TRA transcriptome during acute GVHD (Figure 32). However, 2 weeks after acute GVHD induction, the TRA spectrum was not preserved by Fgf7, although Aire<sup>+</sup>mTEC<sup>high</sup> had recovered to normal levels yet. At 7 weeks post-transplantation, a broader array of TRA was expressed, which resembled the situation in normal (i.e. syngeneically transplanted) mice. I interpret these data such that the amelioration of TRA expression is secondary to the recovery of the mTEC compartment. Individual TRA expression patterns were differentially affected by Fgf7 as some but not all Aire-dependent TRA returned to nearly normal expression in the observation period (Figure 33). The molecular mechanism for this biased profile remains to date unknown. I cannot exclude from my data that mTEC<sup>high</sup> had also at the individual cell level a decrease in the number of TRA transcribed. This hypothesis may be testable by the analysis of single cell mTEC<sup>high</sup> transcriptomics.

To test if different signal intensities and Aire-dependency influenced the restoration of the TRA pool, multidensity histogram analysis was performed. Since signal intensities were similar between Ub, TRA, and Aire-dependent TRA, these data clearly suggested that Fgf7 restored gene expression independently of signal intensities (Figure 35). Such bias in gene regulation is indeed not a common observation in gene expression analysis (personal communication R. Ivanek, bioinformatician). These data also revealed that there was no significant preferential restoration of Aire-dependent TRA compared to Aire-independent TRA. I interpret these data such that Fgf7 restored the whole mTEC<sup>high</sup> pool, and did not favour the Aire<sup>+</sup>mTEC<sup>high</sup>. In consequence, both, Aire-dependent and -independent TRA, are efficiently restored by Fgf7. Confirming the data that TRA restoration is an arbitrary process, there was no preferential effect of Fgf7 on genes that are expressed mainly in chronic GVHD target tissues observed (Figure 36).

In summary, these data suggest that normal numbers of Aire<sup>+</sup>mTEC<sup>high</sup> and TRA diversity after engraftment of donor HSC possibly result in effective negative thymic selection and support of thymic T<sub>reg</sub> development. Such a mechanism would prevent the emergence of autoreactive T cells in the periphery and consequently result in the absence of chronic GVHD with its autoimmune manifestations. Nevertheless, there are open questions, which have not been addressed in this study. I did not investigate the effect of Fgf7 on already established acute or chronic GVHD. The question arises whether there are enough residual mTEC or progenitor cells in a recipient with already established thymic acute GVHD to respond to Fgf7. Does Fgf7 have any positive or negative effects on other epithelial cells than TEC? Since the Fgf7 administration was not locally directed at the thymus, Fgf7 might act in addition to TEC also on other cell types in the periphery.

Whether peritransplant administration of Fgf7 results in a decreased occurrence of chronic GVHD and autoimmune syndrome in allogeneic HSCT patients, remains unknown so far. Clinical studies about Fgf7 (Palifermin) are contradictory in this respect. One retrospective study concluded that Fgf7 decreases the incidence of acute GVHD<sup>268</sup> but another one did not find any ameliorating effect of Fgf7 on GVHD in allogeneic HSCT.<sup>269</sup> Moreover, prospective trials could not show differences in acute

GVHD incidence, severity, survival, and incidence of chronic GVHD between Fgf7 and placebo cohort in humans.<sup>270,271</sup>

The rationale of my study was to provide mechanistic explanations and cell biological principles that ascribe how autoimmunity may develop in the context of antecedent alloimmunity. Fgf7 was used to test the hypothesis that interventions directed at epithelial cytoprotection maintain the integrity of the mTEC compartment after transplantation and reverse the loss of TRA diversity. Since promiscuous gene expression for the deletion of self-reactive T cells is not the only way how the self-reactive potential of the immune system is regulated (see above), such cytoprotection may not necessarily equate to an outright protection from autoimmunity. While Fgf7 effects the peripheral immune system,<sup>272</sup> it may be incorrect to assume that its administration can prevent autoimmunity arising from a central in lieu of a peripheral defect in tolerance. However, interventions focused on mTEC cytoprotection, such as Fgf7, may contribute to prevent the emergence of thymus-dependent autoreactive T cells and thus alter autoimmune outcome. Although the successful results of Fgf7 from animal models have not yet been confirmed in human transplantation,<sup>273</sup> the present data suggest to focus on new therapies that treat or prevent chronic GVHD by targeting the thymic microenvironment, rather than lymphohaematopoietic cells.

## 6. CONCLUSIONS

Although, acute GVHD has been implicated as a risk factor for chronic GVHD, it remains unknown whether and how autoimmunity is linked to antecedent alloimmunity. My data provide a mechanism for how autoimmunity may develop in the context of acute GVHD (Figure 38). This mechanism is based on a contracted mTEC cellularity and consequently impaired TRA representation due to altered gene expression. In conclusion, the weakened platform for negative selection might provide the explanation for the emergence of autoreactive T cells seen in the murine transplantation models. Because thymic negative selection is sensitive to small changes in TRA expression, approaches for mTEC cytoprotection, as shown here with the administration of Fgf7, may prevent the emergence of thymus-dependent autoreactive T cells. In consequence, this might alter autoimmune outcome. The identification in chronic GVHD of the yet undefined specificities of autoreactive effector T cells will allow to test this argument directly in experimental systems and ultimately in clinical allogeneic HSCT.



## 7. REFERENCES

1. Appelbaum FR. Hematopoietic-cell transplantation at 50. *N Engl J Med.* 2007;357:1472-1475.
2. Copelan EA. Hematopoietic stem-cell transplantation. *N Engl J Med.* 2006;354:1813-1826.
3. Gratwohl A, Baldomero H. Trends of hematopoietic stem cell transplantation in the third millennium. *Curr Opin Hematol.* 2009;16:420-426.
4. Passweg JR, Baldomero H, Gratwohl A, Bregni M, Cesaro S, et al. The EBMT activity survey: 1990-2010. *Bone Marrow Transplant.* 2012;47:906-923.
5. Passweg JR, Baldomero H, Bregni M, Cesaro S, Dreger P, et al. Hematopoietic SCT in Europe: data and trends in 2011. *Bone Marrow Transplant.* 2013;48:1161-1167.
6. Passweg JR, Halter J, Bucher C, Gerull S, Heim D, et al. Hematopoietic stem cell transplantation: a review and recommendations for follow-up care for the general practitioner. *Swiss Med Wkly.* 2012;142:w13696.
7. Koreth J, Schlenk R, Kopecky KJ, Honda S, Sierra J, et al. Allogeneic stem cell transplantation for acute myeloid leukemia in first complete remission: systematic review and meta-analysis of prospective clinical trials. *JAMA.* 2009;301:2349-2361.
8. Pasquini MC, Wang Z. Current use and outcome of hematopoietic stem cell transplantation: CIBMTR Summary Slides, 2012. Available at: <http://www.cibmtr.org>.
9. Reisner Y, Hagin D, Martelli MF. Haploidentical hematopoietic transplantation: current status and future perspectives. *Blood.* 2011;118:6006-6017.
10. Turner BE, Collin M, Rice AM. Reduced intensity conditioning for hematopoietic stem cell transplantation: has it achieved all it set out to? *Cytotherapy.* 2010;12:440-454.
11. Gyurkocza B, Storb R, Storer BE, Chauncey TR, Lange T, et al. Nonmyeloablative allogeneic hematopoietic cell transplantation in patients with acute myeloid leukemia. *J Clin Oncol.* 2010;28:2859-2867.

12. Gooley TA, Chien JW, Pergam SA, Hingorani S, Sorrow ML, et al. Reduced mortality after allogeneic hematopoietic-cell transplantation. *N Engl J Med*. 2010;363:2091-2101.
13. Deeg HJ, Sandmaier BM. Who is fit for allogeneic transplantation? *Blood*. 2010;116:4762-4770.
14. Pidala J, Anasetti C, Jim H. Quality of life after allogeneic hematopoietic cell transplantation. *Blood*. 2009;114:7-19.
15. Baker KS, Bresters D, Sande JE. The burden of cure: long-term side effects following hematopoietic stem cell transplantation (HSCT) in children. *Pediatr Clin North Am*. 2010;57:323-342.
16. Bacigalupo A, Sormani MP, Lamparelli T, Gualandi F, Occhini D, et al. Reducing transplant-related mortality after allogeneic hematopoietic stem cell transplantation. *Haematologica*. 2004;89:1238-1247.
17. Morris ES, Hill GR. Advances in the understanding of acute graft-versus-host disease. *Br J Haematol*. 2007;137:3-19.
18. Small TN, Papadopoulos EB, Boulad F, Black P, Castro-Malaspina H, et al. Comparison of immune reconstitution after unrelated and related T-cell-depleted bone marrow transplantation: effect of patient age and donor leukocyte infusions. *Blood*. 1999;93:467-480.
19. Storek J, Gooley T, Witherspoon RP, Sullivan KM, Storb R. Infectious morbidity in long-term survivors of allogeneic marrow transplantation is associated with low CD4 T cell counts. *Am J Hematol*. 1997;54:131-138.
20. Storek J, Joseph A, Espino G, Dawson MA, Douek DC, et al. Immunity of patients surviving 20 to 30 years after allogeneic or syngeneic bone marrow transplantation. *Blood*. 2001;98:3505.
21. Barker JN, Hough RE, van Burik JA, DeFor TE, MacMillan ML, et al. Serious infections after unrelated donor transplantation in 136 children: impact of stem cell source. *Biol Blood Marrow Transplant*. 2005;11:362-370.
22. Marr KA, Carter RA, Boeckh M, Martin P, Corey L. Invasive aspergillosis in allogeneic stem cell transplant recipients: changes in epidemiology and risk factors. *Blood*. 2002;100:4358-4366.
23. Ochs L, Shu XO, Miller J, Enright H, Wagner J, et al. Late infections after allogeneic bone marrow transplantations: comparison of incidence

- in related and unrelated donor transplant recipients. *Blood*. 1995;86:3979.
24. Cavazzana-Calvo M, André-Schmutz I, Dal Cortivo L, Neven B, Hacein-Bey-Abina S, Fischer A. Immune reconstitution after haematopoietic stem cell transplantation: obstacles and anticipated progress. *Curr Opin Immunol*. 2009;21:544-548.
  25. Seggewiss R, Einsele H. Immune reconstitution after allogeneic transplantation and expanding options for immunomodulation: an update. *Blood*. 2010;115:3861-3868.
  26. Storek J, Zhao Z, Lin E, Berger T, McSweeney PA, et al. Recovery from and consequences of severe iatrogenic lymphopenia (induced to treat autoimmune diseases). *Clin Immunol*. 2004;113:285-298.
  27. Muraro PA, Douek DC. Renewing the T cell repertoire to arrest autoimmune aggression. *Trends Immunol*. 2006;27:61-67.
  28. Crooks GM, Weinberg K, Mackall C. Immune reconstitution: from stem cells to lymphocytes. *Biol Blood Marrow Transplant*. 2006;12:42-46.
  29. Storek J. Immunological reconstitution after hematopoietic cell transplantation - its relation to the contents of the graft. *Expert Opin Biol Ther*. 2008;8:583-597.
  30. Parkman R, Cohen G, Carter SL, Weinberg KI, Masinsin B, et al. Successful immune reconstitution decreases leukemic relapse and improves survival in recipients of unrelated cord blood transplantation. *Biol Blood Marrow Transplant*. 2006;12:919-927.
  31. Haddad E, Landais P, Friedrich W, Gerritsen B, Cavazzana-Calvo M, et al. Long-term immune reconstitution and outcome after HLA-nonidentical T-cell-depleted bone marrow transplantation for severe combined immunodeficiency: a European retrospective study of 116 patients. *Blood*. 1998;91:3646-3653.
  32. Porrata LF, Litzow MR, Tefferi A, Letendre L, Kumar S, et al. Early lymphocyte recovery is a predictive factor for prolonged survival after autologous hematopoietic stem cell transplantation for acute myelogenous leukemia. *Leukemia*. 2002;16:1311-1318.
  33. Clave E, Rocha V, Talvensaaari K, Busson M, Douay C, et al. Prognostic value of pretransplantation host thymic function in HLA-identical sibling hematopoietic stem cell transplantation. *Blood*. 2005;105:2608-2613.

34. Ege H, Gertz MA, Markovic SN, Lacy MQ, Dispenzieri A, et al. Prediction of survival using absolute lymphocyte count for newly diagnosed patients with multiple myeloma: a retrospective study. *Br J Haematol.* 2008;141:792-798.
35. van Den Brink M, Leen AM, Baird K, Merchant M, Mackall C, Bollard CM. Enhancing immune reconstitution: from bench to bedside. *Biol Blood Marrow Transplant.* 2013;19:S79-S83.
36. Krenger W, Blazar BR, Holländer GA. Thymic T-cell development in allogeneic stem cell transplantation. *Blood.* 2011;117:6768-6776.
37. Hollander G, Gill J, Zuklys S, Iwanami N, Liu C, Takahama Y. Cellular and molecular events during early thymus development. *Immunological reviews.* 2006;209:28-46.
38. Gill J, Malin M, Sutherland J, Gray D, Hollander G, Boyd R. Thymic generation and regeneration. *Immunol Rev.* 2003;195:28-50.
39. Guidos C. Thymus and T-lymphocyte development: what is new in the 21st century? *Immunol Rev.* 2006;209:5-9.
40. Boehm T. Thymus development and function. *Curr Opin Immunol.* 2008;20:178-184.
41. Rothenberg EV, Moore JE, Yui MA. Launching the T-cell-lineage developmental programme. *Nat Rev Immunol.* 2008;8:9-21.
42. Zlotoff DA, Schwarz BA, Bhandoola A. The long road to the thymus: the generation, mobilization, and circulation of T-cell progenitors in mouse and man. *Seminars in Immunopathology.* 2008;30:371-382.
43. Petrie HT, Zúñiga-Pflücker JC. Zoned out: functional mapping of stromal signaling microenvironments in the thymus. *Annu Rev Immunol.* 2007;25:649-679.
44. Anderson G, Jenkinson EJ. Lymphostromal interactions in thymic development and function. *Nat Rev Immunol.* 2001;1:31-40.
45. van Ewijk W, Shores EW, Singer A. Crosstalk in the mouse thymus. *Immunol Today.* 1994;15:214-217.
46. Ceredig R, Rolink T. A positive look at double-negative thymocytes. *Nat Rev Immunol.* 2002;2:888-897.
47. Godfrey DI, Kennedy J, Suda T, Zlotnik A. A developmental pathway involving four phenotypically and functionally distinct subsets of CD3-CD4-CD8- triple-negative adult mouse thymocytes defined by CD44 and CD25 expression. *J Immunol.* 1993;150:4244-4252.

48. von Boehmer H, Aifantis I, Feinberg J, Lechner O, Saint-Ruf C, et al. Pleiotropic changes controlled by the pre-T-cell receptor. *Curr Opin Immunol.* 1999;11:135-142.
49. Aliahmad P, Kaye J. Commitment issues: linking positive selection signals and lineage diversification in the thymus. *Immunological reviews.* 2006;209:253-273.
50. Singer A, Bosselut R. CD4/CD8 coreceptors in thymocyte development, selection, and lineage commitment: analysis of the CD4/CD8 lineage decision. *Adv Immunol.* 2004;83:91-131.
51. Takahama Y. Journey through the thymus: stromal guides for T-cell development and selection. *Nat Rev Immunol.* 2006;6:127-135.
52. Witt CM, Raychaudhuri S, Schaefer B, Chakraborty AK, Robey EA. Directed migration of positively selected thymocytes visualized in real time. *PLoS Biol.* 2005;3:e160.
53. Palmer E. Negative selection--clearing out the bad apples from the T-cell repertoire. *Nat Rev Immunol.* 2003;3:383-391.
54. Holländer GA, Peterson P. Learning to be tolerant: how T cells keep out of trouble. *J Intern Med.* 2009;265:541-561.
55. van Ewijk W, Wang B, Hollander G, Kawamoto H, Spanopoulou E, et al. Thymic microenvironments, 3-D versus 2-D? *Semin Immunol.* 1999;11:57-64.
56. Gray D, Abramson J, Benoist C, Mathis D. Proliferative arrest and rapid turnover of thymic epithelial cells expressing Aire. *J Exp Med.* 2007;204:2521-2528.
57. Gray DH, Seach N, Ueno T, Milton MK, Liston A, et al. Developmental kinetics, turnover, and stimulatory capacity of thymic epithelial cells. *Blood.* 2006;108:3777-3785.
58. Klug DB, Carter C, Gimenez-Conti IB, Richie ER. Cutting edge: thymocyte-independent and thymocyte-dependent phases of epithelial patterning in the fetal thymus. *J Immunol.* 2002;169:2842-2845.
59. Zuklys S, Gill J, Keller MP, Hauri-Hohl M, Zhanybekova S, et al. Stabilized beta-catenin in thymic epithelial cells blocks thymus development and function. *J Immunol.* 2009;182:2997-3007.
60. Lee EN, Park JK, Lee JR, Oh SO, Baek SY, et al. Characterization of the expression of cytokeratins 5, 8, and 14 in mouse thymic epithelial cells during thymus regeneration following acute thymic involution. *Anat Cell Biol.* 2011;44:14-24.

61. Bowlus CL, Ahn J, Chu T, Gruen JR. Cloning of a novel MHC-encoded serine peptidase highly expressed by cortical epithelial cells of the thymus. *Cell Immunol.* 1999;196:80-86.
62. Farr A, Nelson A, Truex J, Hosier S. Epithelial heterogeneity in the murine thymus: a cell surface glycoprotein expressed by subcapsular and medullary epithelium. *Journal of Histochemistry & Cytochemistry.* 1991;39:645-653.
63. Gray DH, Fletcher AL, Hammett M, Seach N, Ueno T, et al. Unbiased analysis, enrichment and purification of thymic stromal cells. *J Immunol Methods.* 2008;329:56-66.
64. Derbinski J, Gäbler J, Brors B, Tierling S, Jonnakuty S, et al. Promiscuous gene expression in thymic epithelial cells is regulated at multiple levels. *J Exp Med.* 2005;202:33-45.
65. Dooley J, Erickson M, Farr AG. An organized medullary epithelial structure in the normal thymus expresses molecules of respiratory epithelium and resembles the epithelial thymic rudiment of nude mice. *J Immunol.* 2005;175:4331-4337.
66. Gillard GO, Farr AG. Features of medullary thymic epithelium implicate postnatal development in maintaining epithelial heterogeneity and tissue-restricted antigen expression. *J Immunol.* 2006;176:5815-5824.
67. Zuklys S, Mayer CE, Zhanybekova S, Stefanski HE, Nusspaumer G, et al. MicroRNAs control the maintenance of thymic epithelia and their competence for T lineage commitment and thymocyte selection. *J Immunol.* 2012;189:3894-3904.
68. Farr AG, Dooley JL, Erickson M. Organization of thymic medullary epithelial heterogeneity: implications for mechanisms of epithelial differentiation. *Immunol Rev.* 2002;189:20-27.
69. Koble C, Kyewski B. The thymic medulla: a unique microenvironment for intercellular self-antigen transfer. *J Exp Med.* 2009;206:1505-1513.
70. Kyewski B, Klein L. A central role for central tolerance. *Annu Rev Immunol.* 2006;24:571-606.
71. Derbinski J, Schulte A, Kyewski B, Klein L. Promiscuous gene expression in medullary thymic epithelial cells mirrors the peripheral self. *Nat Immunol.* 2001;2:1032-1039.

72. Anderson MS, Venanzi ES, Klein L, Chen Z, Berzins SP, et al. Projection of an immunological self shadow within the thymus by the aire protein. *Science*. 2002;298:1395-1401.
73. Liston A, Gray DH, Lesage S, Fletcher AL, Wilson J, et al. Gene dosage--limiting role of Aire in thymic expression, clonal deletion, and organ-specific autoimmunity. *J Exp Med*. 2004;200:1015-1026.
74. Johnnidis JB, Venanzi ES, Taxman DJ, Ting JP, Benoist CO, Mathis DJ. Chromosomal clustering of genes controlled by the aire transcription factor. *Proc Natl Acad Sci U S A*. 2005;102:7233-7238.
75. Derbinski J, Pinto S, Rösch S, Hexel K, Kyewski B. Promiscuous gene expression patterns in single medullary thymic epithelial cells argue for a stochastic mechanism. *Proc Natl Acad Sci U S A*. 2008;105:657-662.
76. Anderson MS, Venanzi ES, Chen Z, Berzins SP, Benoist C, Mathis D. The cellular mechanism of Aire control of T cell tolerance. *Immunity*. 2005;23:227-239.
77. Hubert FX, Kinkel SA, Webster KE, Cannon P, Crewther PE, et al. A specific anti-Aire antibody reveals aire expression is restricted to medullary thymic epithelial cells and not expressed in periphery. *J Immunol*. 2008;180:3824-3832.
78. Finnish-German APECED Consortium. An autoimmune disease, APECED, caused by mutations in a novel gene featuring two PHD-type zinc-finger domains. *Nat Genet*. 1997;17:399-403.
79. Nagamine K, Peterson P, Scott HS, Kudoh J, Minoshima S, et al. Positional cloning of the APECED gene. *Nature genetics*. 1997;17:393-398.
80. Betterle C, Greggio NA, Volpato M. Clinical review 93: Autoimmune polyglandular syndrome type 1. *J Clin Endocrinol Metab*. 1998;83:1049-1055.
81. Vogel A, Strassburg CP, Obermayer-Straub P, Brabant G, Manns MP. The genetic background of autoimmune polyendocrinopathy-candidiasis-ectodermal dystrophy and its autoimmune disease components. *J Mol Med (Berl)*. 2002;80:201-211.
82. Hamazaki Y, Fujita H, Kobayashi T, Choi Y, Scott HS, et al. Medullary thymic epithelial cells expressing Aire represent a unique lineage derived from cells expressing claudin. *Nat Immunol*. 2007;8:304-311.

83. Ramsey C, Winqvist O, Puhakka L, Halonen M, Moro A, et al. Aire deficient mice develop multiple features of APECED phenotype and show altered immune response. *Hum Mol Genet.* 2002;11:397-409.
84. Kuroda N, Mitani T, Takeda N, Ishimaru N, Arakaki R, et al. Development of autoimmunity against transcriptionally unrepressed target antigen in the thymus of Aire-deficient mice. *J Immunol.* 2005;174:1862-1870.
85. DeVoss J, Hou Y, Johannes K, Lu W, Liou GI, et al. Spontaneous autoimmunity prevented by thymic expression of a single self-antigen. *J Exp Med.* 2006;203:2727-2735.
86. Gavanescu I, Kessler B, Ploegh H, Benoist C, Mathis D. Loss of Aire-dependent thymic expression of a peripheral tissue antigen renders it a target of autoimmunity. *Proc Natl Acad Sci U S A.* 2007;104:4583-4587.
87. Mathis D, Benoist C. Aire. *Annual review of immunology.* 2009;27:287-312.
88. Derbinski J, Kyewski B. How thymic antigen presenting cells sample the body's self-antigens. *Curr Opin Immunol.* 2010;22:592-600.
89. Danzl NM, Donlin LT, Alexandropoulos K. Regulation of medullary thymic epithelial cell differentiation and function by the signaling protein Sin. *J Exp Med.* 2010;207:999-1013.
90. Boehm T, Scheu S, Pfeiffer K, Bleul CC. Thymic medullary epithelial cell differentiation, thymocyte emigration, and the control of autoimmunity require lympho-epithelial cross talk via LTbetaR. *J Exp Med.* 2003;198:757-769.
91. Engel M, Sidwell T, Vasanthakumar A, Grigoriadis G, Banerjee A. Thymic Regulatory T Cell Development: Role of Signalling Pathways and Transcription Factors. *Clin Dev Immunol.* 2013;2013:617595.
92. Fontenot JD, Rudensky AY. A well adapted regulatory contrivance: regulatory T cell development and the forkhead family transcription factor Foxp3. *Nat Immunol.* 2005;6:331-337.
93. Miyara M, Sakaguchi S. Natural regulatory T cells: mechanisms of suppression. *Trends Mol Med.* 2007;13:108-116.
94. Cowan JE, Parnell SM, Nakamura K, Caamano JH, Lane PJ, et al. The thymic medulla is required for Foxp3+ regulatory but not conventional CD4+ thymocyte development. *J Exp Med.* 2013;210:675-681.



95. Coquet JM, Ribot JC, Bąbala N, Middendorp S, van der Horst G, et al. Epithelial and dendritic cells in the thymic medulla promote CD4<sup>+</sup>Foxp3<sup>+</sup> regulatory T cell development via the CD27-CD70 pathway. *J Exp Med*. 2013;210:715-728.
96. Leavy O. Regulatory T cells: the thymic medulla - a cradle for TReg cell development. *Nat Rev Immunol*. 2013;13:304.
97. Kurts C, Heath WR, Carbone FR, Allison J, Miller JF, Kosaka H. Constitutive class I-restricted exogenous presentation of self antigens in vivo. *J Exp Med*. 1996;184:923-930.
98. Gallegos AM, Bevan MJ. Central tolerance to tissue-specific antigens mediated by direct and indirect antigen presentation. *J Exp Med*. 2004;200:1039-1049.
99. Barnden MJ, Heath WR, Rodda S, Carbone FR. Peptide antagonists that promote positive selection are inefficient at T cell activation and thymocyte deletion. *Eur J Immunol*. 1994;24:2452-2456.
100. Barnden MJ, Allison J, Heath WR, Carbone FR. Defective TCR expression in transgenic mice constructed using cDNA-based alpha- and beta-chain genes under the control of heterologous regulatory elements. *Immunol Cell Biol*. 1998;76:34-40.
101. Hakim FT, Gress RE. Reconstitution of the lymphocyte compartment after lymphocyte depletion: a key issue in clinical immunology. *Eur J Immunol*. 2005;35:3099-3102.
102. Williams KM, Hakim FT, Gress RE. T cell immune reconstitution following lymphodepletion. *Semin Immunol*. 2007;19:318-330.
103. Bahceci E, Epperson D, Douek DC, Melenhorst JJ, Childs RC, Barrett AJ. Early reconstitution of the T-cell repertoire after non-myeloablative peripheral blood stem cell transplantation is from post-thymic T-cell expansion and is unaffected by graft-versus-host disease or mixed chimaerism. *Br J Haematol*. 2003;122:934-943.
104. Mackall CL, Granger L, Sheard MA, Cepeda R, Gress RE. T-cell regeneration after bone marrow transplantation: differential CD45 isoform expression on thymic-derived versus thymic-independent progeny. *Blood*. 1993;82:2585-2594.
105. Fallen PR, McGreavey L, Madrigal JA, Potter M, Ethell M, et al. Factors affecting reconstitution of the T cell compartment in allogeneic haematopoietic cell transplant recipients. *Bone Marrow Transplant*. 2003;32:1001-1014.

106. Hakim FT, Memon SA, Cepeda R, Jones EC, Chow CK, et al. Age-dependent incidence, time course, and consequences of thymic renewal in adults. *Journal of Clinical Investigation*. 2005;115:930-939.
107. Storek J, Geddes M, Khan F, Huard B, Helg C, et al. Reconstitution of the immune system after hematopoietic stem cell transplantation in humans. *Semin Immunopathol*. 2008;30:425-437.
108. Rapoport AP, Stadtmauer EA, Aqui N, Badros A, Cotte J, et al. Restoration of immunity in lymphopenic individuals with cancer by vaccination and adoptive T-cell transfer. *Nat Med*. 2005;11:1230-1237.
109. Baron F, Sandmaier BM. Chimerism and outcomes after allogeneic hematopoietic cell transplantation following nonmyeloablative conditioning. *Leukemia*. 2006;20:1690-1700.
110. Baron F, Baker JE, Storb R, Gooley TA, Sandmaier BM, et al. Kinetics of engraftment in patients with hematologic malignancies given allogeneic hematopoietic cell transplantation after nonmyeloablative conditioning. *Blood*. 2004;104:2254-2262.
111. Bourgeois C, Stockinger B. T cell homeostasis in steady state and lymphopenic conditions. *Immunol Lett*. 2006;107:89-92.
112. Jameson SC. T cell homeostasis: keeping useful T cells alive and live T cells useful. *Semin Immunol*. 2005;17:231-237.
113. Roux E, Dumont-Girard F, Starobinski M, Siegrist CA, Helg C, et al. Recovery of immune reactivity after T-cell-depleted bone marrow transplantation depends on thymic activity. *Blood*. 2000;96:2299-2303.
114. Almeida AR, Borghans JA, Freitas AA. T cell homeostasis: thymus regeneration and peripheral T cell restoration in mice with a reduced fraction of competent precursors. *J Exp Med*. 2001;194:591-599.
115. Brugnani D, Airò P, Pennacchio M, Carella G, Malagoli A, et al. Immune reconstitution after bone marrow transplantation for combined immunodeficiencies: down-modulation of Bcl-2 and high expression of CD95/Fas account for increased susceptibility to spontaneous and activation-induced lymphocyte cell death. *Bone Marrow Transplant*. 1999;23:451-457.
116. Lin MT, Tseng LH, Frangoul H, Gooley T, Pei J, et al. Increased apoptosis of peripheral blood T cells following allogeneic hematopoietic cell transplantation. *Blood*. 2000;95:3832-3839.

117. Warren EH, Deeg HJ. Dissecting graft-versus-leukemia from graft-versus-host-disease using novel strategies. *Tissue Antigens*. 2013;81:183-193.
118. Jenq RR, van den Brink MR. Allogeneic haematopoietic stem cell transplantation: individualized stem cell and immune therapy of cancer. *Nat Rev Cancer*. 2010;10:213-221.
119. Ringdén O, Karlsson H, Olsson R, Omazic B, Uhlin M. The allogeneic graft-versus-cancer effect. *Br J Haematol*. 2009;147:614-633.
120. Vincent K, Roy DC, Perreault C. Next-generation leukemia immunotherapy. *Blood*. 2011;118:2951-2959.
121. Mutis T, Verdijk R, Schrama E, Esendam B, Brand A, Goulmy E. Feasibility of immunotherapy of relapsed leukemia with ex vivo-generated cytotoxic T lymphocytes specific for hematopoietic system-restricted minor histocompatibility antigens. *Blood*. 1999;93:2336-2341.
122. Bleakley M, Riddell SR. Molecules and mechanisms of the graft-versus-leukaemia effect. *Nat Rev Cancer*. 2004;4:371-380.
123. Mommaas B, Kamp J, Drijfhout JW, Beekman N, Ossendorp F, et al. Identification of a novel HLA-B60-restricted T cell epitope of the minor histocompatibility antigen HA-1 locus. *J Immunol*. 2002;169:3131-3136.
124. Maecker B, Sherr DH, Vonderheide RH, von Bergwelt-Baildon MS, Hirano N, et al. The shared tumor-associated antigen cytochrome P450 1B1 is recognized by specific cytotoxic T cells. *Blood*. 2003;102:3287-3294.
125. Siegel S, Wagner A, Kabelitz D, Marget M, Coggin J, et al. Induction of cytotoxic T-cell responses against the oncofetal antigen-immature laminin receptor for the treatment of hematologic malignancies. *Blood*. 2003;102:4416-4423.
126. Ferrara JLM, Levine JE, Reddy P, Holler E. Graft-versus-host disease. *The Lancet*. 2009;373:1550-1561.
127. Vigorito AC, Campregher PV, Storer BE, Carpenter PA, Moravec CK, et al. Evaluation of NIH consensus criteria for classification of late acute and chronic GVHD. *Blood*. 2009;114:702-708.
128. Pidala J. Graft-vs-host disease following allogeneic hematopoietic cell transplantation. *Cancer Control*. 2011;18:268-276.
129. Bacigalupo A, Palandri F. Management of acute graft versus host disease (GvHD). *Hematol J*. 2004;5:189-196.

130. Cahn JY, Klein JP, Lee SJ, Milpied N, Blaise D, et al. Prospective evaluation of 2 acute graft-versus-host (GVHD) grading systems: a joint Société Française de Greffe de Moëlle et Thérapie Cellulaire (SFGM-TC), Dana Farber Cancer Institute (DFCI), and International Bone Marrow Transplant Registry (IBMTR) prospective study. *Blood*. 2005;106:1495-1500.
131. Jagasia M, Arora M, Flowers ME, Chao NJ, McCarthy PL, et al. Risk factors for acute GVHD and survival after hematopoietic cell transplantation. *Blood*. 2012;119:296-307.
132. Flowers ME, Inamoto Y, Carpenter PA, Lee SJ, Kiem HP, et al. Comparative analysis of risk factors for acute graft-versus-host disease and for chronic graft-versus-host disease according to National Institutes of Health consensus criteria. *Blood*. 2011;117:3214-3219.
133. Wolf D, von Lilienfeld-Toal M, Wolf AM, Schleuning M, von Bergwelt-Baildon M, et al. Novel treatment concepts for graft-versus-host disease. *Blood*. 2012;119:16-25.
134. Loiseau P, Busson M, Balere ML, Dormoy A, Bignon JD, et al. HLA Association with hematopoietic stem cell transplantation outcome: the number of mismatches at HLA-A, -B, -C, -DRB1, or -DQB1 is strongly associated with overall survival. *Biol Blood Marrow Transplant*. 2007;13:965-974.
135. Flomenberg N, Baxter-Lowe LA, Confer D, Fernandez-Vina M, Filipovich A, et al. Impact of HLA class I and class II high-resolution matching on outcomes of unrelated donor bone marrow transplantation: HLA-C mismatching is associated with a strong adverse effect on transplantation outcome. *Blood*. 2004;104:1923-1930.
136. Lee SJ, Klein JP, Barrett AJ, Ringden O, Antin JH, et al. Severity of chronic graft-versus-host disease: association with treatment-related mortality and relapse. *Blood*. 2002;100:406.
137. Stewart BL, Storer B, Storek J, Deeg HJ, Storb R, et al. Duration of immunosuppressive treatment for chronic graft-versus-host disease. *Blood*. 2004;104:3501-3506.
138. Fraser CJ, Bhatia S, Ness K, Carter A, Francisco L, et al. Impact of chronic graft-versus-host disease on the health status of hematopoietic cell transplantation survivors: a report from the Bone Marrow Transplant Survivor Study. *Blood*. 2006;108:2867-2873.

139. Filipovich AH, Weisdorf D, Pavletic S, Socie G, Wingard JR, et al. National Institutes of Health consensus development project on criteria for clinical trials in chronic graft-versus-host disease: I. Diagnosis and staging working group report. *Biol Blood Marrow Transplant.* 2005;11:945-956.
140. Pidala J, Kurland B, Chai X, Majhail N, Weisdorf DJ, et al. Patient-reported quality of life is associated with severity of chronic graft-versus-host disease as measured by NIH criteria: report on baseline data from the Chronic GVHD Consortium. *Blood.* 2011;117:4651-4657.
141. Arora M, Klein JP, Weisdorf DJ, Hassebroek A, Flowers ME, et al. Chronic GVHD risk score: a Center for International Blood and Marrow Transplant Research analysis. *Blood.* 2011;117:6714-6720.
142. Pavletic SZ, Carter SL, Kernan NA, Henslee-Downey J, Mendizabal AM, et al. Influence of T-cell depletion on chronic graft-versus-host disease: results of a multicenter randomized trial in unrelated marrow donor transplantation. *Blood.* 2005;106:3308-3313.
143. Linhares YP, Pavletic S, Gale RP. Chronic GVHD: Where are we? Where do we want to be? Will immunomodulatory drugs help? *Bone Marrow Transplant.* 2013;48:203-209.
144. Filipovich AH. Diagnosis and manifestations of chronic graft-versus-host disease. *Best Pract Res Clin Haematol.* 2008;21:251-257.
145. Arai S, Jagasia M, Storer B, Chai X, Pidala J, et al. Global and organ-specific chronic graft-versus-host disease severity according to the 2005 NIH Consensus Criteria. *Blood.* 2011;118:4242-4249.
146. Hess AD. Equal opportunity targeting in chronic GVHD. *Blood.* 2012;119:6183-6184.
147. Martin PJ. Biology of Chronic Graft-versus-Host Disease: Implications for a Future Therapeutic Approach. *Keio J Med.* 2008;57:177-183.
148. Pavletic SZ, Lee SJ, Socie G, Vogelsang G. Chronic graft-versus-host disease: implications of the National Institutes of Health consensus development project on criteria for clinical trials. *Bone Marrow Transplant.* 2006;38:645-651.
149. Pavletic SZ, Fowler DH. Are we making progress in GVHD prophylaxis and treatment? *Hematology Am Soc Hematol Educ Program.* 2012;2012:251-264.
150. Schroeder MA, DiPersio JF. Mouse models of graft-versus-host disease: advances and limitations. *Dis Model Mech.* 2011;4:318-333.

151. Matzinger P. The danger model: a renewed sense of self. *Science*. 2002;296:301-305.
152. Hill GR, Ferrara JL. The primacy of the gastrointestinal tract as a target organ of acute graft-versus-host disease: rationale for the use of cytokine shields in allogeneic bone marrow transplantation. *Blood*. 2000;95:2754-2759.
153. Zeiser R, Penack O, Holler E, Idzko M. Danger signals activating innate immunity in graft-versus-host disease. *J Mol Med (Berl)*. 2011;89:833-845.
154. Wilhelm K, Ganesan J, Müller T, Dürr C, Grimm M, et al. Graft-versus-host disease is enhanced by extracellular ATP activating P2X7R. *Nat Med*. 2010;16:1434-1438.
155. Chakraverty R, Sykes M. The role of antigen-presenting cells in triggering graft-versus-host disease and graft-versus-leukemia. *Blood*. 2007;110:9-17.
156. Teshima T, Ordemann R, Reddy P, Gagin S, Liu C, et al. Acute graft-versus-host disease does not require alloantigen expression on host epithelium. *Nature medicine*. 2002;8:575-581.
157. Ferrara JL, Reddy P. Pathophysiology of graft-versus-host disease. *Semin Hematol*. 2006;43:3-10.
158. Goulmy E. Minor histocompatibility antigens: from transplantation problems to therapy of cancer. *Hum Immunol*. 2006;67:433-438.
159. Hambach L, Spierings E, Goulmy E. Risk assessment in haematopoietic stem cell transplantation: minor histocompatibility antigens. *Best Pract Res Clin Haematol*. 2007;20:171-187.
160. Fowler DH, Kurasawa K, Smith R, Eckhaus MA, Gress RE. Donor CD4-enriched cells of Th2 cytokine phenotype regulate graft-versus-host disease without impairing allogeneic engraftment in sublethally irradiated mice. *Blood*. 1994;84:3540-3549.
161. Yang Y-G, Dey BR, Sergio JJ, Pearson DA, Sykes M. Donor-derived interferon gamma is required for inhibition of acute graft-versus-host disease by interleukin 12. *Journal of Clinical Investigation*. 1998;102:2126.
162. Hauri-Hohl MM, Keller MP, Gill J, Hafen K, Pachlatko E, et al. Donor T-cell alloreactivity against host thymic epithelium limits T-cell development after bone marrow transplantation. *Blood*. 2007;109:4080-4088.

163. McCormick LL, Zhang Y, Tootell E, Gilliam AC. Anti-TGF-beta treatment prevents skin and lung fibrosis in murine sclerodermatous graft-versus-host disease: a model for human scleroderma. *J Immunol.* 1999;163:5693-5699.
164. Zhang C, Todorov I, Zhang Z, Liu Y, Kandeel F, et al. Donor CD4+ T and B cells in transplants induce chronic graft-versus-host disease with autoimmune manifestations. *Blood.* 2006;107:2993-3001.
165. Cutler C, Miklos D, Kim HT, Treister N, Woo SB, et al. Rituximab for steroid-refractory chronic graft-versus-host disease. *Blood.* 2006;108:756-762.
166. Chen X, Vodanovic-Jankovic S, Johnson B, Keller M, Komorowski R, Drobyski WR. Absence of regulatory T-cell control of TH1 and TH17 cells is responsible for the autoimmune-mediated pathology in chronic graft-versus-host disease. *Blood.* 2007;110:3804-3813.
167. Anderson BE, McNiff JM, Matte C, Athanasiadis I, Shlomchik WD, Shlomchik MJ. Recipient CD4+ T cells that survive irradiation regulate chronic graft-versus-host disease. *Blood.* 2004;104:1565-1573.
168. Fujita S, Sato Y, Sato K, Eizumi K, Fukaya T, et al. Regulatory dendritic cells protect against cutaneous chronic graft-versus-host disease mediated through CD4+CD25+Foxp3+ regulatory T cells. *Blood.* 2007;110:3793-3803.
169. Miura Y, Thoburn CJ, Bright EC, Phelps ML, Shin T, et al. Association of Foxp3 regulatory gene expression with graft-versus-host disease. *Blood.* 2004;104:2187-2193.
170. Zorn E, Kim HT, Lee SJ, Floyd BH, Litsa D, et al. Reduced frequency of FOXP3+ CD4+CD25+ regulatory T cells in patients with chronic graft-versus-host disease. *Blood.* 2005;106:2903-2911.
171. Meignin V, Peffault de Latour R, Zuber J, Régnault A, Mounier N, et al. Numbers of Foxp3-expressing CD4+CD25high T cells do not correlate with the establishment of long-term tolerance after allogeneic stem cell transplantation. *Exp Hematol.* 2005;33:894-900.
172. Arimoto K, Kadowaki N, Ishikawa T, Ichinohe T, Uchiyama T. FOXP3 expression in peripheral blood rapidly recovers and lacks correlation with the occurrence of graft-versus-host disease after allogeneic stem cell transplantation. *International journal of hematology.* 2007;85:154-162.

173. Rieger K, Loddenkemper C, Maul J, Fietz T, Wolff D, et al. Mucosal FOXP3<sup>+</sup> regulatory T cells are numerically deficient in acute and chronic GvHD. *Blood*. 2006;107:1717-1723.
174. Matsuoka K, Kim HT, McDonough S, Bascug G, Warshauer B, et al. Altered regulatory T cell homeostasis in patients with CD4<sup>+</sup> lymphopenia following allogeneic hematopoietic stem cell transplantation. *J Clin Invest*. 2010;120:1479-1493.
175. Koreth J, Matsuoka K, Kim HT, McDonough SM, Bindra B, et al. Interleukin-2 and regulatory T cells in graft-versus-host disease. *N Engl J Med*. 2011;365:2055-2066.
176. Morohashi T, Ogasawara K, Kitaichi N, Iwabuchi K, Onoé K. Abrogation of negative selection by GVHR induced by minor histocompatibility antigens or H-2D antigen alone. *Immunobiology*. 2000;202:268-279.
177. Holländer GA, Widmer B, Burakoff SJ. Loss of normal thymic repertoire selection and persistence of autoreactive T cells in graft vs host disease. *J Immunol*. 1994;152:1609-1617.
178. van den Brink MR, Moore E, Ferrara JL, Burakoff SJ. Graft-versus-host-disease-associated thymic damage results in the appearance of T cell clones with anti-host reactivity. *Transplantation*. 2000;69:446-449.
179. Teshima T, Reddy P, Liu C, Williams D, Cooke KR, Ferrara JL. Impaired thymic negative selection causes autoimmune graft-versus-host disease. *Blood*. 2003;102:429-435.
180. Zhang Y, Hexner E, Frank D, Emerson SG. CD4<sup>+</sup> T cells generated de novo from donor hemopoietic stem cells mediate the evolution from acute to chronic graft-versus-host disease. *J Immunol*. 2007;179:3305-3314.
181. Sakoda Y, Hashimoto D, Asakura S, Takeuchi K, Harada M, et al. Donor-derived thymic-dependent T cells cause chronic graft-versus-host disease. *Blood*. 2007;109:1756-1764.
182. Hakim FT, Payne S, Shearer GM. Recovery of T cell populations after acute graft-vs-host reaction. *The Journal of Immunology*. 1994;152:58-64.
183. Zhao D, Young JS, Chen YH, Shen E, Yi T, et al. Alloimmune response results in expansion of autoreactive donor CD4<sup>+</sup> T cells in transplants that can mediate chronic graft-versus-host disease. *J Immunol*. 2011;186:856-868.



184. Rangarajan H, Yassai M, Subramanian H, Komorowski R, Whitaker M, et al. Emergence of T cells that recognize nonpolymorphic antigens during graft-versus-host disease. *Blood*. 2012;119:6354-6364.
185. Tivol E, Komorowski R, Drobyski WR. Emergent autoimmunity in graft-versus-host disease. *Blood*. 2005;105:4885-4891.
186. Sung AD, Chao NJ. Concise review: acute graft-versus-host disease: immunobiology, prevention, and treatment. *Stem Cells Transl Med*. 2013;2:25-32.
187. Ho VT, Soiffer RJ. The history and future of T-cell depletion as graft-versus-host disease prophylaxis for allogeneic hematopoietic stem cell transplantation. *Blood*. 2001;98:3192-3204.
188. Platzbecker U, Ehninger G, Bornhäuser M. Allogeneic transplantation of CD34+ selected hematopoietic cells--clinical problems and current challenges. *Leuk Lymphoma*. 2004;45:447-453.
189. Wagner JE, Thompson JS, Carter SL, Kernan NA, Unrelated Donor Marrow Transplantation Trial. Effect of graft-versus-host disease prophylaxis on 3-year disease-free survival in recipients of unrelated donor bone marrow (T-cell Depletion Trial): a multi-centre, randomised phase II-III trial. *Lancet*. 2005;366:733-741.
190. Couriel DR, Saliba RM, Giralt S, Khouri I, Andersson B, et al. Acute and chronic graft-versus-host disease after ablative and nonmyeloablative conditioning for allogeneic hematopoietic transplantation. *Biology of Blood and Marrow Transplantation*. 2004;10:178-185.
191. Sorror ML, Maris MB, Storer B, Sandmaier BM, Diaconescu R, et al. Comparing morbidity and mortality of HLA-matched unrelated donor hematopoietic cell transplantation after nonmyeloablative and myeloablative conditioning: influence of pretransplantation comorbidities. *Blood*. 2004;104:961-968.
192. Mielcarek M, Martin PJ, Leisenring W, Flowers ME, Maloney DG, et al. Graft-versus-host disease after nonmyeloablative versus conventional hematopoietic stem cell transplantation. *Blood*. 2003;102:756-762.
193. Pérez-Simón JA, Kottaridis PD, Martino R, Craddock C, Caballero D, et al. Nonmyeloablative transplantation with or without alemtuzumab: comparison between 2 prospective studies in patients with lymphoproliferative disorders. *Blood*. 2002;100:3121-3127.

194. Socié G, Schmoor C, Bethge WA, Ottinger HD, Stelljes M, et al. Chronic graft-versus-host disease: long-term results from a randomized trial on graft-versus-host disease prophylaxis with or without anti-T-cell globulin ATG-Fresenius. *Blood*. 2011;117:6375-6382.
195. Soiffer RJ, Lerademacher J, Ho V, Kan F, Artz A, et al. Impact of immune modulation with anti-T-cell antibodies on the outcome of reduced-intensity allogeneic hematopoietic stem cell transplantation for hematologic malignancies. *Blood*. 2011;117:6963-6970.
196. Inamoto Y, Flowers ME. Treatment of chronic graft-versus-host disease in 2011. *Current Opinion in Hematology*. 2011;18:414-420.
197. Clave E, Busson M, Douay C, Peffault de Latour R, Berrou J, et al. Acute graft versus host disease transiently impairs thymic output in young patients after allogeneic hematopoietic stem cell transplantation. *Blood*. 2009;113:6477-6484.
198. Olkinuora H, von Willebrand E, Kantele JM, Vainio O, Talvensaaari K, et al. The impact of early viral infections and graft-versus-host disease on immune reconstitution following paediatric stem cell transplantation. *Scand J Immunol*. 2011;73:586-593.
199. Perales MA, Ishill N, Lomazow WA, Weinstock DM, Papadopoulos EB, et al. Long-term follow-up of patients treated with daclizumab for steroid-refractory acute graft-vs-host disease. *Bone Marrow Transplant*. 2007;40:481-486.
200. Willenbacher W, Basara N, Blau IW, Fauser AA, Kiehl MG. Treatment of steroid refractory acute and chronic graft-versus-host disease with daclizumab. *Br J Haematol*. 2001;112:820-823.
201. Arai S, Margolis J, Zahurak M, Anders V, Vogelsang GB. Poor outcome in steroid-refractory graft-versus-host disease with antithymocyte globulin treatment. *Biology of Blood and Marrow Transplantation*. 2002;8:155-160.
202. McCaul KG, Nevill TJ, Barnett MJ, Toze CL, Currie CJ, et al. Treatment of steroid-resistant acute graft-versus-host disease with rabbit antithymocyte globulin. *J Hematother Stem Cell Res*. 2000;9:367-374.
203. Remberger M, Ringden O, Aschan J, Ljungman P, Lönnqvist B, Markling L. Long-term follow-up of a randomized trial comparing T-cell depletion with a combination of methotrexate and cyclosporine in

- adult leukemic marrow transplant recipients. *Transplant Proc.* 1994;26:1829-1830.
204. Khoury H, Kashyap A, Adkins DR, Brown RA, Miller G, et al. Treatment of steroid-resistant acute graft-versus-host disease with anti-thymocyte globulin. *Bone Marrow Transplant.* 2001;27:1059-1064.
205. Weinberg K, Blazar BR, Wagner JE, Agura E, Hill BJ, et al. Factors affecting thymic function after allogeneic hematopoietic stem cell transplantation. *Blood.* 2001;97:1458-1466.
206. Hakim FT, Gress RE. Reconstitution of thymic function after stem cell transplantation in humans. *Curr Opin Hematol.* 2002;9:490-496.
207. Talvensaari K, Clave E, Douay C, Rabian C, Garderet L, et al. A broad T-cell repertoire diversity and an efficient thymic function indicate a favorable long-term immune reconstitution after cord blood stem cell transplantation. *Blood.* 2002;99:1458.
208. Seddik M, Seemayer TA, Lapp WS. T cell functional defect associated with thymic epithelial cell injury induced by a graft-versus-host reaction. *Transplantation.* 1980;29:61-66.
209. Seemayer TA, Lapp WS, Bolande RP. Thymic epithelial injury in graft-versus-host reactions following adrenalectomy. *Am J Pathol.* 1978;93:325-338.
210. Lapp WS, Ghayur T, Mendes M, Seddik M, Seemayer TA. The functional and histological basis for graft-versus-host-induced immunosuppression. *Immunol Rev.* 1985;88:107-133.
211. Seemayer TA, Bolande RP. Thymic involution mimicking thymic dysplasia: a consequence of transfusion-induced graft versus host disease in a premature infant. *Arch Pathol Lab Med.* 1980;104:141-144.
212. Krenger W, Holländer GA. The immunopathology of thymic GVHD. *Semin Immunopathol.* 2008;30:439-456.
213. Krenger W, Schmidlin H, Cavadini G, Holländer GA. On the relevance of TCR rearrangement circles as molecular markers for thymic output during experimental graft-versus-host disease. *J Immunol.* 2004;172:7359-7367.
214. Lewin SR, Heller G, Zhang L, Rodrigues E, Skulsky E, et al. Direct evidence for new T-cell generation by patients after either T-cell-depleted or unmodified allogeneic hematopoietic stem cell transplantations. *Blood.* 2002;100:2235-2242.

215. Storek J, Joseph A, Dawson MA, Douek DC, Storer B, Maloney DG. Factors influencing T-lymphopoiesis after allogeneic hematopoietic cell transplantation. *Transplantation*. 2002;73:1154-1158.
216. Rossi S, Blazar BR, Farrell CL, Danilenko DM, Lacey DL, et al. Keratinocyte growth factor preserves normal thymopoiesis and thymic microenvironment during experimental graft-versus-host disease. *Blood*. 2002;100:682-691.
217. Krenger W, Rossi S, Holländer GA. Apoptosis of thymocytes during acute graft-versus-host disease is independent of glucocorticoids. *Transplantation*. 2000;69:2190-2193.
218. Kumamoto T, Inaba M, Toki J, Adachi Y, Imamura H, Ikehara S. Cytotoxic effects of irradiation and deoxyguanosine on fetal thymus. *Immunobiology*. 1995;192:365-381.
219. Pénit C, Lucas B, Vasseur F. Cell expansion and growth arrest phases during the transition from precursor (CD4-8-) to immature (CD4+8+) thymocytes in normal and genetically modified mice. *J Immunol*. 1995;154:5103-5113.
220. Rodewald HR, Fehling HJ. Molecular and cellular events in early thymocyte development. *Adv Immunol*. 1998;69:1-112.
221. Krenger W, Rossi S, Piali L, Holländer GA. Thymic atrophy in murine acute graft-versus-host disease is effected by impaired cell cycle progression of host pro-T and pre-T cells. *Blood*. 2000;96:347-354.
222. Krenger W, Holländer GA. The thymus in GVHD pathophysiology. *Best Pract Res Clin Haematol*. 2008;21:119-128.
223. Na IK, Lu SX, Yim NL, Goldberg GL, Tsai J, et al. The cytolytic molecules Fas ligand and TRAIL are required for murine thymic graft-versus-host disease. *J Clin Invest*. 2010;120:343-356.
224. Wu T, Young JS, Johnston H, Ni X, Deng R, et al. Thymic damage, impaired negative selection, and development of chronic graft-versus-host disease caused by donor CD4+ and CD8+ T cells. *J Immunol*. 2013;191:488-499.
225. Dertschnig S, Nusspaumer G, Ivanek R, Hauri-Hohl MM, Holländer GA, Krenger W. Epithelial cytoprotection sustains ectopic expression of tissue-restricted antigens in the thymus during murine acute GVHD. *Blood*. 2013;122:837-841.
226. Weinberg KI. ProTEction from posttransplantation immune deficiency? *Blood*. 2007;109:3617-2618.

227. Holländer GA, Krenger W, Blazar BR. Emerging strategies to boost thymic function. *Curr Opin Pharmacol*. 2010.
228. Finch PW, Rubin JS. Keratinocyte growth factor/fibroblast growth factor 7, a homeostatic factor with therapeutic potential for epithelial protection and repair. *Adv Cancer Res*. 2004;91:69-136.
229. Spielberger R, Stiff P, Bensinger W, Gentile T, Weisdorf D, et al. Palifermin for oral mucositis after intensive therapy for hematologic cancers. *N Engl J Med*. 2004;351:2590-2598.
230. Radtke ML, Kolesar JM. Palifermin (Kepivance) for the treatment of oral mucositis in patients with hematologic malignancies requiring hematopoietic stem cell support. *J Oncol Pharm Pract*. 2005;11:121-125.
231. Siddiqui MA, Wellington K. Palifermin: in myelotoxic therapy-induced oral mucositis. *Drugs*. 2005;65:2139-46; discussion 2147-9.
232. Turner N, Grose R. Fibroblast growth factor signalling: from development to cancer. *Nature Reviews Cancer*. 2010;10:116-129.
233. Werner S. Keratinocyte growth factor: a unique player in epithelial repair processes. *Cytokine & growth factor reviews*. 1998;9:153-165.
234. Moroni E, Dell'Era P, Rusnati M, Presta M. Fibroblast growth factors and their receptors in hematopoiesis and hematological tumors. *J Hematother Stem Cell Res*. 2002;11:19-32.
235. Erickson M, Morkowski S, Lehar S, Gillard G, Beers C, et al. Regulation of thymic epithelium by keratinocyte growth factor. *Blood*. 2002;100:3269-3278.
236. Revest JM, Suniara RK, Kerr K, Owen JJ, Dickson C. Development of the thymus requires signaling through the fibroblast growth factor receptor R2-IIIb. *J Immunol*. 2001;167:1954-1961.
237. Revest JM, Spencer-Dene B, Kerr K, De Moerlooze L, Rosewell I, Dickson C. Fibroblast growth factor receptor 2-IIIb acts upstream of Shh and Fgf4 and is required for limb bud maintenance but not for the induction of Fgf8, Fgf10, Msx1, or Bmp4. *Dev Biol*. 2001;231:47-62.
238. Suniara RK, Jenkinson EJ, Owen JJ. An essential role for thymic mesenchyme in early T cell development. *J Exp Med*. 2000;191:1051-1056.
239. Rossi SW, Jeker LT, Ueno T, Kuse S, Keller MP, et al. Keratinocyte growth factor (KGF) enhances postnatal T-cell development via

- enhancements in proliferation and function of thymic epithelial cells. *Blood*. 2007;109:3803-3811.
240. Alpdogan O, Hubbard VM, Smith OM, Patel N, Lu S, et al. Keratinocyte growth factor (KGF) is required for postnatal thymic regeneration. *Blood*. 2006;107:2453-2460.
  241. Min D, Panoskaltis-Mortari A, Kuro-O M, Holländer GA, Blazar BR, Weinberg KI. Sustained thymopoiesis and improvement in functional immunity induced by exogenous KGF administration in murine models of aging. *Blood*. 2007;109:2529-2537.
  242. Chu -W, Hakim T. KGF boosts thymic archiTECture. *Blood*. 2007;109:3613-3614.
  243. Wang Y, Chen G, Qiao S, Ma X, Tang X, et al. Keratinocyte growth factor enhanced immune reconstitution in murine allogeneic umbilical cord blood cell transplant. *Leukemia & Lymphoma*. 2011;52:1556-1566.
  244. Ben-Sasson SZ, Gerstel R, Hu-Li J, Paul WE. Cell division is not a "clock" measuring acquisition of competence to produce IFN-gamma or IL-4. *J Immunol*. 2001;166:112-120.
  245. Irizarry RA, Hobbs B, Collin F, Beazer-Barclay YD, Antonellis KJ, et al. Exploration, normalization, and summaries of high density oligonucleotide array probe level data. *Biostatistics*. 2003;4:249-264.
  246. Grunkemeier GL, Wu Y. What are the odds? *Ann Thorac Surg*. 2007;83:1240-1244.
  247. Gotter J. Medullary epithelial cells of the human thymus express a highly diverse selection of tissue-specific genes colocalized in chromosomal clusters. *J Exp Med*. 2004;199:155-166.
  248. Anderson MS, Su MA. Aire and T cell development. *Curr Opin Immunol*. 2011;23:198-206.
  249. Klein L, Hinterberger M, Wirnsberger G, Kyewski B. Antigen presentation in the thymus for positive selection and central tolerance induction. *Nat Rev Immunol*. 2009;9:833-844.
  250. Hu Q, Nicol SA, Suen AY, Baldwin TA. Examination of thymic positive and negative selection by flow cytometry. *J Vis Exp*. 2012.
  251. Suen AY, Baldwin TA. Proapoptotic protein Bim is differentially required during thymic clonal deletion to ubiquitous versus tissue-restricted antigens. *Proc Natl Acad Sci U S A*. 2012;109:893-898.

252. Hubert FX, Kinkel SA, Davey GM, Phipson B, Mueller SN, et al. Aire regulates the transfer of antigen from mTECs to dendritic cells for induction of thymic tolerance. *Blood*. 2011;118:2462-2472.
253. Metzger TC, Khan IS, Gardner JM, Mouchess ML, Johannes KP, et al. Lineage tracing and cell ablation identify a post-aire-expressing thymic epithelial cell population. *Cell Rep*. 2013;5:166-179.
254. Martinez RJ, Zhang N, Thomas SR, Nandiwada SL, Jenkins MK, et al. Arthritogenic self-reactive CD4<sup>+</sup> T cells acquire an FR4hiCD73hi anergic state in the presence of Foxp3<sup>+</sup> regulatory T cells. *J Immunol*. 2012;188:170-181.
255. Kobie JJ, Shah PR, Yang L, Rebhahn JA, Fowell DJ, Mosmann TR. T regulatory and primed uncommitted CD4 T cells express CD73, which suppresses effector CD4 T cells by converting 5'-adenosine monophosphate to adenosine. *J Immunol*. 2006;177:6780-6786.
256. Yamaguchi T, Hirota K, Nagahama K, Ohkawa K, Takahashi T, et al. Control of immune responses by antigen-specific regulatory T cells expressing the folate receptor. *Immunity*. 2007;27:145-159.
257. Balzar M, Winter J, de Boer J, Not Available SL. The biology of the 17-1A antigen (Ep-CAM). *Journal of Molecular Medicine*. 1999;77:699-712.
258. Blackburn CC, Augustine CL, Li R, Harvey RP, Malin MA, et al. The nu gene acts cell-autonomously and is required for differentiation of thymic epithelial progenitors. *Proc Natl Acad Sci U S A*. 1996;93:5742-5746.
259. Dudakov JA, Hanash AM, Jenq RR, Young LF, Ghosh A, et al. Interleukin-22 drives endogenous thymic regeneration in mice. *Science*. 2012;336:91-95.
260. Fletcher AL, Lowen TE, Sakkal S, Reiseger JJ, Hammett MV, et al. Ablation and regeneration of tolerance-inducing medullary thymic epithelial cells after cyclosporine, cyclophosphamide, and dexamethasone treatment. *J Immunol*. 2009;183:823-831.
261. Su MA, Giang K, Zumer K, Jiang H, Oven I, et al. Mechanisms of an autoimmunity syndrome in mice caused by a dominant mutation in Aire. *J Clin Invest*. 2008;118:1712-1726.
262. Ukena SN, Grosse J, Mischak-Weissinger E, Buchholz S, Stadler M, et al. Acute but not chronic graft-versus-host disease is associated with a

- reduction of circulating CD4(+)CD25 (high)CD127 (low/-) regulatory T cells. *Ann Hematol.* 2011;90:213-218.
263. Hänninen A, Nurmela R, Maksimow M, Heino J, Jalkanen S, Kurts C. Islet beta-cell-specific T cells can use different homing mechanisms to infiltrate and destroy pancreatic islets. *Am J Pathol.* 2007;170:240-250.
264. Gagnerault -C, Luan J, Lotton C, Lepault F. Pancreatic Lymph Nodes Are Required for Priming of Cell Reactive T Cells in NOD Mice. *Journal of Experimental Medicine.* 2002;196:369-377.
265. Shevach EM. Mechanisms of foxp3+ T regulatory cell-mediated suppression. *Immunity.* 2009;30:636-645.
266. Parkman R. A 2-hit model for chronic GVHD. *Blood.* 2013;122:623-624.
267. Enouz S, Carrié L, Merkler D, Bevan MJ, Zehn D. Autoreactive T cells bypass negative selection and respond to self-antigen stimulation during infection. *J Exp Med.* 2012;209:1769-1779.
268. Nasilowska-Adamska B, Rzepecki P, Manko J, Czyz A, Markiewicz M, et al. The influence of palifermin (Kepivance) on oral mucositis and acute graft versus host disease in patients with hematological diseases undergoing hematopoietic stem cell transplant. *Bone Marrow Transplant.* 2007;40:983-988.
269. Langner S, Staber P, Schub N, Gramatzki M, Grothe W, et al. Palifermin reduces incidence and severity of oral mucositis in allogeneic stem-cell transplant recipients. *Bone Marrow Transplant.* 2008;42:275-279.
270. Blazar BR, Weisdorf DJ, DeFor T, Goldman A, Braun T, et al. Phase 1/2 randomized, placebo-control trial of palifermin to prevent graft-versus-host disease (GVHD) after allogeneic hematopoietic stem cell transplantation (HSCT). *Blood.* 2006;108:3216-3222.
271. Levine JE, Blazar BR, DeFor T, Ferrara JL, Weisdorf DJ. Long-term follow-up of a phase I/II randomized, placebo-controlled trial of palifermin to prevent graft-versus-host disease (GVHD) after related donor allogeneic hematopoietic cell transplantation (HCT). *Biol Blood Marrow Transplant.* 2008;14:1017-1021.
272. Krijanovski OI, Hill GR, Cooke KR, Teshima T, Crawford JM, et al. Keratinocyte growth factor separates graft-versus-leukemia effects from graft-versus-host disease. *Blood.* 1999;94:825-831.



273. Jagasia MH, Abonour R, Long GD, Bolwell BJ, Laport GG, et al. Palifermin for the reduction of acute GVHD: a randomized, double-blind, placebo-controlled trial. *Bone Marrow Transplant*. 2012;47:1350-1355.

## 8. ACKNOWLEDGEMENTS

First and foremost a big thank you to Werner Krenger who supported and advised me throughout my PhD years. It was a big pleasure to have you as a supervisor, you taught me a lot, and I think we had a good time, not only science related but also auf den Brettern, die die Welt bedeuten. The second, but not less important, thank you goes to Georg A. Holländer for letting me work in his lab, independently and free, and giving me the right support when it was needed. I always appreciate your feedback. There are many people in and around the lab without whom I would not have been able to finish this work and I would like to mention them here in no specific order. A big thanks to Robert Ivanek for helping me tremendously with the microarray analysis and introducing me into R, Katrin Hafen for teaching me everything about the mouse, Gretel Nusspaumer for supporting me in experiment planning, Mathias M. Hauri for scientific support and shipping boneys from Seattle, to all the other girls and boys from the lab for cheerful moments, for lunch times, for solving my computer problems, for i.p. injections when I was too busy, for watching the royal wedding, for gossip chitchats, and for many other things, thank you Angela, Noriko, Elisa, Chiara, Caroline, Saule, Martha, Elli, Tatjana, Annick, Hong Ying, Sanjay, Carlos, Gabor, Thomas and Saulius. I would also like to acknowledge Prof. Christoph Hess and Prof. Jean Pieters as members of my PhD committee.

Beside the science world, there are many people who are here when I need them and contribute substantially to me being smiley and happy. Daniel, thank you for everything you give me, be it in easy or rather difficult moments. I know, I can be quite "pesante", especially when I'm about to finish my PhD...thanks for being here for me, supporting me and for your love. Danke Papi! Ich möchte keine grossen Worte verlieren, sondern einfach Danke sagen. Last but not least, I would like to remember my mum. I know that she is with me and knowing her support gave me power and strength to reach this and many other targets in my life. She would be happy now.

## 9. APPENDIX

From [bloodjournal.hematologylibrary.org](http://bloodjournal.hematologylibrary.org) at MEDIZINBIBLIOTEK on August 2, 2013. For personal use only.

# blood

2013 122: 837-841  
Prepublished online May 29, 2013;  
doi:10.1182/blood-2012-12-474759

## Epithelial cytoprotection sustains ectopic expression of tissue-restricted antigens in the thymus during murine acute GVHD

Simone Dertschnig, Gretel Nusspaumer, Robert Ivanek, Mathias M. Hauri-Hohl, Georg A. Holländer and Werner Krenger

---

Updated information and services can be found at:  
<http://bloodjournal.hematologylibrary.org/content/122/5/837.full.html>

Articles on similar topics can be found in the following Blood collections  
[Brief Reports](#) (1664 articles)  
[Transplantation](#) (1890 articles)

---

Information about reproducing this article in parts or in its entirety may be found online at:  
[http://bloodjournal.hematologylibrary.org/site/misc/rights.xhtml#repub\\_requests](http://bloodjournal.hematologylibrary.org/site/misc/rights.xhtml#repub_requests)

Information about ordering reprints may be found online at:  
<http://bloodjournal.hematologylibrary.org/site/misc/rights.xhtml#reprints>

Information about subscriptions and ASH membership may be found online at:  
<http://bloodjournal.hematologylibrary.org/site/subscriptions/index.xhtml>

Blood (print ISSN 0006-4971, online ISSN 1528-0020), is published weekly by the American Society of Hematology, 2021 L St, NW, Suite 900, Washington DC 20036.  
Copyright 2011 by The American Society of Hematology; all rights reserved.



## Brief Report

### TRANSPLANTATION

# Epithelial cytoprotection sustains ectopic expression of tissue-restricted antigens in the thymus during murine acute GVHD

Simone Dertschnig,<sup>1</sup> Gretel Nusspaumer,<sup>1</sup> Robert Ivanek,<sup>1</sup> Mathias M. Hauri-Hohl,<sup>2</sup> Georg A. Holländer,<sup>1,3</sup> and Werner Krenger<sup>1</sup>

<sup>1</sup>Department of Biomedicine, University of Basel and Basel University Children's Hospital, Basel, Switzerland; <sup>2</sup>Benaroya Research Institute, Virginia Mason Hospital, Seattle, WA; and <sup>3</sup>Department of Paediatrics and the Weatherall Institute of Molecular Medicine, University of Oxford, Oxford, United Kingdom

#### Key Points

- Acute GVHD predisposes to autoimmune chronic GVHD, but it is currently unclear how autoimmunity is linked to antecedent alloimmunity.
- Loss of central tolerance induction that occurs via functional compromise of thymic epithelial cells may provide such a pathogenic link.

Development of acute graft-versus-host disease (aGVHD) predisposes to chronic GVHD with autoimmune manifestations. A characteristic of experimental aGVHD is the de novo generation of autoreactive T cells. Central tolerance is dependent on the intrathymic expression of tissue-restricted peripheral self-antigens (TRA), which is in mature medullary thymic epithelial cells (mTEC<sup>high</sup>) partly controlled by the autoimmune regulator (Aire). Because TECs are targets of donor T-cell alloimmunity, we tested whether murine aGVHD interfered with the capacity of recipient Aire<sup>+</sup>mTEC<sup>high</sup> to sustain TRA diversity. We report that aGVHD weakens the platform for central tolerance induction because individual TRAs are purged from the total repertoire secondary to a decline in the Aire<sup>+</sup>mTEC<sup>high</sup> cell pool. Peritransplant administration of an epithelial cytoprotective agent, fibroblast growth factor-7, maintained a stable pool of Aire<sup>+</sup>mTEC<sup>high</sup>, with an improved TRA transcriptome despite aGVHD. Taken together, our data provide a mechanism for how autoimmunity may develop in the context of antecedent alloimmunity. (*Blood*. 2013;122(5):837-841)

#### Introduction

Self-tolerance of the nascent T-cell receptor repertoire is attained through negative selection in the thymus.<sup>1</sup> Essential for clonal deletion is the exposure of thymocytes to self-antigens, including those with highly restricted tissue expression. Within the thymus, the ectopic expression of many tissue-restricted peripheral self-antigens (TRAs) is a distinct property of mature medullary thymic epithelial cells (mTEC<sup>high</sup>).<sup>2,3</sup> TRA expression is controlled partly by the transcription factor autoimmune regulator (Aire).<sup>3</sup> Deficits in Aire and/or TRA expression (independent of their causes) impair negative selection and can consequently cause autoimmune disease.<sup>2-5</sup>

Acute and chronic graft-versus-host disease (aGVHD and cGVHD, respectively) remain the primary complications of allogeneic hematopoietic stem cell transplantation (allo-HSCT).<sup>6</sup> aGVHD is initiated by alloreactive donor T cells and targets a restricted set of tissues, including the thymus.<sup>7,8</sup> The development of human aGVHD predisposes to cGVHD, whose autoimmune manifestations are integral components of disease.<sup>9</sup> It remains uncertain, however, whether and how autoimmunity is linked to antecedent alloimmunity. A hallmark of murine aGVHD is the de novo generation of autoreactive T cells from donor HSC<sup>10,11</sup> which can mediate the evolution from acute to chronic GVHD.<sup>12,13</sup> Because the thymic epithelium is a target of donor T-cell alloimmunity,<sup>7,8,14</sup> we hypothesized that thymic aGVHD interferes with the mTEC<sup>high</sup> capacity to sustain TRA diversity, thus decreasing the platform for central tolerance. In this

context, interventions directed at epithelial cytoprotection are expected to maintain posttransplantation mTEC<sup>high</sup> integrity and function. To test these 2 interrelated hypotheses, we used murine allo-HSCT models and investigated the effects of fibroblast growth factor-7 (Fgf7), which boosts thymopoiesis through its mitogenic action on TEC.<sup>15,16</sup>

#### Study design

Female C57BL/6 (B6;H-2<sup>b</sup>), (C57BL/6xDBA/2)F<sub>1</sub> (BDF<sub>1</sub>;H-2<sup>bd</sup>), Balb/c (H-2<sup>d</sup>), CBy.PL(B6)-Thy1<sup>tr</sup>/SerJ (Balb/c-Thy1.1;H-2<sup>d</sup>), 129/Sv (H-2<sup>b</sup>), and B6.SJL-Ptprc<sup>pep3</sup>/BoyJ (B6.CD45.1;H-2<sup>b</sup>) mice were kept in accordance with federal regulations. Thymic aGVHD was induced in unirradiated or total body-irradiated recipients<sup>14</sup> (supplemental Figure 1). Recombinant human Fgf7 (palifermin, Kevivance, Biovitrum, Sweden) was injected intraperitoneally from day -3 to day +3 after allo-HSCT at a dose of 5 mg/kg per day.<sup>15,16</sup>

Confocal microscopy of thymic sections was performed using a Zeiss LSM510 (Carl-Zeiss AG, Switzerland).<sup>17</sup> The TEC compartment was analyzed by flow cytometry (FACSARIA, Becton Dickinson, Mountain View, CA). mTEC<sup>high</sup> were identified as cells with a CD45<sup>+</sup>EpCam<sup>+</sup>Ly51<sup>-</sup>UEA1<sup>+</sup>MHCI<sup>high</sup> phenotype<sup>17-19</sup> (supplemental Figure 2). Global gene expression profiling was used to establish TRA diversity in transplant recipients. Microarray data of triplicate samples of pure mTEC<sup>high</sup> preparations (Mouse Gene 1.0 ST Array, Affymetrix, Santa Clara, CA; data available under

Submitted December 19, 2012; accepted May 17, 2013. Prepublished online as *Blood* First Edition paper, May 29, 2013; DOI 10.1182/blood-2012-12-474759.

G.A.H. and W.K. contributed equally to this study.

The online version of this article contains a data supplement.

There is an Inside *Blood* commentary on this article in this issue.

The publication costs of this article were defrayed in part by page charge payment. Therefore, and solely to indicate this fact, this article is hereby marked "advertisement" in accordance with 18 USC section 1734.

© 2013 by The American Society of Hematology

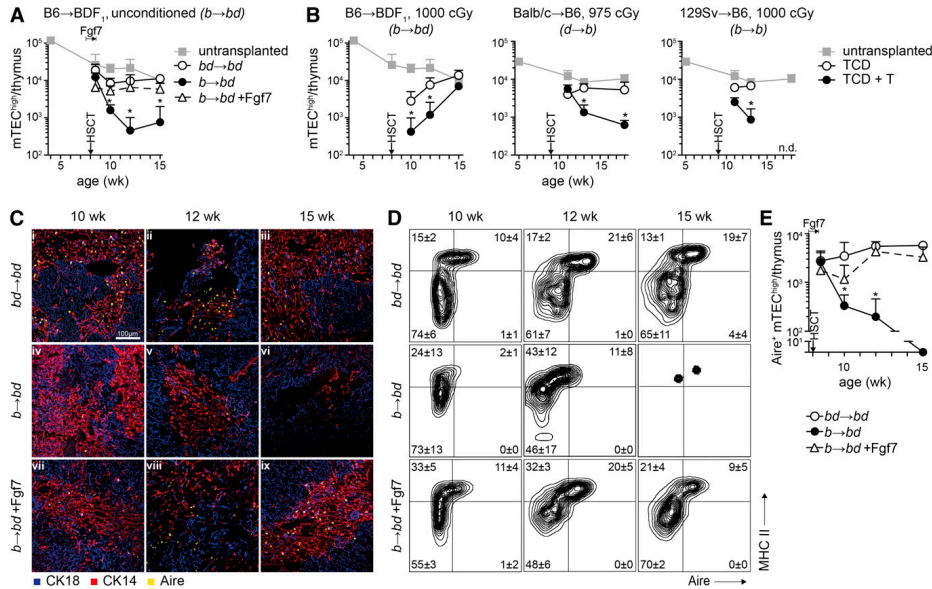


**Figure 1. Acute GVHD impairs mTEC<sup>high</sup> compartment size.** The mTEC<sup>high</sup> compartment was analyzed as a function of recipient age in 4 different murine models of allo-HSCT, as detailed in supplemental Figures 1 and 2. (A) Acute GVHD was induced in 8-week-old unconditioned BDF<sub>1</sub> recipients (*b→bd*, black circles). Untransplanted BDF<sub>1</sub> mice (gray squares) or syngeneically transplanted mice (*bd→bd*, open circles) served as controls. In 1 group, Fgf7 was administered (*b→bd* + Fgf7, triangles) as described.<sup>15</sup> A total of 6 experiments were performed, with 3 to 5 mice per group and experiment. (B) Acute GVHD (TCD+T group, black circles) was induced in irradiated 8-week-old BDF<sub>1</sub> recipients (*b→bd*, left panel), 9-week-old B6 recipients (*d→b*, middle panel) or 8-week-old B6 recipients (*b→b*, right panel) as described in supplemental Figures 1 and 2. Untransplanted BDF<sub>1</sub> or B6 mice (gray squares) and recipients of TCD bone marrow (TCD group, open circles) were used as controls without disease in all models. A total of 3 experiments were performed. The line graphs show total numbers (mean ± SD) of mTEC<sup>high</sup> cells in thymi from individual mice. \**P* < .05, analysis of variance (ANOVA), aGVHD versus transplanted mice without aGVHD. TCD, T-cell-depleted; n.d., not done. (C-E) Qualitative and quantitative analysis of thymic Aire expression, as described in supplemental Methods. Immunohistochemistry and confocal microscope analysis (C) was performed on thymic frozen sections taken from unconditioned transplant recipients at ages 10, 12, and 15 weeks (ie, 2, 4, and 7 weeks after transplantation; [i-iii] *bd→bd*, [iv-vi] *b→bd*, [vii-ix] *b→bd* + Fgf7). Cytokeratin-18 (CK18, blue) and CK14-positive cells (red) denote cTEC and mTEC, respectively.<sup>14,17</sup> Aire<sup>+</sup> cells are yellow in color and localize to the thymus medulla. Syngeneically transplanted mice (*bd→bd*, 18 ± 4 Aire<sup>+</sup> mTEC/0.04 mm<sup>2</sup> medulla) were not different from age-matched untransplanted control mice (data not shown). The flow cytometry plots in (D) depict Aire and MHC class II expression of DAPI<sup>+</sup>CD45<sup>+</sup>EpCam<sup>+</sup>Ly51<sup>+</sup>UEA1<sup>+</sup> mTECs. Numbers represent frequencies (%) of cells (mean ± SD). Total numbers of Aire<sup>+</sup> mTEC<sup>high</sup> in thymi from individual recipient mice (E) was calculated from flow cytometry data (mean ± SD). Groups are the same as in panel (A). A total of 5 experiments were performed, with 3 to 5 mice per group. \**P* < .05, ANOVA, aGVHD vs transplanted mice without aGVHD.

accession number E-MEXP-3745 at <http://www.ebi.ac.uk/arrayexpress>) were verified by quantitative polymerase chain reaction. Gene expression data from multiple published sources<sup>20,21</sup> and from MOE430 and GNF1M gene atlases (<http://biogps.org>) were combined for identification of Aire-dependent and Aire-independent TRA (supplemental Methods). Bioinformatics was implemented using software from “The R Project for Statistical Computing” (<http://www.r-project.org/>).

## Results and discussion

Total numbers of mTEC<sup>high</sup> declined over time in untransplanted adult BDF<sub>1</sub> and B6 mice, confirming age-dependent changes of the thymic stroma<sup>22</sup> (Figure 1A-B). We then investigated 4 mouse models of age-matched allo-HSCT. In unconditioned recipients of haploidentical HSCT (H-2<sup>b</sup>→H-2<sup>bd</sup>; *b→bd*), the induction of thymic aGVHD<sup>14,15</sup> (supplemental Figures 1 and 2) progressively reduced total mTEC<sup>high</sup> numbers to ≤10<sup>3</sup> cells/mouse in animals surviving aGVHD (Figure 1A). This observation was mirrored in allo-HSCT that

included total body-irradiated before MHC-identical, MHC-disparate, or haploidentical transplantation (Figure 1B). In these models, the conditioning initially reduced mTEC<sup>high</sup> numbers independently of aGVHD, but cell loss was either more pronounced (*b→bd*) or more protracted (*d→b*; *b→b*) in the presence of disease. Hence, reduction in mTEC<sup>high</sup> compartment size is a universal manifestation of thymic aGVHD,<sup>7</sup> and radiation injury is not mandatory. Contraction of the total mTEC<sup>high</sup> pool in unconditioned *b→bd* recipients corresponded to progressive decreases in the subset that expresses Aire<sup>+</sup> (Figure 1C-E). In 12-week-old recipients, residual Aire<sup>+</sup> mTEC<sup>high</sup> were low in numbers (<300 cells/thymus) and later became virtually undetectable, owing to the smaller than normal frequencies of Aire-expressing cells among declining mTEC<sup>high</sup> numbers.

Given the intimate associations among Aire-deficiency, TRA repression, and autoimmunity,<sup>3</sup> we determined whether aGVHD interfered with TRA transcription. Development of thymic GVHD (*b→bd*) altered global gene expression profiles in total residual mTEC<sup>high</sup> cell pools isolated at 2 to 4 weeks after transplantation (Figure 2A, supplemental Table 1). Using a special algorithm (supplemental

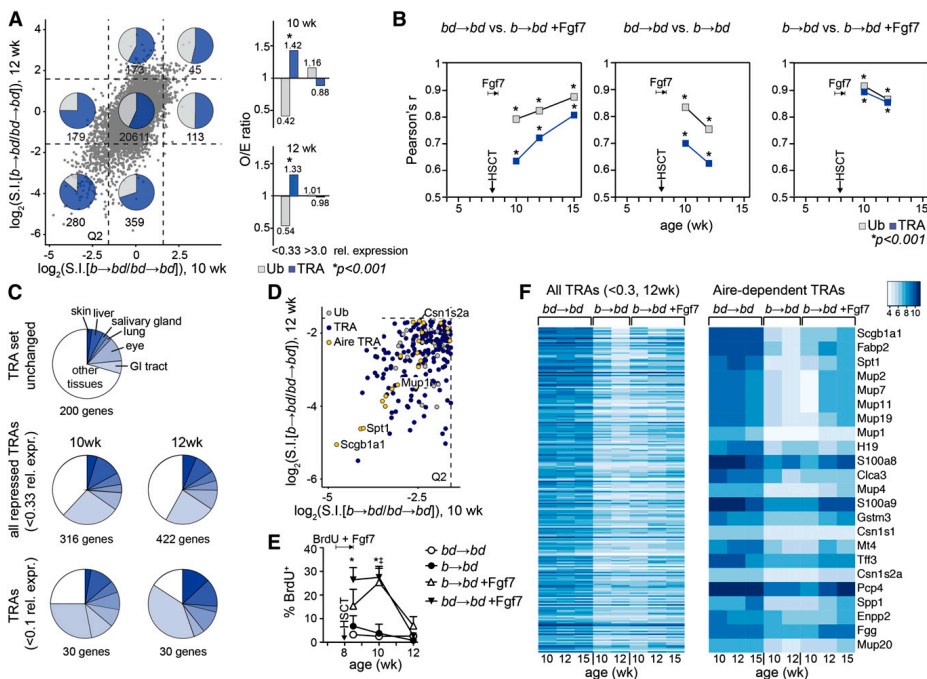


**Figure 2.** Peritransplant administration of Fgf7 sustains a more diverse TRA transcriptome in mTEC<sup>high</sup> during aGVHD. Acute GVHD (*b*-*bd*) was induced in 8-week-old unconditioned recipient BDF<sub>1</sub> mice as in Figure 1A. Global gene expression was analyzed in entire residual mTEC<sup>high</sup> cell pools isolated from individual recipients at 10, 12, and 15 weeks of age (ie, 2, 4, and 7 weeks after transplantation). The figure reflects data from 5 independent experiments, with 2 to 4 mice per group and experiment. (A) Left panel: gene expression profiling of mTEC<sup>high</sup> in transplant recipients using Mouse Gene 1.0 ST arrays (Affymetrix). The x- and y-axes represent relative expression of individual genes (given as log<sub>2</sub> values of signal intensity ratios, S.I.) in mice with aGVHD (*b*-*bd*) vs syngeneically transplanted recipients without disease (*bd*-*bd*). Data were plotted as a function of recipient age (10 vs 12 weeks). Genes whose expression levels were enhanced or decreased more than threefold relative to the control group (corresponding to relative expression values given by the S.I. ratios of <math>< -0.33</math> and <math>> 3.0</math>, respectively, or <math>< -1.6</math> and <math>> +1.6</math> on the log<sub>2</sub> scale) were considered to be significantly altered in consequence of aGVHD (threshold is indicated by dashed lines). Q2 is the lower left quadrant, denoting genes whose expression levels were depressed at both 2 and 4 weeks after allo-HSCT (10- and 12-week-old recipients). The inserted numbers denote the absolute numbers of genes in the respective quadrants. Transcripts from a total of 21 759 genes were analyzed. An annotated list of the genes most affected by aGVHD is given in supplemental Table 1. Ub (ubiquitously expressed genes, gray squares) and TRA (dark blue squares). (Right panel) O/E performance analysis (O, observed number of events; E, expected hypergeometric statistical analysis). A value of O/E = 1.0 represents a distribution among TRA and Ub according to expectations (that is sequestration according to the relative frequencies of TRA and Ub in adult mice without disease). (B) The linear relationship between 2 experimental groups was tested for Ub and TRA using a correlation matrix, as detailed in supplemental Figure 3. The variation of each gene was calculated using the interquartile range, a measure of statistical dispersion. Pearson's correlation coefficient *r* is shown as a function of age and time after transplantation. The asterisk (\*) symbol indicates a statistical *P* value for the quality of each measured *r* at any given time point for TRA and Ub, respectively; \**P* < .001 of Pearson's *r*. (C) Tissue representation of TRA repressed during aGVHD (<math>< -0.1</math> and <math>< -0.33</math> relative expression, respectively), vs mice without GVHD (relative expression = 1). Many repressed TRAs were specific for tissues of the gastrointestinal tract, skin, and eye. Changes in expression of these genes in response to Fgf7 are given in supplemental Figure 4. (D) Aire dependency of TRA repressed in mTEC<sup>high</sup> during aGVHD in 10- and 12-week-old recipients (quadrant Q2; the axes are the same as in panel A). Examples shown are the following: Scgb1a1, secretoglobulin; Csn1s2a, casein  $\gamma$ ; Mup1, major urinary protein 1; Spt1, salivary protein 1 (see supplemental Table 1). Aire-independent TRA (dark blue circles), Aire-dependent TRA (yellow circles), and Ub (gray circles). (E) Analysis of TEC proliferation in response to Fgf7. Eight-week-old BDF<sub>1</sub> mice were left untreated or were treated with Fgf7 from days -3 to +3 after allo-HSCT. All mice simultaneously received 0.8 mg/mL BrdU in their drinking water. mTECs were analyzed for BrdU incorporation at the indicated ages after transplantation. BrdU<sup>+</sup> cells (%)  $\pm$  SD. \**P* < .001, ANOVA, aGVHD vs mice without aGVHD. (F) Expression levels of individual genes expressed in mTEC<sup>high</sup> is given in a heatmap as color-coded log<sub>2</sub> value of signal intensities. (Left panel) The map was sorted according to relative expression of genes in mTEC<sup>high</sup> (*b*-*bd* vs *bd*-*bd* mice; 12 weeks old) and contains all TRA with a relative expression of <math>< -0.3</math> during aGVHD in age-matched mice. Enhancement of TRA expression in response to Fgf7 was detectable by higher signal intensities of individual genes. (Right panel) Aire-dependent TRAs were sorted as listed before.

Methods: "Bioinformatics"), we discriminated between TRA and ubiquitously expressed transcripts (Ub) in mTEC<sup>high</sup>. Several hundred transcripts were expressed at reduced levels (>3-fold change) in mice with aGVHD (Figure 2A). Notably, the TRA/Ub ratios for repressed transcripts were significantly higher than would have been

expected to be observed by chance (O/E ratio >1.0 TRA; <1.0 Ub; *P* < .001; Figure 2A, right panel). A low correlation coefficient between TRA expression in *b*-*bd* vs *bd*-*bd* mice (Pearson's *r* = 0.700 and *r* = 0.625 in 10- and 12-week-old recipients, respectively) indicated a sizable number of TRAs being reduced during lethal

aGVHD (Figure 2B, supplemental Figure 3). We interpreted these data such that a contraction in TRA diversity during aGVHD was caused by cellular loss of mTEC<sup>high</sup>, in particular Aire-positive mTEC. This explanation was based on the fact that ectopic TRA expression is a stochastic process in which only a limited number of mTEC<sup>high</sup> express a given TRA.<sup>2,18</sup> A comprehensive coverage of TRA expression is therefore only achieved by a sufficiently large mTEC<sup>high</sup> pool, which is, however, missing under conditions of aGVHD. The most substantially reduced TRAs were found to be enriched for genes that are characteristically expressed in tissues known to be targets of cGVHD<sup>9</sup> (Figure 2C). Many of these genes belonged to the subset of Aire-dependent TRAs<sup>20</sup> (Figure 2D,F, supplemental Figure 3).

Because efficient central tolerance requires the full scope of TRA, we next asked whether mTEC<sup>high</sup> compartment size and heterogeneity is sustained by using strategies for epithelial cytoprotection. Peritransplant administration of the TEC mitogen Fgf7<sup>15,16</sup> failed to prevent initial mTEC<sup>high</sup> cell loss in *b→bd* recipients (Figure 1A). However, Fgf7 maintained stable numbers of mTEC<sup>high</sup>, including the subset expressing Aire (~3000 cells/mouse during aGVHD; Figure 1C-E). Consistent with reports that mTEC are continuously replaced in adulthood,<sup>18,22</sup> ~5% of mTECs underwent cell division within 1 week in the *b→bd* and *bd→bd* transplant groups (Figure 2E). This frequency increased to ~15% in mice with aGVHD but that treated with Fgf7. Label retention analyses indicated high turnover of mTEC in response to Fgf7 in *b→bd* recipients (Figure 2E). Rescue of mTEC<sup>high</sup> numbers was therefore the consequence of enhanced proliferation within the entire mTEC compartment. During early aGVHD, the TRA spectrum was not preserved by Fgf7 (Pearson's  $r = 0.635$  vs *bd→bd* mice; Figure 2B, supplemental Figure 3). However, a broader array of TRA was expressed by 7 weeks after allo-HSCT as indicated by an expression profile that was closer to that of age-matched *bd→bd* controls ( $r = 0.807$ ). Hence, peritransplant administration of Fgf7 sustained a more diverse TRA transcriptome during aGVHD. Individual TRA expression patterns were differentially affected by aGVHD and Fgf7 as some but not all Aire-dependent TRA returned to nearly normal expression in the observation period (Figure 2F, supplemental

Figures 3 and 4). However, the molecular mechanism for this biased profile remains to date unknown.

Taken together, our data provide a mechanism for how autoimmunity may develop in the context of aGVHD (supplemental Figure 5). Because thymic-negative selection is sensitive to small changes in TRA expression,<sup>4,5</sup> approaches for mTEC cytoprotection may prevent the emergence of thymus-dependent autoreactive T cells<sup>12</sup> and thus alter autoimmune outcome. The identification in cGVHD of the yet undefined specificities of autoreactive effector T cells<sup>24</sup> will allow to test this argument directly in experimental systems and ultimately in clinical allo-HSCT.

## Acknowledgments

The authors thank Philippe Demougin (Life Sciences Training Facility, LSTF, Biocenter, University of Basel) for DNA microarray analyses, and Dr Gabor Szinnai (University Children's Hospital, Basel) for critically reviewing our manuscript.

This work was supported by Swiss National Science Foundation grants 310030-129838 (W.K.) and 310010-122558 (G.A.H.), and by a grant from the Hematology Research Foundation, Basel, Switzerland (W.K.).

## Authorship

Contribution: S.D., G.N., and M.M.H.-H. designed and performed work; R.I. implemented bioinformatics and statistics; and W.K. and G.A.H. share senior authorship and both designed the work and wrote the paper.

Conflict-of-interest disclosure: The authors declare no competing financial interests.

Correspondence: Werner Krenger, Department of Biomedicine, University of Basel, Mattenstrasse 28, 4058 Basel, Switzerland; e-mail: werner.krenger@unibas.ch.

## References

- Vicente R, Swainson L, Marty-Grès S, et al. Molecular and cellular basis of T cell lineage commitment. *Semin Immunol*. 2010;22(5):270-275.
- Klein L, Hinterberger M, Wirmsberger G, Kyewski B. Antigen presentation in the thymus for positive selection and central tolerance induction. *Nat Rev Immunol*. 2009;9(12):833-844.
- Anderson MS, Su MA. Aire and T cell development. *Curr Opin Immunol*. 2011;23(2):198-206.
- Chentoufi AA, Polychronakos C. Insulin expression levels in the thymus modulate insulin-specific autoreactive T-cell tolerance: the mechanism by which the IDDM2 locus may predispose to diabetes. *Diabetes*. 2002;51(5):1383-1390.
- Liston A, Gray DH, Lesage S, et al. Gene dosage—limiting role of Aire in thymic expression, clonal deletion, and organ-specific autoimmunity. *J Exp Med*. 2004;200(8):1015-1026.
- Blazar BR, Murphy WJ, Abedi M. Advances in graft-versus-host disease biology and therapy. *Nat Rev Immunol*. 2012;12(6):443-458.
- Na IK, Lu SX, Yim NL, et al. The cytolytic molecules Fas ligand and TRAIL are required for murine thymic graft-versus-host disease. *J Clin Invest*. 2010;120(1):343-356.
- Krenger W, Blazar BR, Holländer GA. Thymic T-cell development in allogeneic stem cell transplantation. *Blood*. 2011;117(25):6768-6776.
- Martin PJ. Biology of chronic graft-versus-host disease: implications for a future therapeutic approach. *Keio J Med*. 2008;57(4):177-183.
- Holländer GA, Widmer B, Burakoff SJ. Loss of normal thymic repertoire selection and persistence of autoreactive T cells in graft vs host disease. *J Immunol*. 1994;152(4):1609-1617.
- van den Brink MR, Moore E, Ferrara JL, Burakoff SJ. Graft-versus-host-disease-associated thymic damage results in the appearance of T cell clones with anti-host reactivity. *Transplantation*. 2000;69(3):446-449.
- Zhang Y, Hexner E, Frank D, Emerson SG. CD4<sup>+</sup> T cells generated de novo from donor hematopoietic stem cells mediate the evolution from acute to chronic graft-versus-host disease. *J Immunol*. 2007;179(5):3305-3314.
- Sakoda Y, Hashimoto D, Asakura S, et al. Donor-derived thymic-dependent T cells cause chronic graft-versus-host disease. *Blood*. 2007;109(4):1756-1764.
- Hauri-Hohl MM, Keller MP, Gill J, et al. Donor T-cell alloreactivity against host thymic epithelium limits T-cell development after bone marrow transplantation. *Blood*. 2007;109(9):4080-4088.
- Rossi S, Blazar BR, Farrell CL, et al. Keratinocyte growth factor preserves normal thymopoiesis and thymic microenvironment during experimental graft-versus-host disease. *Blood*. 2002;100(2):682-691.
- Rossi SW, Jeker LT, Ueno T, et al. Keratinocyte growth factor (KGF) enhances postnatal T-cell development via enhancements in proliferation and function of thymic epithelial cells. *Blood*. 2007;109(9):3803-3811.
- Zuklys S, Mayer CE, Zhanybekova S, et al. MicroRNAs control the maintenance of thymic epithelia and their competence for T lineage commitment and thymocyte selection. *J Immunol*. 2012;189(8):3894-3904.
- Gillard GO, Farr AG. Features of medullary thymic epithelium implicate postnatal development in maintaining epithelial heterogeneity and tissue-restricted antigen expression. *J Immunol*. 2006;176(10):5815-5824.



19. Gray DH, Fletcher AL, Hammett M, et al. Unbiased analysis, enrichment and purification of thymic stromal cells. *J Immunol Methods*. 2008; 329(1-2):56-66.
20. Anderson MS, Venanzi ES, Klein L, et al. Projection of an immunological self shadow within the thymus by the aire protein. *Science*. 2002; 298(5597):1395-1401.
21. Derbinski J, Gäbler J, Brors B, et al. Promiscuous gene expression in thymic epithelial cells is regulated at multiple levels. *J Exp Med*. 2005; 202(1):33-45.
22. Gray DH, Seach N, Ueno T, et al. Developmental kinetics, turnover, and stimulatory capacity of thymic epithelial cells. *Blood*. 2006;108(12): 3777-3785.
23. Hubert FX, Kinkel SA, Webster KE, et al. A specific anti-Aire antibody reveals aire expression is restricted to medullary thymic epithelial cells and not expressed in periphery. *J Immunol*. 2008;180(6): 3824-3832.
24. Hess AD. Equal opportunity targeting in chronic GVHD. *Blood*. 2012;119(26):6183-6184.

From [bloodjournal.hematologylibrary.org](http://bloodjournal.hematologylibrary.org) at MEDIZINBIBLIOTEK on August 2, 2013. For personal use only.

# blood

2013 122: 623-624  
doi:10.1182/blood-2013-06-507376

## A 2-hit model for chronic GVHD

Robertson Parkman

---

Updated information and services can be found at:  
<http://bloodjournal.hematologylibrary.org/content/122/5/623.full.html>  
Articles on similar topics can be found in the following Blood collections  
[Free Research Articles](#) (1825 articles)

---

Information about reproducing this article in parts or in its entirety may be found online at:  
[http://bloodjournal.hematologylibrary.org/site/misc/rights.xhtml#repub\\_requests](http://bloodjournal.hematologylibrary.org/site/misc/rights.xhtml#repub_requests)

Information about ordering reprints may be found online at:  
<http://bloodjournal.hematologylibrary.org/site/misc/rights.xhtml#reprints>

Information about subscriptions and ASH membership may be found online at:  
<http://bloodjournal.hematologylibrary.org/site/subscriptions/index.xhtml>

Blood (print ISSN 0006-4971, online ISSN 1528-0020), is published weekly by the American Society of Hematology, 2021 L St, NW, Suite 900, Washington DC 20036.  
Copyright 2011 by The American Society of Hematology; all rights reserved.



in eosinophilic esophagitis. *Immunol Allergy Clin North Am*. 2009;29(1):197-211, xiii-xiv.

5. Lee JJ, Dimina D, Macias MP, et al. Defining a link with asthma in mice congenitally deficient in eosinophils. *Science*. 2004;305(5691):1773-1776.

6. Humbles AA, Lloyd CM, McMillan SJ, et al. A critical role for eosinophils in allergic airways remodeling. *Science*. 2004;305(5691):1776-1779.

7. Jacobsen EA, Ochkur SI, Pero RS, et al. Allergic pulmonary inflammation in mice is dependent on eosinophil-induced recruitment of effector T cells. *J Exp Med*. 2008;205(5):699-710.

8. Nair P, Pizzichini MM, Kjarsgaard M, et al. Mepolizumab for prednisone-dependent asthma with sputum eosinophilia. *N Engl J Med*. 2009;360(10):985-993.

9. Rothenberg ME, Klion AD, Roufosse FE, et al; Mepolizumab HES Study Group. Treatment of patients with the hyper-eosinophilic syndrome with mepolizumab. *N Engl J Med*. 2008;358(12):1215-1228.

10. Rosenberg HF, Gallin JL. Neutrophil-specific granule deficiency includes eosinophils. *Blood*. 1993;82(1):268-273.

© 2013 by The American Society of Hematology

## ● ● ● TRANSPLANTATION

Comment on Dertschnig et al, page 837

# A 2-hit model for chronic GVHD

Robertson Parkman<sup>1,2</sup> <sup>1</sup>CHILDREN'S HOSPITAL LOS ANGELES; <sup>2</sup>UNIVERSITY OF SOUTHERN CALIFORNIA KECK SCHOOL OF MEDICINE

In this issue of *Blood*, Dertschnig and colleagues<sup>1</sup> demonstrate in mice that acute graft-versus-host disease (GVHD) results in a marked reduction of autoimmune receptor-expressing medullary thymic epithelial cells (Aire<sup>+</sup> mTEC) and a decrease in the diversity of Aire-dependent tissue-restricted peripheral self-antigens (TRAs) required for effective negative thymic selection. Both of these abnormalities are reversed by the peritransplant administration of the epithelial protectant drug, fibroblast growth factor 7 (Fgf7).

Chronic GVHD continues to be a major cause of both morbidity and mortality after allogeneic hematopoietic stem cell transplantation (HSCT).<sup>2</sup> Chronic GVHD has been assumed to be caused by the continuation of the pathogenic mechanisms that cause acute GVHD, primarily donor-derived T lymphocytes specific for histocompatibility antigens uniquely expressed by recipient cells.<sup>3</sup> As a consequence, therapy for chronic GVHD has traditionally been directed at suppressing the donor antirecipient immune response. However, during the last 25 years, a series of murine experiments have indicated that donor-derived, autoreactive T lymphocytes (ie, T lymphocytes specific for antigens expressed by both donor and recipient cells) are present in murine HSCT recipients with chronic GVHD and that the chronic GVHD could be transferred by the donor-derived T lymphocytes into both donor and recipient mice.<sup>4-6</sup>

More recently, a clinical trial of low-dose subcutaneous IL-2 in human HSCT recipients with established chronic GVHD demonstrated that an increase in circulating regulatory T lymphocytes (Treg) resulted in clinical

improvement, suggesting that deficiencies in Treg lymphocytes play a role in the pathogenesis of human chronic GVHD.<sup>7</sup>

Dertschnig et al report that mice with acute GVHD have a profound decrease in the frequency of Aire<sup>+</sup> mTEC, which are necessary for the thymic production of naturally occurring Treg lymphocytes. Other investigators have previously demonstrated that the diverse expression of TRA by Aire<sup>+</sup> mTEC is required for the effective thymic elimination of autoreactive T lymphocytes by negative selection.<sup>8</sup> Using microarray analyses of isolated Aire<sup>+</sup> mTEC, the present investigators report the decreased expression and diversity of TRA with a selective decrease in the TRA associated with the tissues that are the target organs of human chronic GVHD (skin, liver, salivary glands, lung, eye, and gastrointestinal tract). The result of the restricted diversity of TRA expression would be the extrathymic presence of autoreactive T lymphocytes. Their present results suggest a 2-hit model for chronic GVHD, in which the presence of extrathymic autoreactive T lymphocytes (Hit 1) in the context of immune dysregulation (deficiencies in

Treg lymphocytes, Hit 2) can result in the development of chronic GVHD.

The peri-HSCT administration of the epithelial protectant drug, Fgf7, does not affect the initial post-HSCT decrease in mTEC but does hasten the recovery of Aire<sup>+</sup> mTEC and improves the diversity of TRA expression. Fgf7 acts by stimulating the proliferation and differentiation of TEC progenitors and the proliferation of residual mTEC.<sup>9</sup> The relative contribution of the 2 populations to the recovery of Aire<sup>+</sup> mTEC is unclear. The presence of normal numbers of Aire<sup>+</sup> mTEC with normal TRA diversity during the recapitulation of immunologic ontogeny, which occurs after the engraftment of donor hematopoietic stem cells, may result in the presence of adequate numbers of circulating Treg lymphocytes and effective negative thymic selection, which would eliminate the peripheral presence of autoreactive T lymphocytes, and an absence of chronic GVHD. As such, clinical trials to determine whether the peritransplant administration of Fgf7 results in a decreased incidence of chronic GVHD in human HSCT recipients are indicated.

The present murine experiments, however, do not address several potentially important clinical questions: (1) What would be the impact of the administration of Fgf7 to patients with established chronic GVHD?; (2) Do HSCT recipients with established chronic GVHD have an adequate number of TEC progenitors and residual mTEC for the Fgf7 to be effective?; (3) Do the TEC progenitors and mTEC in chronic GVHD patients become refractory to the action of Fgf7?; and (4) Is the loss of Aire<sup>+</sup> mTEC during acute GVHD paralleled by a decrease in TRA diversity, or are they separable biological processes? If they differ, then some HSCT recipients may have a deficiency of Treg lymphocytes without the concomitant presence of peripheral autoreactive T lymphocytes, whereas other recipients may have adequate numbers of Treg lymphocytes with the presence of peripheral autoreactive T lymphocytes. Only HSCT recipients with both the presence of peripheral autoreactive T lymphocytes (Hit 1) and deficiencies in Treg lymphocytes (Hit 2) would be at risk of developing chronic GVHD. The immunophenotypic identification of functional human Treg lymphocytes will aid in the evaluation of

human chronic GVHD; however, the inability to identify immunophenotypic human autoreactive T lymphocytes is still a major limitation to our better understanding.<sup>10</sup>

Finally, the present results suggest that the focus of future research into new therapies to prevent or treat chronic GVHD should be directed at the thymic microenvironment rather than at lymphohematopoietic cells.

**Conflict-of-interest disclosure:** The author declares no competing financial interests. ■

#### REFERENCES

1. Dertschnig S, Nusspaumer G, Ivanek R, Hauri-Hohl MM, Holländer GA, Krenger W. Epithelial cytoprotection sustains ectopic expression of tissue-restricted antigens in the thymus during murine acute GVHD. *Blood*. 2013;122(5):837-841.
2. Martin PJ, Inamoto Y, Carpenter PA, Lee SJ, Flowers ME. Treatment of chronic graft-versus-host disease: Past, present and future. *Korean J Hematol*. 2011;46(3):153-163.
3. Blazar BR, Murphy WJ, Abedi M. Advances in graft-versus-host disease biology and therapy. *Nat Rev Immunol*. 2012;12(6):443-458.
4. Parkman R. Clonal analysis of murine graft-vs-host disease. I. Phenotypic and functional analysis of T lymphocyte clones. *J Immunol*. 1986;136(10):3543-3548.
5. Sakoda Y, Hashimoto D, Asakura S, et al. Donor-derived thymic-dependent T cells cause chronic graft-versus-host disease. *Blood*. 2007;109(4):1756-1764.
6. Zhang Y, Hexner E, Frank D, Emerson SG. CD4+ T cells generated de novo from donor hemopoietic stem cells mediate the evolution from acute to chronic graft-versus-host disease. *J Immunol*. 2007;179(5):3305-3314.
7. Koreth J, Matsuoka K, Kim HT, et al. Interleukin-2 and regulatory T cells in graft-versus-host disease. *N Engl J Med*. 2011;365(22):2055-2066.
8. Klein L, Hinterberger M, Wirnsberger G, Kyewski B. Antigen presentation in the thymus for positive selection and central tolerance induction. *Nat Rev Immunol*. 2009;9(12):833-844.
9. Rossi SW, Jeker LT, Ueno T, et al. Keratinocyte growth factor (KGF) enhances postnatal T-cell development via enhancements in proliferation and function of thymic epithelial cells. *Blood*. 2007;109(9):3803-3811.
10. Miyara M, Yoshioka Y, Kitoh A, et al. Functional delineation and differentiation dynamics of human CD4+ T cells expressing the FoxP3 transcription factor. *Immunity*. 2009;30(6):899-911.

© 2013 by The American Society of Hematology

#### ● ● ● VASCULAR BIOLOGY

Comment on Moxon et al, page 842

## The endothelial protein C receptor and malaria

Tom van der Poll<sup>1</sup> <sup>1</sup>UNIVERSITY OF AMSTERDAM

In this issue of *Blood*, Moxon et al provide novel insight into the pathogenesis of cerebral malaria, linking loss of the endothelial protein C receptor (EPCR) on brain vessels, caused by cytoadherent infected erythrocytes, with localized coagulation, inflammation, and disruption of endothelial barrier function.<sup>1</sup>

**M**alaria is caused by parasites of the genus *Plasmodium*, of which *P falciparum* is the most virulent.<sup>2</sup> One of the most fatal manifestations of *P falciparum* infection is cerebral malaria, which especially affects children <6 years of age and is responsible for an annual death toll of nearly a million infants in Africa alone. In recent years, the cycle of coagulation and inflammation has emerged as a pivotal component of malaria pathogenesis.<sup>3</sup> In normal homeostasis, activation of coagulation is compensated by concurrent induction of anticoagulant mechanisms.<sup>4</sup> In areas of excessive activation of the clotting cascade, thrombin acts as a feedback inhibitor of coagulation by binding to the

endothelial receptor thrombomodulin (see figure). The thrombomodulin-thrombin complex converts the zymogen protein C into activated protein C (APC), a reaction that is greatly accelerated by EPCR.<sup>5,6</sup> APC acts as an anticoagulant by virtue of its capacity to proteolytically inactivate clotting factors Va and VIIIa. When attached to EPCR, APC in addition can exert anti-inflammatory, antiapoptotic, and vasculoprotective signals via protease activated receptor (PAR)1. In case of impaired function of the protein C system, high thrombin levels can activate PAR1, resulting in effects that are opposite to those transduced by APC, disrupting endothelial barrier function.

A hallmark feature of severe malaria is sequestration of infected erythrocytes in blood vessels.<sup>2</sup> The elegant investigations by Moxon et al provide a long-sought explanation of why red blood cell sequestration especially leads to damage in the brain.<sup>1</sup> In postmortem studies in children that had died of cerebral malaria, endothelial sites of adherent erythrocytes were shown to colocalize with loss of EPCR. Moreover, the authors developed a novel approach that enabled examination of blood vessels with relevance for the brain vasculature in children with cerebral malaria directly after admission to the hospital. For this, they used subcutaneous tissue microvessels as an ex vivo surrogate for brain endothelium and demonstrated reduced expression of both EPCR and thrombomodulin in cerebral malaria patients compared with healthy controls. Children with cerebral malaria had higher levels of soluble EPCR and thrombomodulin in their cerebrospinal fluid than febrile control patients, suggesting that the loss of these receptors at least in part was caused by shedding.

Importantly, in plasma, the balance between the production of thrombin (measured by the levels of the prothrombin F1+2 fragment) and APC was not altered in cerebral malaria compared with healthy children and children with mild febrile disease or uncomplicated malaria, indicating that at the systemic level, coagulation activation was compensated. Together, these data strongly suggest that cerebral malaria is associated with a localized disturbance of coagulation and inflammation caused by a local loss of EPCR and thrombomodulin initiated by sequestration of infected erythrocytes, changes that damage the brain due to the already low constitutive expression of EPCR and thrombomodulin in healthy brain vessels.<sup>1,7</sup>

Another recent study has implicated EPCR in the pathogenesis of malaria by a completely different mechanism.<sup>8</sup> In malaria, adherence of red blood cells to endothelium is caused by an interaction between *P falciparum* erythrocyte membrane protein-1 (PEMP1) family members, transported to the erythrocyte membrane as a consequence of parasite infection, and receptors on the vascular endothelium.<sup>2</sup> In this respect, PEMP1 subtypes containing domain cassettes 8 and 13 are important for sequestration of infected erythrocytes in severe childhood malaria.<sup>9</sup> Turner et al very recently revealed EPCR as the endothelial receptor for PEMP1 domain

# Curriculum Vitae

**Simone Dertschnig**

**Nationality: Swiss, Austrian**

**Date of birth: 7. September 1986, Basel CH**

**Marital status: unmarried**

## **LANGUAGES:**

**German** (mother tongue)

**English** (C2) very good (Certificate of Proficiency in English, University of Cambridge ESOL Examinations)

**French** (good)

**Italian** (A2 basics)

## **EDUCATION:**

2010 May – 2014 Feb

**University of Basel and University Children's Hospital (UKBB) Basel, Department of Biomedicine, Basel, Switzerland**

**PhD student in Biomedical Research**

2009 Jan – 2010 Feb

**University of Basel and University Children's Hospital (UKBB) Basel, Department of Biomedicine, Basel, Switzerland**

**Master of Science in Molecular Biology, Major in Immunology**

2008 Sep – 2008 Dec

**Wimbledon School of English, London UK**

2005 – 2008 **University of Basel**

**Bachelor of Science in Biology, Major in Molecular Biology**

2000 - 2005 **Gymnasium Kirschgarten, Basel, Switzerland**

### AWARDS:

- 2012 Mai Prize for the best oral presentation in the category of basic/translational research at the “Young Researcher Day in Pediatrics” held during the Annual Meeting of the Swiss Society for Paediatrics.  
Title of the talk: Fibroblast growth factor-7 sustains thymic expression of tissue-restricted antigens during experimental graft-versus-host disease

### PUBLICATIONS:

- Dertschnig S, Nusspaumer G, Ivanek R, Hauri-Hohl MM, Holländer GA, Krenger W, EPITHELIAL CYTOPROTECTION SUSTAINS ECTOPIC EXPRESSION OF TISSUE-RESTRICTED ANTIGENS IN THE THYMUS DURING MURINE ACUTE GVHD. *Blood*. 2013 Aug 1;122(5):837-41.

### ATTENDANCE AT CONFERENCES:

- 40<sup>th</sup> Annual Meeting of the European Group for Blood and Marrow Transplantation (EBMT), 30 March-2 April 2014, Milan IT  
Oral presentation: **Dertschnig S**, Hauri-Hohl M, Holländer GA, Krenger W, “Impaired thymic expression of a tissue-restricted antigen licenses the *de novo* generation of autoreactive CD4<sup>+</sup> T cells during murine acute graft-versus-host disease”
- Research Day of the Children’s University Hospital Basel 2013, 26 September 2013, Basel CH  
Poster: **Dertschnig S**, Holländer GA, Krenger W, “Acute GVHD weakens the platform for central tolerance”
- Annual Meeting of the Swiss Society for Paediatrics (Schweizerische Gesellschaft für Pädiatrie) 2013, 21 June 2013, Geneva CH  
Poster: **Dertschnig S**, Bucher C, Holländer GA, Krenger W, “Epithelial cytoprotection sustains ectopic expression of tissue-restricted antigens in the thymus medulla during acute graft-versus-host disease”
- 39<sup>th</sup> Annual Meeting of the European Group for Blood and Marrow Transplantation (EBMT), 7-10 April 2013, London UK

- Oral presentation: **Dertschnig S**, Bucher C, Ivanek R, Hauri-Hohl M, Holländer GA, Krenger W, “Epithelial cytoprotection sustains ectopic expression of tissue-restricted antigens in the thymus medulla during murine acute graft-versus-host disease”
- Research Day of the Children’s University Hospital Basel 2012, 23 August 2012, Basel CH
    - Poster: **Dertschnig S**, Nusspaumer G, Holländer GA, Krenger W, “Fgf7 rescues thymic expression of tissue-restricted self-antigens in experimental acute GVHD”
  - Young Researcher Day in Pediatrics, Annual Meeting of the Swiss Society for Paediatrics 2012, 31 May 2012, Lucerne CH
    - Oral presentation: **Dertschnig S**, Nusspaumer G, Holländer GA, Krenger W, “Fibroblast growth factor-7 sustains thymic expression of tissue-restricted antigens during experimental graft-versus-host disease”
  - 38<sup>th</sup> Annual Meeting of the European Group for Blood and Marrow Transplantation (EBMT), 1-4 April 2012, Geneva CH
    - Oral presentation: **Dertschnig S**, Nusspaumer G, Holländer GA, Krenger W, “Fibroblast growth factor-7 sustains thymic expression of tissue-restricted antigens during experimental acute graft-versus-host disease”
    - Oral presentation (given by Bucher C): Bucher C, Krenger W, **Dertschnig S**, Stern M, Gerull S, Heim D, Halter J, Buser A, Lehmann T, Graf L, Rovo A, Tichelli A, Passweg J, “Busulfan-based versus total body irradiation-based myelo-ablative conditioning in patients with AML: reduction of acute graft-versus-host disease incidence, mucositis and duration of hospitalization”
  - Research Day of the Children’s University Hospital Basel 2011, 25 August 2011, Basel CH
    - Poster: **Dertschnig S**, Nusspaumer G, Holländer GA, Krenger W, “Fgf7 sustains thymic expression of tissue-restricted antigens during acute GVHD”
  - EUTHyme-Rolduc Meeting 2011, 21-24 May 2011, Noordwijkerhout NL

Poster: **Dertschnig S**, Krenger W, “Acute graft-versus-host disease targets thymic epithelial cells”

- 23<sup>rd</sup> Meeting of the Swiss Immunology PhD Students, 30 March – 1 April 2011, Wolfsberg CH

Poster: **Dertschnig S**, Krenger W, “Graft-versus-host disease targets thymic epithelial cells”